

Lehrstuhl für Fluidmechanik und Prozessautomation
Technische Universität München

Optical In-Situ Measurement of the pH -Value During High Pressure Treatment of Fluid Food

Volker Michael Stippl

Vollständiger Abdruck der von der Fakultät Wissenschaftszentrum
Weihenstephan für Ernährung, Landnutzung und Umwelt der Technischen
Universität München zur Erlangung des akademischen Grades eines

Doktor-Ingenieurs (Dr.-Ing.)

genehmigten Dissertation.

Vorsitzender: Univ.-Prof. Dr.-Ing. habil. R. Meyer-Pittroff

Prüfer der Dissertation: 1. Univ.-Prof. Dr.-Ing. habil. A. Delgado
2. Univ.-Prof. Dr.-Ing. habil. Th. Becker
Universität Hohenheim
3. Univ.-Prof. Dr.-Ing. Dr.h.c. P.A. Wilderer, i.R.

Die Dissertation wurde am 16.02.2005 bei der Technischen Universität München eingereicht und durch die Fakultät Wissenschaftszentrum Weihenstephan für Ernährung, Landnutzung und Umwelt am 27.07.2005 angenommen.

Und wenn de amme Chrüzweg stohsch
Und nümme weisch, wo's ane goht,
Halt still, und frog di G'wisse z'erst -
's cha dütsch, gottlob! - und folg sim Rot!

Johann Peter Hebel

meinen Eltern gewidmet

Danksagung

Diese Arbeit entstand in der Zeit von 2001 bis 2005 am Lehrstuhl für Fluidmechanik und Prozessautomation der Technischen Universität München auf Anregung von Herrn Prof. Dr.-Ing. A. Delgado. Ihm möchte ich meinen ganz herzlichen Dank aussprechen. Neben der Tatsache, dass er mir die Möglichkeit geboten hat, an seinem Lehrstuhl zu forschen, möchte ich die konzeptionelle Unterstützung hervorheben, die er mir gewidmet hat.

Des weiteren möchte ich meinem Betreuer Prof. Dr.-Ing. habil. T.M. Becker für seine fachlich kompetente Betreuung aber vor allem für seine Geduld mit mir bedanken. Besonders die Unterstützung mit seinen weitreichenden Kenntnisse in der Chemometrie trugen wesentlich zum Gelingen dieser Arbeit bei.

Herrn Prof. Dr.-Ing., Dr. h.c. P.A. Wilderer danke ich für das Interesse an der Arbeit sowie für die Anfertigung des Gutachtens und Herrn Prof. Dr.-Ing. R. Meyer-Pittroff für die Übernahme des Prüfungsvorsitzes.

Mein besonderer Dank gilt weiterhin M. Anderton, der als "native speaker" mit viel Mühe mein erbärmliches Englisch korrigierte.

Dem Werkstatt-Team, W. Seidl, J. Rohrer und ihren Azubis sei ein besonderer Dank für die vielen anfallenden Arbeiten an der Versuchsanlage ausgesprochen. Es war ein großer Glücksfall mit so kompetenten und guten Mechanikern zusammen arbeiten zu können.

Meinem Diplomanten W. Danzl danke ich für seine engagierte und kreative Mitarbeit bei den Optoden und die vielen kompetenden wissenschaftlichen Diskussionen und Anregungen. H. Petermeier gilt mein Dank für die Unterstützung bei meinen mathematischen Problemen. Für die gute Mitarbeit im Labor möchte ich meinem studentischen Mitarbeitern L. Rodriguez und M. Kasseris danken.

Frau K. Fraunhofer, Frau B. Weber und vor allem Frau H. Gerzer danke ich für die Beratung und Hilfe bei verwaltungstechnischen Aufgaben. Allen bisher nicht genannten Mitarbeitern des Lehrstuhls und der Forschergruppe sei mein Dank für die gute Zusammenarbeit und die schöne Atmosphäre hier am Lehrstuhl ausgesprochen.

Dank auch an die Firma PreSens die ihre Optoden und Messgeräte kostenlos zur Verfügung stellten und deren Mitarbeiter sich viel Zeit für unsere Probleme nahmen.

Zuletzt will ich schliesslich meinen Mitbewohnern C. Munz, W. Danzl, L. Sarreiter, R. Brasse, H. Schlaffke, M. und E. Anderton, R. Meyer, H. Huikmann†, M. Hicke, K. Kaltenbacher, R. Schmidt, H. Peterson, J. Meier, M. Lang, A. Kilimann und C. Fenn für die Gemeinschaft danken die ich mit ihnen in Itzling erfahren habe. Ohne die Möglichkeit hier abzuschalten zu können hätte ich diese Arbeit sicher nicht durchgehalten.

Freising, im Oktober 2005

Volker Stippl

Contents

1	Introduction	1
1.1	High Pressure Treatment of Food	1
1.1.1	Brief Historical Remarks	3
1.1.2	Fundamentals of High Pressure Technology	4
1.2	<i>pH</i> -Value	15
1.3	<i>pH</i> -Value and High Pressure Food Technology	16
1.4	Conceptual Formulation	19
2	Methods Used for Measuring <i>pH</i>-Value	20
2.1	Overview	20
2.2	Determination of the <i>pH</i> -Value Using the Electrical Potential Difference Caused by Phase Boundary Reactions	26
2.3	Determination of the <i>pH</i> -Value Using Indicator Dyes	38
2.3.1	Indicator Dyes	38
2.3.2	Possible Errors in <i>pH</i> -Measurements using Indicator Dyes	44
2.3.3	Methods for <i>pH</i> -Measurements using Indicator Dyes	47
2.4	Comparison of the Different Methods	58
3	Performance of Experiments	63
3.1	Calculation of the <i>pH</i> -Value of the Calibration and Validation Buffer Solutions	63
3.2	Measurement of <i>pH</i> -Value Using Solved Absorption Indicator Dyes	67
3.2.1	Experimental Setup for <i>pH</i> -Measurements Using Solved Absorption Indicator Dyes	67
3.2.2	Selection of Indicator Dyes	69
3.3	Measurement of <i>pH</i> -Value Using Immobilised Indicator Dyes	72
3.3.1	Techniques Used for Immobilising Indicator Dyes	73
3.3.2	Manufacture of Optodes	74
3.3.3	Experimental Setup for <i>pH</i> -Measurements with Optodes	78
3.4	Investigations of <i>pH</i> -Inhomogeneities in High Pressure Vessels	79
3.5	Sources of Chemicals and Equipment	81

4	Presentation and Discussion of Results	83
4.1	Discussion of the <i>pH</i> -Measurements Using Solved Indicator Dyes .	83
4.1.1	Data Analysis of the <i>pH</i> -Measurements Using Solved Indicator Dyes	83
4.1.2	Results of the <i>pH</i> -Measurements Using Solved Indicator Dyes	88
4.2	Discussion of the <i>pH</i> -Measurements Using Immobilised Indicator Dyes	97
4.2.1	Data Analysis of the <i>pH</i> -Measurements Using Immobilised Indicator Dyes	97
4.2.2	Results of the <i>pH</i> -Measurements Using Optodes	100
4.3	Results of the Investigations into <i>pH</i> -Inhomogeneities in High Pressure Vessels	110
4.4	Conclusions and Outlook	113
5	Appendix	116
5.1	Auxiliary Calculations	116
5.1.1	Derivation of Equations Used in the Text	116
5.1.2	A Program to Select and Pre-treat the Values from Spectral Data Files	119
5.2	Bibliography	126

Index of Symbols

a_i	Activity of the Species i	-
a_Σ	Sum of the Activities of an Acid and all Associated Anions	-
b	Constant in the Equation (1.9)	9.2 GPa ⁻¹
c_i	Concentration of the Species i	$\frac{\text{mol}}{\text{dm}^3}$
c_o	Standard Concentration	$1 \frac{\text{mol}}{\text{dm}^3}$
c_Σ	Sum of the Concentrations of an Acid and all Associated Anions	$\frac{\text{mol}}{\text{dm}^3}$
e	Error	-
d	Length of the Optical Path	cm
i, j, l	Index of an Element	-
k	Rate Constant	-
m_i	Molality of the Species i	$\frac{\text{mol}}{\text{kg}}$
m_o	Standard Molality	$1 \frac{\text{mol}}{\text{kg}}$
m_i^o	Molality of the Species i at Standard Pressure	$\frac{\text{mol}}{\text{kg}}$
m_Σ	Sum of the Molalities of an Acid and all Associated Anions	$\frac{\text{mol}}{\text{kg}}$
p	Pressure	Pa
p_o	Standard Pressure	101.325 kPa
p_{max}	Value to Normalize Pressure Data	450 MPa
pH	Negative Logarithm of the Hydrogen Ion Activity	$pH = -\lg a_{H^+}$
pOH	Negative Logarithm of the Hydroxide Ion Activity	$pOH = -\lg a_{OH^-}$
pK	Negative Logarithm of an Equilibrium Constant (Related to Activities)	$pK = -\lg K$
pK_a	Negative Logarithm of an Equilibrium Constant for an Acid Dissociation (Related to Activities)	$pK_a = -\lg K_a$
pK_a^*	Negative Logarithm of an Equilibrium Constant for an Acid Dissociation (Related to the Activity of H^+ and the Molalities of the Acid and the Corresponding Base)	$pK_a^* = -\lg K_a^*$
pK_W	Negative Logarithm of the Equilibrium Constant for the Dissociation of Water (Related to the Activities)	$pK_W = -\lg K_W$

r_i	Debye Radius of the Ion i	nm
t	Time	s
z_i	Number of Elementary Charges of the Ion i	-
B	Parameter in Equations (1.3) and (1.6)	Pa
C	Constant in Equation (1.6)	0.725
F	Faraday Constant	$96485.3415 \frac{\text{C}}{\text{mol}}$
ΔH	Molar Enthalpy Difference of a Reaction	$\frac{\text{J}}{\text{mol}}$
I	Ionic Strength	-
I_λ	Intensity of Light at the Wavelength λ	-
I_λ^0	Intensity of Light at the Wavelength λ in Absence of the Analyte	-
J, L	Quantity of a Group of Elements	-
K	Equilibrium Constant (Related to Activities)	-
K_a	Equilibrium Constant of an Acid Dissociation (Related to Activities)	-
K_a^*	Equilibrium Constant of an Acid Dissociation (Related to the Activity of H^+ and the Molalities of the Acid and the Corresponding Base)	$K_a^* = K_a \cdot \frac{\gamma(HA)}{\gamma(A^-)}$
K_W	Equilibrium Constant of the Dissociation of Water (Related to Activities)	-
R	Gas Constant	$8.314571 \frac{\text{J}}{\text{K} \cdot \text{mol}}$
ΔS	Molar Entropy Difference of a Reaction	$\frac{\text{J}}{\text{K} \cdot \text{mol}}$
T	Temperature	K
U_i	Electric Potential Difference of a Reaction i	mV
U_i^*	Standard Electric Potential Difference of a Reaction i ($\forall a_j = 1$)	mV
V	Volume	m^3
$V_{W,0}$	Molar Volume of Water at Standard Pressure and Standard Temperature	$18.02 \frac{\text{cm}^3}{\text{mol}}$
ΔV	Molar Volume Difference of a Reaction	$\frac{\text{cm}^3}{\text{mol}}$
ΔV^0	Molar Volume Difference of a Reaction at Standard Pressure	$\frac{\text{cm}^3}{\text{mol}}$

ΔV_W^o	Molar Volume Difference of the Dissociation of Water at Standard Pressure and Standard Temperature	$22.414 \frac{\text{cm}^3}{\text{mol}}$
$\Delta V^\#$	Molar Volume of Activation of a Reaction	$\frac{\text{cm}^3}{\text{mol}}$
Y_l, Y_r	Functions of pH -Value and of Light Intensities to Fit their Correlation.	-
$\alpha_{(\lambda)}$	Absorption Index at the Wavelength λ	$\frac{\text{m}^2}{\text{mol}}$
ϵ	Relative Dielectric Permittivity	-
ϵ^o	Relative Dielectric Permittivity at Standard Pressure	-
γ_i	Activity Coefficient of the Species i	-
η_i	Number of Bonded Water Molecules on the Molecule/Ion i	-
κ	Molar Compressibility	$\frac{\text{m}^3}{\text{mol} \cdot \text{Pa}}$
$\Delta \kappa$	Difference of the Molar Compressibilities of Products and Reactants in Solution	$\frac{\text{m}^3}{\text{mol} \cdot \text{Pa}}$
$\Delta \kappa^o$	Difference of the Molar Compressibilities of Products and Reactants in Solution at Standard Pressure	$\frac{\text{m}^3}{\text{mol} \cdot \text{Pa}}$
λ	Wavelength	nm
ρ	Density	$\frac{\text{kg}}{\text{dm}^3}$
ρ^o	Density at Standard Pressure	$\frac{\text{kg}}{\text{dm}^3}$
σ	Sensitivity Dependant on Concentration	-
σ_I	Sensitivity Dependant on Light Intensity of Absorbance Measurements	-
Λ	Coefficient in Equations (3.2), (3.4) and (3.6)	$503 \frac{\sqrt{\text{K}}}{\text{nm}}$
Φ	Phase Shift between Exciting and Emitted Light	-
Φ_m	Measured Phase Shift (Average of Two Fluorescence Dyes) between Exciting and Emitted Light	-
Φ_R	Reference Phase Shift between Exciting and Emitted Light of a pH -Insensitive Fluorescence Dye	-
Θ	Angle of Reflection	-
Ω	Coefficient in Equations (3.2), (3.4) and (3.6)	$1.82 \cdot 10^6 \text{K}^{-\frac{3}{2}}$

Prefix

Publications

V.M. Stippl, T.M. Becker, A. Delgado:
Optical Method for the In-situ Measurement of the pH -Value
during High Pressure Treatment of Foods
in *High Pressure Research* (2002) **22** [3], 757.

A. Molina-Gutierrez, V.M. Stippl, A. Delgado, M.G. Gänzle, R.F. Vogel:
In Situ Determination of the Intracellular pH of *Lactococcus lactis*
and *Lactobacillus plantarum* during Pressure Treatment
in *Applied and Environmental Microbiology* (2002) **68** [9], 4399.

V.M. Stippl, A. Delgado, T.M. Becker:
Hochdruckbehandlung von Getränken
in *Braumanager* (2004) **4**, 26.

V.M. Stippl, A. Delgado, T.M. Becker:
Optical In-situ Detection of pH -Value
during High Pressure Treatment of Fluid Foods
in *Innovative Food Science & Emerging Technologies* (2004) **5** [3], 285.

V.M. Stippl, A. Delgado, T.M. Becker:
Ionization Equilibria at High Pressure
in *European Food Research and Technology* (2005) **221**, 151

Zusammenfassung

Neben der thermischen Behandlung zum Haltbarmachen von Lebensmitteln gewinnt die Anwendung von hydrostatischen Drücken immer größere Bedeutung. Es hat sich gezeigt, dass bei Drücken von mehreren 100 MPa viele lebensmittelverderbende Mikroorganismen vollständig abgetötet werden können, während wertvolle Inhaltsstoffe wie Vitamine, Farb-, Aroma- und Geschmacksstoffe weitgehend erhalten bleiben.

Bei einer Veränderung des Druckes ändern sich die Gleichgewichtskonstanten¹. Infolgedessen ändert sich sowohl der pH -Wert einer Lösung als auch das Verhalten von pH sensitiven Reaktionen, wie z.B. das pH -Optimum eines Enzyms oder der pH -Wert, dessen Unterschreitung zu einer Proteindenaturierung führt.

Wenngleich die Forschung auf dem Gebiet der Hochdruckbehandlung von Lebensmitteln in den letzten Jahrzehnten intensiviert wurde, so fehlt es doch noch an in-situ Messmethoden für viele grundlegende physikalische und chemische Größen, wie den pH -Wert. Zielsetzung dieser Arbeit war es, ein System zur optischen Messung des pH -Wertes von Lebensmitteln unter Drücken bis 450 MPa zu entwickeln.

Das dafür entwickelte System beruht auf Absorptionsmessungen eines Indikatorgemisches in einer Hochdrucksichtzelle. Es wurden 14 Indikatoren verwendet, die bei Normaldruck einen pH -Bereich von 2 bis 8 abdecken. Das System wurde mit verschiedenen Pufferlösungen unter Druck kalibriert. Da sich Säure/Basen-Gleichgewichte unter Druck verschieben, musste das Druckverhalten der verwendeten Puffer berechnet werden. Dazu wurden verschiedene Verfahren aus der Literatur vorgestellt und diskutiert und das Verfahren mit der besten Übereinstimmung mit Messwerten ausgewählt.

Die Modellierung der spektroskopischen Daten erfolgte mit chemometrischen Methoden, um die komplizierten überlagerten Spektren beherrschen zu können und um den Einfluss von Matrixeffekten klein zu halten. Es wurden verschiedene mathematische Verfahren getestet. Die PCR (Principal Component Regression) mit 3 Hauptkomponenten erwies sich als die genaueste. Bei der Validierung wurde damit eine empirische Varianz von 0,25 pH -Einheiten erreicht.

¹Der Begriff *Konstante* ist irreführend, da Gleichgewichte nicht *konstant* sind, sondern eine Funktion von Druck und Temperatur.

Abstract

In addition to heat treatment of food used to enhance shelf life, the relevance of the application of hydrostatic pressures is increasing. With treatment of several 100 MPa many food-spoiling microorganisms can be completely eliminated, while valuable properties such as vitamins, colouring, smell and taste are mostly preserved.

Equilibrium constants² change with pressure. Consequently, both the pH -value of a solution and the behaviour of pH -sensitive reactions change, e.g. the pH -optimum of an enzyme or the pH -value under which a protein is denatured.

Although research into high pressure treatment of food has been intensified in the last decades, there is still a deficiency in in-situ measuring methods for many fundamental physical and chemical quantities such as the pH -value. The aim of this work was to develop a system for the optical measurement of the pH -value of food during pressure treatment of up to 450 MPa.

The system developed is based on absorption measurements using indicator dyes in an optical high pressure cell. The calibration took place using different buffer solutions under pressure. A mixture of 14 indicator dyes was used, covering a pH -range from 2 to 8 at standard pressure. Since acid/base equilibria shift under pressure, the pressure behaviour of the buffer systems had to be calculated. For this purpose, different procedures described in literature were presented and discussed. The procedure which showed the best agreement with measured data was selected for the calculations. The modelling of the spectroscopic data took place using chemometric methods in order to be able to cope with the complicated overlapping spectra and to keep the influence of matrix effects small. Different mathematical procedures were tested and the PCR (Principal Component Regression) with 3 principal components was considered to be the best. In validation, an empirical variance of 0.25 pH -units was reached using the calculations with PCR.

²The term *constant* is misleading, as equilibria are not *constant* but a function of pressure and temperature.

Chapter 1

Introduction

The subject of this thesis is the in-situ-measurement of pH during high pressure treatment of food. The introduction is divided into sections, the first introducing high pressure treatment of food, the second pH -value. In the last part, both sections will be merged to show their connections.

1.1 High Pressure Treatment of Food

An abundance of literature is available which describes high pressure treatment of food. Good summaries are given by Matser et al. [1], by Smelt [2] and by Hoover et al. [3].

With high pressure treatment of food it is possible, as with thermal treatment, to inactivate vegetative cells and some microbial spores resulting in food products having an enhanced shelf life [3, 4, 5, 6, 7, 8, 9]. As the inactivation of spores is incomplete even at pressures of up to 1 000 MPa, it is not cost-effective to use only this method for food in which spores can exist. Here often a combination of pressure and temperature treatment is expedient, where the self-heating of the medium by compression can be utilised [1, 10]. This self-heating can be increased by the choice of a pressure transmission medium with high compressibility [11]. But there exist also some spores in which pressure resistance increases with temperature [12]. The inactivation of vegetative cells by pressure is caused mostly by membrane damage [13, 14, 15, 16] and protein denaturing (especially the denaturing of enzymes).

The major advantage over thermal processes is that high pressure only slightly affects colour, taste, smell and nutritional qualities: the natural flavour of raw meat and fish as well as fresh fruits and juices remain in most cases unaffected. Most vitamins, sensitive to heat, survive pressure treatment. In addition, hardly any colour changes arise, since most natural dyes such as Chlorophyll or β -Carotene are not affected by pressure [17].

Enzymes, which play an important role in food technology, are affected by

pressure. This influence can concern the kinetics of enzyme reactions [18, 19] and inactivation by coagulation [18, 19, 20, 21, 22]. The kinetics of enzyme catalysed reactions can be altered by the influence of high pressure on each catalytic step, the result being either increased or decreased activity or changing selectivities [23].

Furthermore, pressure influences important chemical reactions such as Maillard Browning [24, 25] and Lipid Autoxidation, and possible interactions between both [26]. In addition, the structure and function of biopolymers such as proteins [18, 27, 28, 29], starch [30], pectin [31] and other polysaccharides and lipids and mixtures of them are sensitive to pressure [17, 32]. This enables pressure to be used to develop products with novel eating characteristics: for example structural characteristics –such as the creamy sensation of chocolate or yoghurt or the texture of vegetables [33]– can be affected by the use of high pressure [27, 28, 34].

In general, high pressure methods require a shorter processing time than thermal treatment. Unlike heat, pressure spreads uniformly throughout the whole vessel, though the conclusion should not be drawn that each changing physical property is evenly distributed. Because food has often no homogenous composition, pressure dependent properties such as heating by compression or pH -change vary inhomogeneously. Even in homogenous liquids, thermal variations are possible due to heat loss through the vessel walls [35, 36, 37, 38, 39, 40, 41, 42, 43].

The process conditions depend on the product. At a pressure of between 200 and 800 MPa, temperatures of up to 328 K and holding-times of between 5 and 30 minutes, enzymes and bacteria are inactivated while colour, vitamins, taste and smell remain mostly unaffected.

Another possible method of food treatment is *high pressure freezing and thawing* and *liquid storage at subzero temperatures* [44, 45, 46]. The effects of high pressure on the liquid-solid behaviour of water open this way to new applications in food technology. The melting temperature of ice decreases with pressure to 252 K at 210 MPa, while the opposite effect is observed above this pressure. The method involves cooling unfrozen food that consists mainly of water under pressure and then suddenly releasing the pressure, thus causing a high degree of *undercooling*. Undercooling (or supercooling) is the process of retaining the liquid state of a substance at a temperature/pressure beyond the melting point and is only possible if pressure release occurs faster than the crystallisation velocity¹. After decompression, nucleation will occur and a very rapid freezing takes place (known as *recalcescence*). This sudden freezing forms glassy state ice nucleations distributed uniformly throughout the sample. Ice made in this way does not have the ability to form large crystals. This leads to less damage of cell membranes, which is responsible for the mushy consistency of conventional frozen and thawed food [44, 45, 47].

¹A small undercooling over long time is also possible as the temperature for building seed crystals is a little lower than that for crystal growth.

1.1.1 Brief Historical Remarks

The first experiments at pressures above 100 MPa were performed more than 100 years ago [48, 49, 50]. These experiments were made to verify fundamental thermodynamic theories. The first papers about killing rates of microorganisms and preservation of food were published around 1900 [51, 52], about a quarter of a century after Pasteur's discovery of thermal inactivation of microorganisms. Hite reported that subjecting milk to a pressure of 450 MPa or greater considerably reduces the bacterial count. He also investigated the high pressure preservation of meat, fruit and vegetables [53].

In 1914, Bridgeman demonstrated that high hydrostatic pressure could coagulate egg albumin [54]. In the same year, papers about fruit preservation were published [53]. Following these early investigations, a number of publications [5, 55, 56, 57] have dealt with the effect of high pressure on microorganisms and proteins. Phase diagrams of various solutions and solvents, which were measured in extensive work (e.g. [58]), created the basis for the present development of methods for high pressure freezing and thawing and subzero liquid storage.

Literature from following years about hydrostatic high pressure describes mostly research into sea biology (e.g. [59, 60]). Investigations into pressure-induced germination of bacterial spores were carried out in the late 1960's [61] and the early 1970's [62, 63], but no industrial applications were realised. In the same period, high pressure technology for the use in the production of ceramics, steel, carbide components, superalloys, artificial diamonds and polymers were developed. These experiences in plant engineering and construction provided the basis for the development of food processing vessels.

In the last decades of the 20th century researchers begin to study potential commercialisation of high pressure technology in the food industry: in 1982 the University of Delaware (USA) and in 1987 the University of Kyoto (Japan) started research projects leading to industrial food applications. The first commercial products (high pressure combined with careful thermal pasteurisation) arrived in 1990 on the Japanese market. Since 1996, further high pressure-treated food is available on the market: in France orange juice, in Spain ham, in England high pressure-homogenised milk and in the USA avocado purée. In France in September 1998 an application for acceptance of high pressure-treated food (fruit preparation) was placed for the first time under the "Novel Food" regulation. The present situation in high pressure technology is expatiated by Palou et al. [64]. Up to now, most of the new procedures are used mainly for fruit and vegetables. In Japan, for example, one million litres per year of high pressure treated tangerine juice is already being produced.

1.1.2 Fundamentals of High Pressure Technology

Influence of High Pressure on Chemical Reactions

Temperature and pressure are two important factors in thermodynamics. Like temperature, pressure also affects chemical reactions, such as denaturing processes [18, 19, 21, 22, 56, 65, 66], organic-chemical reactions [67] or ionisation processes [68, 69, 70, 71].

At constant temperature, the influence of pressure on the reaction rates depends exclusively on the activation volume of the reaction $\Delta V^\#$ and the effect of pressure on the equilibria depends exclusively on the volume change of a reaction ΔV . The principle of Le Chatelier, Brown and Thomson states that, under equilibrium conditions, reactions associated with a decrease in volume (including changes of conformations or phase transitions) are favoured by pressure. A numerical expression for the influence of pressure on reactions was given by M. Planck [49]:

$$\left(\frac{\partial \ln K}{\partial p}\right)_T = -\frac{\Delta V(p)}{RT}. \quad (1.1)$$

Here K is an equilibrium constant, p the pressure, R the gas constant ($R = 8.314 \frac{\text{J}}{\text{K}\cdot\text{mol}}$) and T the absolute temperature in kelvin. The volume change ΔV (in $\frac{\text{m}^3}{\text{mol}}$) is the difference between the partial molal volumes of products and reactants in an infinitesimally diluted solution.

The equation describing the correlation of the pressure dependency of rate constants and the activation volume $\Delta V^\#$ is shown in (1.2). It has a similar form to Equation (1.1) as the equilibrium is the state in which the reaction rate from reactants to products is equal to that of the reverse reaction².

$$\left(\frac{\partial \ln k}{\partial p}\right)_T = -\frac{\Delta V^\#(p)}{RT} \quad (1.2)$$

For rough classification it is possible to divide reactions into groups: reactions leading to new interactions show mostly a decrease in volume. These interactions can be the forming of covalent bonds, charge-transfer complexes, ion-solvent interaction, dipole-solvent interaction or hydrophilic interaction. Among the reactions changing covalent bonds, only those with a changing number of molecules have a large volume change and consequently a high pressure dependency. A decreasing number of molecules normally leads to a decrease in volume.

²One of the first publications about the theory of the activated complex [72] includes the influence of activation volume on pressure dependency of rates. Extensive work on this phenomena can be found in the publications of Buchanan and Hamann [73] and Élyanov et al. [74, 75, 76, 77, 78]. A review discussing and itemising activation and reaction volumes is given by Asano and Le Noble [69, 71].

A special case can be found in the large volume reductions associated with reactions forming ions in aqueous solutions such as the dissociation of acids. The reason for this is the intense interaction between the electric field of ions and water.

With increased pressure, ionization reactions such as the dissociation of a neutral acid HA tend to shift more to the side of H^+ and A^- -ions [79, 80, 81]. Pressure lowers the free enthalpy required to dissolve the ions or, in other words, enhances the appearance of electrical charges as it is accompanied by a contraction of the surrounding solvent. Water is substantially more closely packed in the vicinity of ions. This phenomenon is known as electrostriction. According to the equation of Planck (1.1) such reactions will tend to smaller volumes with increasing pressure. As the molar volume change, ΔV , changes with pressure an equation is required to describe this pressure behaviour. To develop a comprehensive theory describing this pressure behaviour to be used in solving the differential Equation (1.1), several factors must be taken into account:

1. **Steric Arrangement:** it describes the volume change of a reaction if both products and reactants are treated as being uncharged and nonpolar. The volume change in this case depends on both the geometric arrangement of the products and reactants and the ability of the solvent molecules to arrange around the reactants.
2. **Hydration:** the water molecules in close proximity to the ion are tightly bonded and can be regarded as being immobilized, strongly polarized and highly compressed. The number and geometry of these water molecules has often a stiff arrangement, but unlike Hydrogen bonds in water such ion-water interactions tend mostly to decrease volume.
3. **Electric Field of the Ion:** the Columbic field produced by the charge of an ion attracts the partial charges of opposite polarity to the water dipoles and tends to crowd the water molecules closer to it. Therefore the transference of an ion into water has the same effect as applying additional pressure. But in contrast to hydrostatic pressure, this "pressure" is not uniformly distributed but decreases with greater distance to the ion.

The magnitude of the influence of steric arrangements on the volume change is approximately that of neutral reactions. Reactions in which all the molecules involved are neutral usually have volume changes of a few $\frac{\text{cm}^3}{\text{mol}}$, while most of the ion forming reactions have volume changes of between -10 and -35 $\frac{\text{cm}^3}{\text{mol}}$ [69]. Therefore, the factors of hydration and the influence of the electric field predominate.

Ions have an important influence on the water molecules surrounding them, these interactions being especially important at high pressures as they lead to changes in density. An important part in understanding these interactions and

their pressure behaviour is the interplay between different types of water structures. The interaction between molecules in liquid water is a complex system and many models have been developed to describe this behaviour³. All have in common the supposition that water can be regarded as a type of associated liquid in which the associations are present throughout the whole of the liquid forming three-dimensional networks of Hydrogen-bonds, several different configurations of which can coexist simultaneously. The proportion of these structured associations decreases with increasing pressure. At pressures above 100-150 MPa (at 298 K) these associations disappear and water behaves as a normal liquid. The different structures are mostly described as being similar to those of ice modifications. Each of the coexisting constituents corresponds to characteristic values, such as dielectric permittivity and density [82].

Thermodynamically, the behaviour of water can be seen as the result of competitive forces. The formation of Hydrogen bonds is associated with an increase in enthalpy, but to a decrease in entropy owing to the stiff arrangement. Additionally, at higher pressures, mechanical work plays an important role in increasing the volume which is needed to accommodate these structures.

If ions are present, a further influence is the tendency for dipoles to arrange in the direction of the electric field; therefore the structure with the better possibility of such an arrangement will be preferred. Also, denser constituents will be found in the proximity of ions.

A change in the characteristics of water is the result of both the sum of the changes of every component and the modification of the composition. In the vicinity of small ions, the electric field strength and pressure are in an order of magnitude where little experimental data is available. Whalley [88] has shown in a rough estimation that the maximum pressure, caused by the electrostatic field of a small unit charged ion with a diameter of 0.3 nm is approximately 1.4 GPa and the maximum electric field is approximately $2 \frac{\text{GV}}{\text{m}}$.

On the basis of theoretical considerations and numerical simulations, a saturation of the dielectric permittivity should take place somewhere between 10 and $1000 \frac{\text{MV}}{\text{m}}$ (see [89, 90] and the literature cited therein). Saturation means that nearly every dipole is aligned with the field followed by a strong decrease in dielectric permittivity. Such a parallel alignment can lead to new structures.

The hydration of ions can also be regarded as a structure in a strong electric field and at high pressure. While this structure is not only a result of the effort to achieve a dense structure with many dipoles being aligned with the field, interactions with outer-orbitals of the ion also play a role. However, these interactions are similar to the angle directed forces of Hydrogen bonds which are responsible for the arrangement of the structures. But a continuation of the "hydration structure" is impossible as a regular lattice cannot be expanded while maintaining a spherical symmetry.

³For an overview see [82], more recent publications are [83, 84, 85, 86, 87].

It must be pointed out that uncharged polar molecules, such as undissociated neutral acids, also have an influence on all of the aforementioned items with regard to charge [88]. Therefore, the electrical part of the reaction volume change is caused by the difference in the effect of charged products and that of uncharged polar reactants on the density of surrounding water.

Until now, no comprehensive theory exists which considers all influences on the volume of the solvent. But several semi-empirical functions can be found in the literature to describe ΔV as a function of pressure. All of them treat water as a homogenous medium, neglecting the changes caused by the strong electrical field and high pressure in the proximity of ions. No publication considers the structural changes of water directly. But these structural changes have an influence on the pressure behaviour of solvent properties such as density, compressibility and dielectric permittivity. While most authors use empirical values or equations for these properties, there is an indirect account for these structural changes.

An early Equation (1.3) was given by Owen and Brinkley [91]. They used an equation of Gibson [92, 93] to describe the compression of water due to ions, based on Tammann's hypothesis [48, 50, 94] which treats the influence of ions on water as an additional pressure. This additional "internal pressure" is equal to the pressure in which pure water has the same compressibility as the solution at standard pressure. Therefore, the compressibility at standard pressure, κ_o , is a measure for the electrical influence of ions, its value determining how the volume changes with pressure. The influence of steric arrangements on the volume change included in the volume change at standard pressure ΔV_o is assumed to be not influenced by pressure.

$$RT \ln \frac{K(p)}{K(p_o)} = - \Delta V_o(p - p_o) + \Delta \kappa_o(B + p_o) \cdot \left[(p - p_o) - (B + p_o) \ln \left(\frac{B + p}{B + p_o} \right) \right] \quad (1.3)$$

where the parameter B is a function of temperature (B (298 K) = 299.6 MPa) and the subscript $_o$ denotes that the values are at standard pressure. $\Delta \kappa_o$, the difference in the molar compressibilities is the derivative $\left(\frac{\partial \Delta V}{\partial p} \right)_{p_o}$ and can be seen as the difference in the influence of products and reactants on the compressibility of the solution at standard pressure. Uncharged molecules are assumed to have no influence.

Lown et al. [79] have reported that there is a rough but simple correlation between ΔV_o and $\Delta \kappa_o$:

$$\Delta \kappa_o \approx 2.13 \text{ GPa}^{-1} \cdot \Delta V_o \quad (1.4)$$

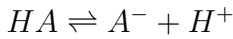
and they suggested using this equation to calculate the difference in compressibility from volume change data if no compressibility data are available. This

means that the pressure increase caused by the ions is assumed to be responsible for both the change in volume and the change in compressibility.

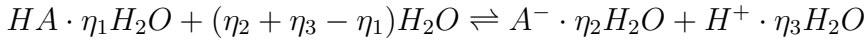
A shortcoming of Tammann's hypothesis is in treating all water molecules as being influenced in the same way. But as shown previously, there is a large difference in the internal pressure in the proximity of ions and that further away.

North [95] derived an equation similar to (1.3) in a completely different way: he considered only water molecules which were strictly bound in close proximity to the ion. This "hydration" is included in the complete reaction.

Instead of



he formulated the equilibrium so:



where η_i specifies the number of bonded water molecules. Assuming that other water molecules are not influenced by the ions, the volume change of this reaction is:

$$\begin{aligned} \Delta V = & V_{(H^+ \cdot \eta_3 H_2O)} + V_{(A^- \cdot \eta_2 H_2O)} \\ & - V_{(HA \cdot \eta_1 H_2O)} - (\eta_2 + \eta_3 - \eta_1) V_{H_2O}. \end{aligned} \quad (1.5)$$

He also approximated that the bonded water is incompressible, likewise the ions H^+ and A^- and the acid HA . Therefore the change of ΔV with changing pressure can be calculated as only the volume change of the $(\eta_2 + \eta_3 - \eta_1)$ water molecules. In a similar manner to Owen and Brinkley [91] he used an equation from Tait to describe the pressure behaviour of water and obtained:

$$\begin{aligned} RT \ln \frac{K(p)}{K(p_o)} = & - \Delta V_o (p - p_o) \\ & + \eta_{tot} C V_{W,o} \left[(p - p_o) - (B + p_o) \cdot \ln \left(\frac{B + p}{B + p_o} \right) \right] \end{aligned} \quad (1.6)$$

where $V_{W,o}$ is the molar volume of water at standard pressure and C a constant ($V_{W,o} (298 \text{ K}) = 18.02 \text{ cm}^3/\text{mol}$; $C = 0.725$). B is the same as in Equation (1.3) and $\eta_{tot} = \eta_2 + \eta_3 - \eta_1$.

Él'Yanov and Hamann [96] reported that North enhanced his Equation (1.6) with $\eta_{tot} \approx 0.213 \frac{\text{mol}}{\text{cm}^3} \cdot \Delta V_o$ as the number of bonded water molecules is often not known. This means that the change in the number of bonded water molecules can be calculated by the volume change at standard pressure. When this term is

included in (1.6), an equation is reached which requires only the volume change at standard pressure as a parameter depending on the individual reaction:

$$RT \ln \frac{K_a(p)}{K_a(p_o)} = -\Delta V_o \left[(p - p_o) + 2.78 \left\langle (p - p_o) - (B + p_o) \ln \left(\frac{B+p}{B+p_o} \right) \right\rangle \right]. \quad (1.7)$$

This approach is similar to that of Owen and Brinkley with the correlation between the reaction volume change and the change in compressibilities. Indeed, if the second derivative of Equation (1.7) with respect to pressure is taken, then one obtains the compressibility change at ambient pressure, which is similar to the correlation (1.4) of Lown et al.:

$$\Delta \kappa_o \approx 2.28 \text{ GPa}^{-1} \cdot \Delta V_o. \quad (1.8)$$

A higher accuracy at higher pressures was obtained by authors which calculate the pressure dependency of the equilibrium constant by the change in the dielectric permittivity of the solvent [96, 97, 98, 99, 100, 101], their line of argument was that pressure enhances the electric permittivity of water. An increase in electric permittivity lowers the electrical work needed to separate opposing charges which happens when an acid dissociates or a salt is dissolved [99, 102]. A change in this electrical work also means a change in the Gibbs free energy. While a minimum of Gibbs free energy is a precondition for equilibrium, the change in the equilibrium constant can be calculated by the change of the dielectric permittivity. This would seem to be an additional influence on the pressure dependency of the equilibrium constants, but is just another way to formulate the previously mentioned compression of water by the electric field of an ion. That is due to both the attractive forces between the ion and water and the electric permittivity being dependent directly on the ability of the permanent dipoles to orientate in the electric field and on the degree of the induced dipole moment. Furthermore, as a consequence of the equation of Planck (1.1), it is essential for each physical value changing with pressure and having influence on an equilibrium (such as the dielectric permittivity) to be accompanied by a volume change. Or in other words, a part of the electrical work expended in separating the charges is used to compress the surrounding solvent. And as this is the only part which is accompanied by a volume change, only this part is influenced by pressure. A change in the dielectric permittivity with pressure is therefore a measure for this part of the electrical work.

While most authors compare only separately measured values, ÉI'Yanov and Hamann [96] gave an equation for the equilibrium constants derived from the pressure dependency of the dielectric permittivity:

$$RT \ln \frac{K(p)}{K(p_o)} = -\frac{\Delta V_o p}{1 + bp}. \quad (1.9)$$

where b is a constant ($b = 0.92 \text{ GPa}^{-1}$). The term describing the pressure dependency is derived from the pressure dependency of the dielectric permittivity. The authors used as the basis for their considerations an equation from Born [102]. Although this equation is based upon a crude model which assumes that the properties of water, such as the dielectric permittivity, are not influenced by the electric field of the ion, it has proven to be useful in describing many effects of ionic solutions.

Nevertheless, Nakahara [103] found a mistake in the derivation of ÉI'Yanov and Hamann's correlation: they showed in their publication an agreement of the interrelation between the pressure behaviour of the equilibrium constants and that of measured values of the dielectric permittivity at 298 K, but the correlation only works at this specific temperature. To prove this, Nakahara derived a function for the pressure behaviour of the equilibrium constant on the basis of a fit to the measurements of the dielectric permittivity using the same assumptions as ÉI'Yanov and Hamann, but using several temperatures, and obtained an equation similar to (1.9), but where the parameter b is now a function of temperature. However, a consideration for the temperature dependency of b in Equation (1.9) leads to a decrease in accuracy compared with measured values. Nakahara concluded that the assumptions used for Equation (1.9) do not lead to the correct findings.

This is at first surprising as the equation of Born has been well proven as a basis for numerous theories such as the description of activity coefficients of ions as a function of ionic strength [104] and the dissociation of salts into ions in solvents of different dielectric permittivities [105, 106, 107, 108, 109] and at different temperatures [110, 111, 112].

Even so, most of these theories show only tendencies or need empirically determined parameters and for some solubility experiments in different solvents the theory fails [113]. Furthermore, Millero [114] described density measurements of aqueous Sodium Chloride solutions and compared his results with the Debye Hückel's theory, which is based on Born's theory. Like Nakahara he found an agreement of a theory based on Born's ideas only at a temperatures of 298 K and a deviation at other temperatures.

For a comparison of all previously mentioned equations, Figure (1.1) shows a graph of calculated pK -values ($pK = -\lg(K)$) using the example of the dissociation reaction of Ammonium Hydroxide at 318 K (Reaction (1)).



Additionally, measured values of this reaction are plotted.

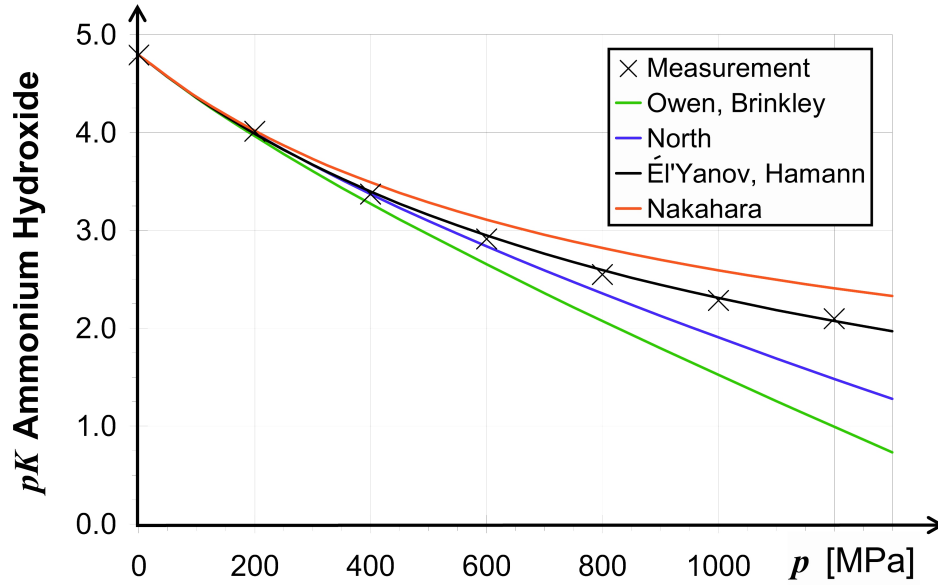


Figure 1.1: pK -values for the dissociation of Ammonium Hydroxide at 318 K as a function of pressure, calculated according to the following equations:

Owen and Brinkley: Equation (1.3) with $B = 308.1 \text{ MPa}$ [115];

and $\Delta\kappa_o = 53.36 \frac{\text{cm}^3}{\text{GPa}}$ [96];

North: Equation (1.7) with $B = 308.1 \text{ MPa}$ [115];

Él'Yanov and Hamann: Equation (1.9) with $b = 0.92 \text{ GPa}^{-1}$ [96];

Nakahara: Equation (1.9) with $b = 1.167 \text{ GPa}^{-1}$ [103];

for all equations: $\Delta V_o = -28.5 \frac{\text{cm}^3}{\text{mol}}$ [96].

Measurements from Hamann and Strauss [97] (corrected according to [96]).

As can be seen from Figure (1.1) there is a good agreement with measurements for all equations for pressures up to 200 MPa. Above this pressure the curves diverge and a good agreement is only reached with the equation of North (1.7) for pressures up to about 600 MPa and the equation from Él'Yanov and Hamann (1.9) for the whole of the pictured range (which, incidentally, is the entire region in which water is liquid at this temperature).

One reason why the theory of Owen and Brinkley shows good agreement with measurements at lower pressures is that they use the volume change and the compressibility change of a reaction at standard pressure as parameters. The volume change is proportional to the first derivative and the compressibility change to the second derivative of the curve in Figure (1.1) (see Equation (1.1)). Therefore their equation has the same slope and curvature at the intercept with the Y axis and thus it is not surprising to find a good agreement in the region where there is no strong change in the curvature. Indeed, Lown et al. [79] proved that it is possible to reach a satisfactory accuracy in this pressure range if the compressibility

is treated as being constant. The conformity of North's Equation (1.7) with the measured values is surprisingly accurate as he neglected to account for influences other than hydration. This may be partly coincidental, but could also show the huge importance of hydration on the volume change of such reactions.

The larger deviation of the curve according to Nakahara than that of El'Yanov and Hamann demonstrates that the basic principle of Born's theory fails. Nevertheless, as a phenomenological description, the equation from El'Yanov and Hamann (1.9) shows a satisfactory agreement with the measurements.

An error of around 0.5 and 1 pK -unit predicted by the equations of North (1.7) and Owen and Brinkley (1.3) respectively for the dissociation of Ammonium Hydroxide at higher pressures leads to an error on the same order of magnitude if, for example, the pOH -value of an Ammonium Hydroxide buffer is calculated using these equations. With the huge relevance of small changes in the pOH -value in many reactions, such errors can lead to a misleading interpretation of the results.

The changes of the pK -values (and also the errors in the calculations) are proportional to the volume change. While, for the example in Figure (1.1), a reaction with a large volume change was used, most equilibria are not so strongly influenced by pressure. Organic carboxylic acids, for example, mostly have a volume change of around $-14 \frac{\text{cm}^3}{\text{mol}}$ (298 K)⁴ [69] which is about half that of the dissociation of Ammonium Hydroxide ($-28.9 \frac{\text{cm}^3}{\text{mol}}$ (298 K)). Reactions in which both products and reactants have the same number (and charge) of ions can have small volume changes. An example of such a reaction is the following:



which has a volume change of $-6.8 \frac{\text{cm}^3}{\text{mol}}$ (298 K). This at first appears surprising as this reaction would seem to be another formulation of Reaction (1), but the difference in both "formulations" is the dissociation reaction of water into H^+ and OH^- , which also shows also a pressure dependency, as two ions are formed. The volume change of the dissociation of water ($-22.1 \frac{\text{cm}^3}{\text{mol}}$ (298 K)) is therefore the difference in the two reactions of Ammonium Hydroxide.

Reactions with changing Hydrogen bond- and Van-der-Waals-forces such as crystallisations, gelifications, swellings and hydrations have also often a large volume change and consequently a considerable pressure dependency.

High pressure has also an influence on the so-called hydrophilic interaction (an overview is given by Asano and Noble [69, 71]). Hydrophilic interaction means interaction between polar solvents and unpolar groups of molecules. Among the unpolar groups only *Van-der-Waals London* forces are relevant. Additionally, between polar solvents and unpolar groups, the stronger *permanent dipole-induced*

⁴An exception is found in the two smallest members in the series of linear carboxylic acids Formic acid ($-8.5 \frac{\text{cm}^3}{\text{mol}}$ (298 K)) and Acetic acid ($-11.3 \frac{\text{cm}^3}{\text{mol}}$ (298 K)) [69]. This is possibly due to the dimerisation of the protonated free acid molecules.

dipole interactions play a role. Also, in water, *permanent dipole-permanent dipole* interactions and *Hydrogen bonds* are present. All these interactions are attracting forces and therefore a volume reduction is to be expected. As previously mentioned an exception is found for Hydrogen bonds in water which form ice-like structures. Accordingly, observations such as the volume decrease when blending alcohol and water are caused more by the decrease in Hydrogen bonds than an increase in hydrophilic interactions. Or in other words: the increase in the interplay between water and unpolar groups with pressure is due to a destruction of the structure of water by hydrophilic groups causing a decrease in volume [69].

The formation and destruction of micelles from Phospholipids, for example, is also a function of pressure. This reaction is of great relevance in biology as damage to cell membranes is often responsible for the killing of microorganisms under pressure [13, 15, 16, 116, 117, 118].

There are many influences on the volume change accompanying the formation of micelles, and until now it has not been possible to estimate the degree of the individual influences. A volume increase due to the formation of micelles is to be expected due to the so called "hydrophobic interactions" discussed above⁵. The arrangement of the hydrophilic groups in a micelle is similar to that of solids and therefore potentially accompanied by a decrease in volume. The melting of hydrocarbons is normally associated with an increase in volume of approximately 10 % and a large volume change can therefore be expected for the "melting" of membranes.

Another important influence to be expected is the repulsion of like charges if the micelle is formed by molecules containing a charged group, such as the Phosphate group in Phospholipids. This repulsion causes an increase in volume due to forming micelles, particularly as it has to be seen according to the state in solution in which this group causes a volume reduction by electrostriction. The effects of destabilising micelles at pressure seem to preponderate as shown by the experiments made so far. Reactions can also be affected by pressure because of their activation volume. For example, less radical chain reactions occur at high pressure, due to the large activation volume necessary for forming radicals.

Influence of High Pressure in Biology

The study of the effects of pressure on living organisms is called barobiology. In general, gram-negative bacteria are inactivated at a lower pressure than gram-positive [120] and cells in the exponential phase are usually more pressure sensitive than cells in the log or stationary phase of growth [120, 121]. Some bacterial spores can resist pressures of more than 1 000 MPa. For inactivation of bacterial spores a combination of high pressure and temperature treatment is an efficient

⁵This is only valid for micelles containing hydrophobic groups. But with the exception of Polyoxomolybdate [119] no micelles without such groups have been described until now. For the pressure stability of Polyoxomolybdate micelles no data is available.

method [1, 122, 123]. In addition, the inducing of germinating by pressure or thermal treatment and killing the vegetative cells by a second pressure or thermal treatment is possible [124, 125, 126]. Viruses appear, as a rule, to be most resistant to pressure [121, 127, 128], though some phages are sensitive to pressures of about 200 MPa [5].

Besides food and health technology where researchers are concerned with the inactivation of microorganisms, another group of scientists are interested in the influence of pressure on living creatures. These are biologists investigating life in extreme conditions such as in deep sea (e.g. [129, 130, 131]), beneath polar ice or in deep ground strata (e.g. [132, 133]). Uwins et al. [132] found indications of life in sandstone sediments at pressures of up to 200 MPa and temperatures between 383 and 443 K.

The first barophilic bacteria from the deep sea were described in 1979 by Yananos et al. [134], and the first paper about obligatory barophilic bacteria was published in 1987 by the same authors [135]. Mammals can also cope with extreme pressures, whales being able to dive up to a depth of 3 000 m with a pressure of about 30 MPa.

In particular, the depth of the sea seems to accommodate various habitats with great biodiversity, comparable with that of the tropical rain forest. An indicator for this large diversity is that numerous new species are discovered with every new expedition to these regions (e.g. [130, 136, 131]). Besides the rich fauna and flora, the deep sea is of great interest as umpteen creatures exist there from early times of life on this planet [32, 131].

Habitats with the highest pressures can be found in deep sediments mostly below the ocean bed. Among the organisms from such sediments which can be cultured at ambient pressure are the smallest and one of the oldest forms of life which have been observed until now [132].

Biochemical changes which are caused by pressure, such as enzyme activities, influence metabolism and growth, and also genetic variances and cell division. Inhibition of cell division is thought to be responsible for filament formation at high pressure, a morphological change observed in many microorganisms. For example, at 40 MPa *Escherichia coli* grows up to 50 times the length than that at 0.1 MPa [23]. Another possible effect of high pressure is the inhibition of the availability of energy from microorganisms due to changes of the energy-producing enzymes. The denaturation of proteins at high pressure has been attributed to the pressure-induced unfolding of protein chains. Conditions for denaturation vary greatly for different enzymes.

The effect of pressure on microorganisms is a combination of the fore mentioned factors. Some changes in cell morphology can be induced which are reversible at low pressure but irreversible at high pressure. At higher pressure the death of microorganisms is believed to be caused by permeabilisation of cell membranes [13, 15, 16, 137, 138] or due to a loosened contact between the membrane surface and attached enzymes [139]. Also the inactivation of DNA [140],

ribosomes [141] or key enzymes, including those involved in DNA replication and transcription [3], are held responsible for inactivation of microorganisms.

Usually, thermal treatment leads to the irreversible denaturation of proteins [56]. In contrast, the effect of applying hydrostatic pressure of between 100 and 400 MPa to proteins is often reversible [19]. This is probably due to conformational changes and sub-unit dissociation/association processes. This phenomenon could be of practical use in controlling certain enzyme reactions [142].

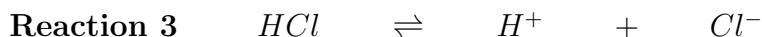
1.2 *pH*-Value

The activity of a Hydrogen ion a_{H^+} is a key factor in describing thermodynamic and kinetic properties of processes occurring in aqueous solutions. Because of the wide range over which a_{H^+} can vary it is common practice to express a_{H^+} in a logarithmic scale as *pH*:

$$pH = -\log(a_{H^+}) = -\log(\gamma_{H^+} \frac{m_{H^+}}{m_o}), \quad (1.10)$$

where m_{H^+} and γ_{H^+} are the molality (in mol/kg) and the activity coefficient of a Hydrogen ion respectively in the system. m_o is a factor to make the activity dimensionless: $m_o = 1\text{mol/kg}$. The definition of *pH* goes back to Sørensen [143] (but is there based on concentrations and without activity coefficients). There is a second "practical" definition noted in IUPAC's Manual on Physical Chemistry Definitions [144] (see also [145]), as the activity coefficient of a Hydrogen ion is an abstract quantity which cannot be measured directly. In this case, the *pH*-value is defined by an electrochemical determination (see Chapter 2) with reference to standard buffer solutions, whose *pH*-values are known.

The *pH*-value of a solution is influenced by all reactions which form or dissipate H^+ ions or change the activity of existing H^+ ions. These reactions are influenced by pressure, temperature and ionic strength. Dissociation of an acid in water is associated with a change in the number and/or the type of ions, e.g.:



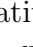

(See also Reactions (1) and (2)). As already mentioned in Chapter 1.1.2, pressure lowers the free solution energy of ions. The influence of temperature on dissociation is due to the enthalpy of both the dissociation and dissolving of the ions.

A major obstacle for studying many different technological and physicochemical processes in aqueous systems at high pressure is the lack of a reliable and generally applicable method for measuring the *pH*-value. If *pH*-values at high pressures could be accurately measured, this would greatly increase the knowledge of protolithic phenomena, including acid-base dissociation, hydrolysis, ion-pairing, solubility processes, and their associated thermodynamic properties. This would

provide the basis for the interpretation of many phenomena, mechanisms and generation of structures in fields such as food technology or microbiology.

1.3 *pH*-Value and High Pressure Food Technology

Besides the direct influence of temperature and pressure on food there are indirect effects from conductance variables such as viscosity, thermal conductivity, electric permittivity, diffusion coefficients, ionic strength and *pH*-value. All of these are influenced by pressure and temperature and all affect processes during high pressure treatment of food. This is illustrated by the interactions between pressure and *pH*-value and the influence of both on a model protein in Figure (1.2).

pH-value influences many phenomena in food technology which are also a function of pressure. For example, a protein can be denatured by pressure and also by *pH*-values which are too low or high. In Figure (1.2), a model protein is pictured with an Amino group which can be protonated. This protein can exist in two states: native (pictured  numbers ① and ③ in Figure (1.2)) and denatured (pictured  numbers ② and ④). A denaturation of the protein takes place if the free enthalpy of the denatured structure is smaller than that of the native structure. A change in the difference between the free enthalpies of both structures can be the consequence of protonation: Reaction ③ \rightleftharpoons ④ tends more to the right, as the structure stabilising interactions between the Amino group and other polar groups (here symbolised by \ominus) is smaller for the deprotonated Amino group than for the protonated. Thus the protein will be denatured by *pH*-values higher than the pK_a -values of Reaction ① \rightleftharpoons ③.

Denaturation by pressure can be caused by different phenomena (or a combination of these phenomena):

- If the volume of ② is smaller than that of ①, the equilibrium ① \rightleftharpoons ② will change according to Equation (1.1). The differences in volume of different structures of proteins in aqueous solutions are mainly a consequence of the ability of water molecules to arrange around the protein chain.
- Like ① \rightleftharpoons ②, the equilibrium ① \rightleftharpoons ③ is influenced by pressure. Here the volume difference is mainly due to the electrostriction of solvent caused by the $-NH_3^+$ group and by H^+ . This leads to a change in the pK_a -values of the Reaction ① \rightleftharpoons ③, or in other words, the *pH*-value necessary to denature the protein changes with pressure.
- Finally, the *pH*-value of the solution can change as a result of other reactions which are influenced by pressure (in the example of Figure (1.2) the reaction

of Phosphoric acid on the right hand side) and the denaturing takes place as a result of the changing pH -values.

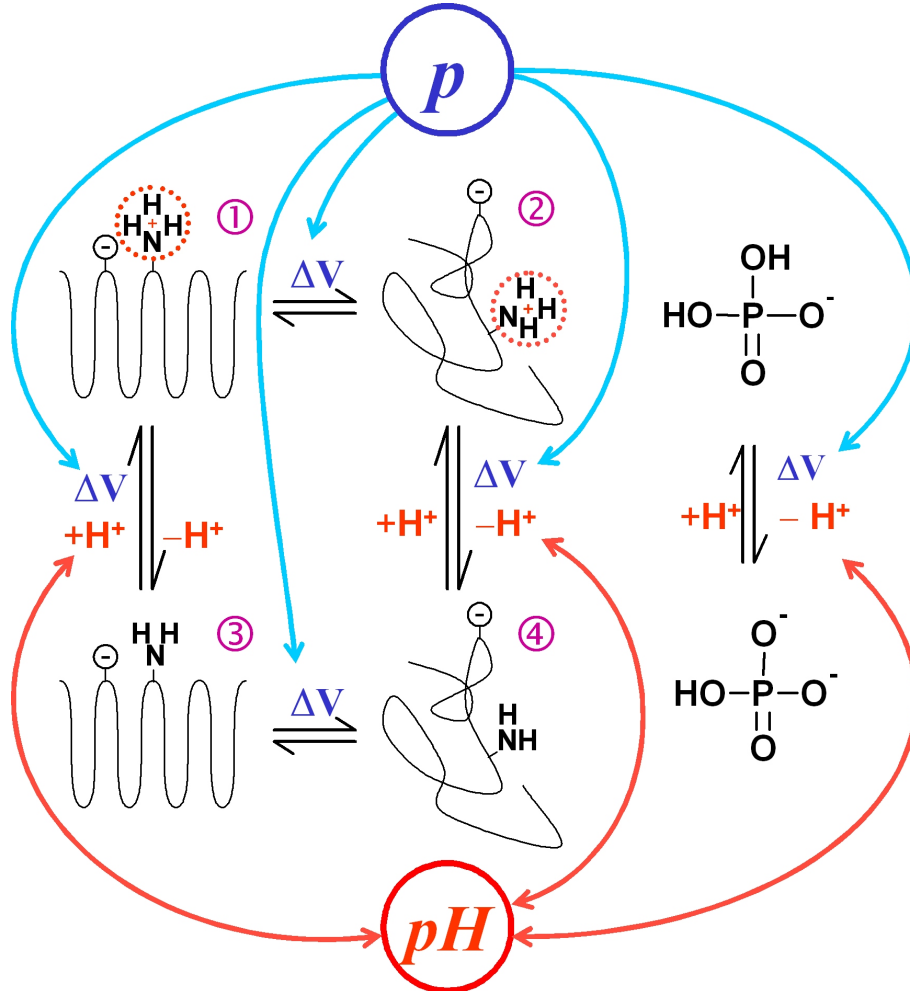


Figure 1.2: Influences of pressure and pH -values on the reactions of a model protein. The ordered wavy line (||||) symbolises the native structure of the protein which contains an Amino group. This Amino group can be protonised ① or deprotonised ③ depending on the pH -value of the solution. The denatured structure is displayed as an unordered clew (||||). In addition, the reaction of Phosphoric acid is shown as influencing the pH -value of the solution and being influenced by pressure and by the pH -value. All reactions are influenced by pressure due to their volume change, symbolised by the blue arrows. Reactions with a changing number of protons are additionally influenced by the pH -value of the solution and have an influence on the pH -value. Therefore, an indirect influence of pressure on protein reactions is possible due to its influence on the equilibrium of reactions such as that of Phosphoric acid followed by changes in the pH -value of the solution. A further indirect influence is the pressure dependency of the pK_a -values of reactions such as that of between ① \rightleftharpoons ③.

In summary, it can be said that all reactions mentioned in Figure (1.2) are directly influenced by pressure due to the volume change accompanying the reaction, but there is a second indirect influence as all reactions with a changing number of protons influence the pH -value and are in turn influenced by the pH -value.

Similar behaviour can be observed in dissolving of ions, crystallisations, gelifications, swellings, hydrations and biochemical and organo-chemical reactions. These changes influence microbiological quantities such as growth, metabolism and mortality of microorganisms and germination of spores.

This means that a change in pressure affects not only the pH -value of a solution, but also pH -sensitive reactions such as the pH -optimum of an enzyme or the pH -range in which a microorganism can exist.

High pressure food research must take into account the change of pH -behaviour of reactions such as enzyme activity and protein denaturing and also the change of pH -values with pressure. To understand the occurrences at high pressure, especially the interactions of pH -dependant reactions, it is necessary to be able to measure the pH -value at high pressure.

The build up of pressure is associated with the generation of inhomogeneities in several physical parameters such as temperature [10, 35, 36, 37, 38, 39, 40, 41, 42, 43, 146] or pH -value. The reason for this could be inhomogeneities in the composition such as in jelly with fruit pieces, where both components show different pH changes with pressure, or inhomogeneous changes of other physical parameters such as temperature which also influence the pH -value. Therefore, the question must be answered to which degree such a distribution of the pH -value can occur. Such observations have not yet been studied under high pressure.

1.4 Conceptual Formulation

The aim of this work is the development of an in-situ method for pH -measurement during high pressure treatment of food and microbiological samples. An understanding of how the pH -value behaves at high pressure would lead to a better comprehension of many phenomena observed at high pressure. As mentioned above, observations such as the coagulation of proteins can be the result of many transformations. It can be the result of a configuration with higher density or a change in the pH -value of the solution. Without the possibility of in-situ pH -determination, it would not be possible in such cases to identify the reason for such occurrences.

In choosing the optimal method for measuring pH , all systems commonly used at ambient pressure were assessed for the possibility of adapting them to high pressure.

An optical system with indicator dyes was proved to be the most appropriate. Therefore indicator dyes and spectroscopic methods will be described in detail. As such systems require calibration at high pressure and the pH -value of the buffer systems depends on pressure, calculations of the pH -changes were made.

For calibration, different chemometrical methods were studied. With the use of the PCR (Principal Component Regression), accuracies of 0.25 pH -units have been achieved.

For opaque and strongly coloured samples which cannot be measured using the described system, an adaptation of the configuration was tested with indicators fixed at the end of a fibre optic cable, or on a film attached at a sapphire window integrated into a high pressure vessel. Instead of the transmitted light, the reflected or emitted light is measured. Further benefits include an easier setup and a better protection of the indicator substances against reactions with solution ingredients such as proteins.

To estimate the influence of inhomogeneities, a setup was developed to observe the distribution of the pH -value in a high pressure cell where two solutions of different pH -values were brought into contact inside an optical cell to observe their mixing behaviour.

Chapter 2

Methods Used for Measuring pH -Value

2.1 Overview

In this section, the different ways of measuring pH -values will be introduced and divided into groups. This classification can be seen in Figure (2.1).

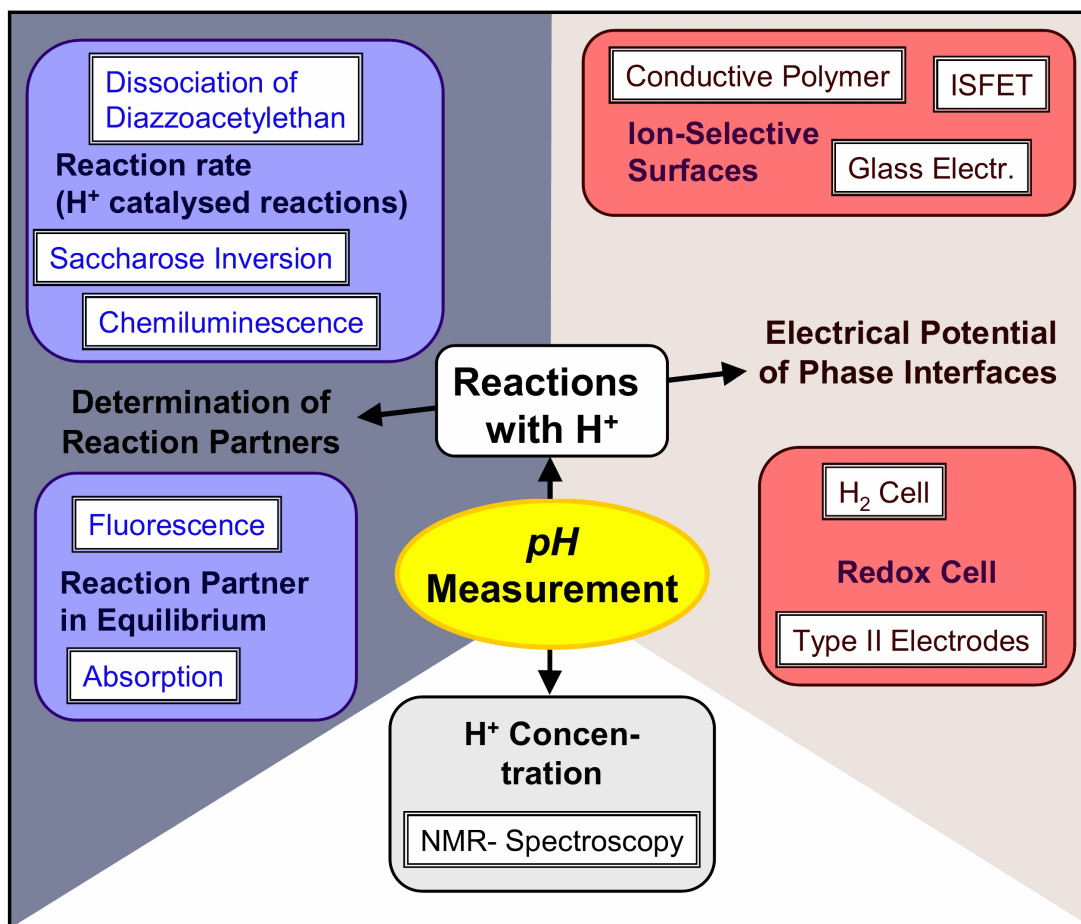
" pH " denotes the negative logarithm of the Hydrogen ion activity. Activity is an abstract thermodynamical quantity, it can only be measured by its influence on chemical reaction equilibria. The activity coefficients of a single ion cannot be determined alone as an ion cannot be observed without the presence of a counter-ion and the influences of both ions cannot be separated.

There are two ways of measuring pH -values indirectly: one is to measure the concentration of H^+ ions, neglecting the difference between the concentration and the activity, or to correct it using thermodynamical approximations. The other way is to assess quantities corresponding to a chemical equilibrium with H^+ ions. Here, equilibria are required with reaction partners which are easily detectable at low concentrations, as the reaction should not influence the activity of H^+ -ions. All systems can be calibrated using buffer solutions whose pH -values are predetermined by definition [144].

Only one publication can be found which describes a direct measurement of H^+ ion *concentrations*. Cho [147] describes a determination of H^+ concentration using NIR spectroscopy. A problem of direct measurement of H^+ concentrations is the large measuring range, due to of the logarithmic scale of pH . The pH -range between 0 and 14 corresponds with H^+ activities of 14 orders of magnitude and no measuring system can be exact over such a range¹.

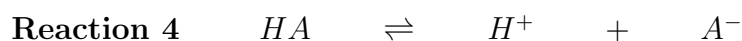
The other way of measuring pH is the determination of H^+ ion activity with suitable reactions. This should not lead to the assumption that these measure-

¹Cho described measurements of pH and pOH -values in the range between 0 and 7, but nevertheless the accuracy near the neutral point was poor.

Figure 2.1: Classification of different ways for pH -measurement.

ment systems are independent of ionic strength, as all reaction partners are influenced. Therefore, either thermodynamical corrections are necessary or reactions must be used in which the agents are mostly unaffected by ionic strength. This is the case for uncharged agents .

A reaction with H^+ can be written as follows:



where A^- is the reaction partner and HA the product, e.g. the deprotonated and the protonated structure of an indicator dye². The Law-of-Mass-Action for this reaction is:

$$K_a = \frac{a_{H^+} \cdot a_{(A^-)}}{a_{(HA)}} \quad (2.1)$$

²Here A^- is characterised to be single negative charged, but this is not generally the case. It is only necessary that HA has one elementary charge more than A .

where K_a is the equilibrium constant for Reaction (4). At least one of the species A^- or HA has to be easily detectable e.g. strongly coloured. With most methods which detect reaction partners of H^+ , *concentrations* of the *reaction partners* are determined and not the activities. Therefore Equation (2.1) must be converted to contain the concentration of the reaction partners. For the concentration of HA (c_{HA}), for example, the following equations are obtained:

$$\begin{aligned} K_a &= \frac{a_{H^+} \cdot \gamma_{(A^-)} \cdot m_{(A^-)}}{\gamma_{(HA)} \cdot m_{(HA)}} \\ &= a_{H^+} \frac{\gamma_{(A^-)} \cdot \frac{m_{\Sigma} - m_{(HA)}}{\rho}}{\gamma_{(HA)} \cdot \frac{c_{(HA)}}{\rho}} \\ 10^{(pH - pK_a^*)} &= \frac{c_{\Sigma} - c_{(HA)}}{c_{(HA)}}. \end{aligned} \quad (2.2)$$

where $c_{\Sigma} = c_{(A^-)} + c_{(HA)} \approx \text{const.}$ ³, $c_i = \frac{m_i}{\rho}$, $K_a^* = K_a \cdot \frac{\gamma_{(HA)}}{\gamma_{(A^-)}}$ and $pK_a^* = -\lg K_a^*$. The modification of K_a into K_a^* was made in order to include the activity coefficients of HA and A^- (but not that of H^+) in the equilibrium constant. K_a^* is therefore additionally a function of the ionic strength.

If the sensitivity σ is defined⁴ as the change of the analyte concentration $c_{(HA)}$ with the change of the pH -value based on the total amount of all forms of the analyte c_{Σ} , the following is obtained:

$$\sigma = \frac{1}{c_{\Sigma}} \left| \frac{dc_{(HA)}}{dpH} \right| \quad (2.3)$$

$$= \left| \frac{\ln(10)}{10^{(pK_a^* - pH)} + 2 + 10^{(pH - pK_a^*)}} \right|. \quad (2.4)$$

The detailed calculation steps which lead from Equations (2.2) and (2.3) to Equation (2.4) are itemised in Equations (5.1) in appendix 5.1.1. Figure (2.2) shows the graph of σ for Equation (2.4) in dependency of $|pH - pK_a^*|$.

As can be seen from Figure (2.2) the sensitivity decreases rapidly if the pH -value diverges from pK_a . Therefore, a measurement on the basis of reactions

³ $c_{\Sigma} = c_{(A^-)} + c_{(HA)}$ (in mol/dm³) is not exactly a constant, as the volume is a function of the composition of $c_{(A^-)}$ and $c_{(HA)}$.

⁴This definition of the sensitivity does not account for the fact that the accuracy of concentration measurements often depend on the concentration of $c_{(HA)}$. For example, the law from Lambert and Beer, $c_i \propto \ln \frac{I}{I^0}$, used for the measurements with indicator dyes, is not linear. I and I^0 represent intensities of the light passing through the sample with and without indicator, respectively. A calculation of the sensitivity of this special case is shown in appendix 5.1 (Equations (5.2) to (5.7)). But the graph in Figure (2.2) would not essentially change.

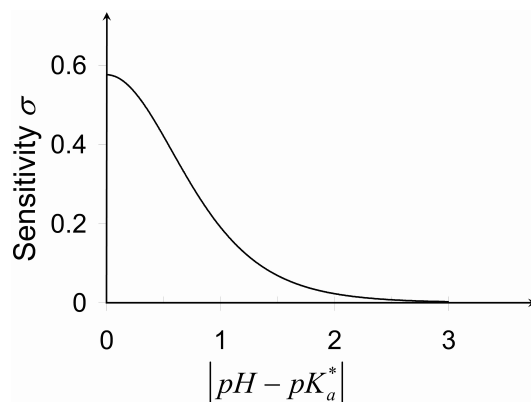


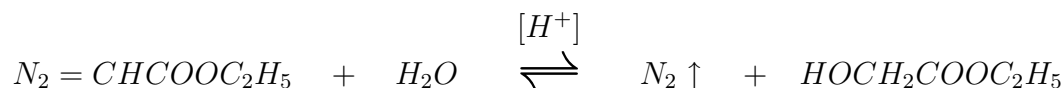
Figure 2.2: Sensitivity $\sigma = \frac{1}{c_{\Sigma}} \left| \frac{dc_{(HA)}}{dpH} \right|$ in dependency of $|pH - pK_a^*|$ (Equation (2.4)). The graph shows the changes of the concentration of a detectable analyte HA (e.g. an indicator dye) with the pH -value. Good accuracy is given with $pK_a^* = pH \pm 0.5$ to 1.

with H^+ -ions is limited in a similar way as the measurement of concentrations. While Reaction (4) itself influences the pH -value, the amount of c_{Σ} should be small compared to $c_{(H^+)}$ and $c_{(OH^-)}$ or to buffering agents. In pure water, for example, this condition is practically unfeasible. The reagent has to be easy detectable in concentrations much smaller than $10^{-7} \frac{\text{mol}}{\text{dm}^3}$. But most food and even tap water contain buffering agents in a magnitude of 10^{-3} to $10^{-1} \frac{\text{mol}}{\text{dm}^3}$. Such solutions could be measured with indicator dyes, as they are intensely coloured even in concentrations of around $10^{-5} \frac{\text{mol}}{\text{dm}^3}$.

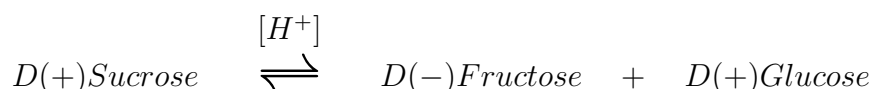
A possible way of taking measurements over the full pH -range is to use a mixture of indicator dyes, where each is responsible for a part of the pH -range. This method combines the high accuracy of measurements with indicator dyes with a large measuring range, but is also associated with a complicated data analysis due to overlapping spectra. However, due to the advances in chemometrics in the last years these problems can be solved now [148, 149, 150].

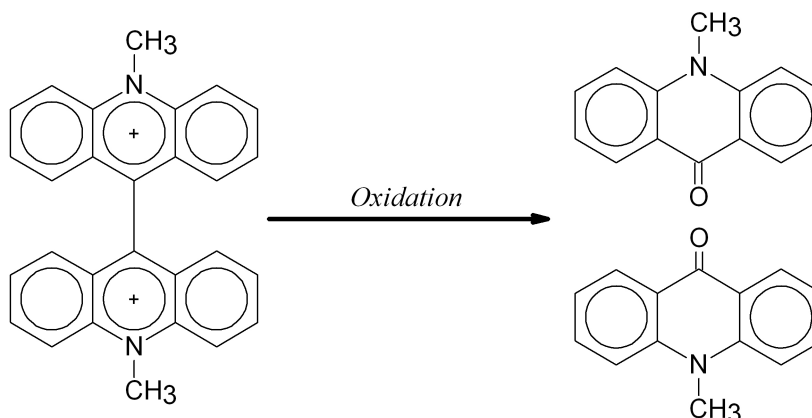
Some reactions which are catalysed by H^+ or OH^- -ions can also be used for measurement of the pH -value. Examples are the dissociation of Diazoacetylene (Reaction (5)), the inversion of Saccharose (Reaction (6)) and the oxidation of Lucigenin (Reaction (7)):

Reaction 5



Reaction 6

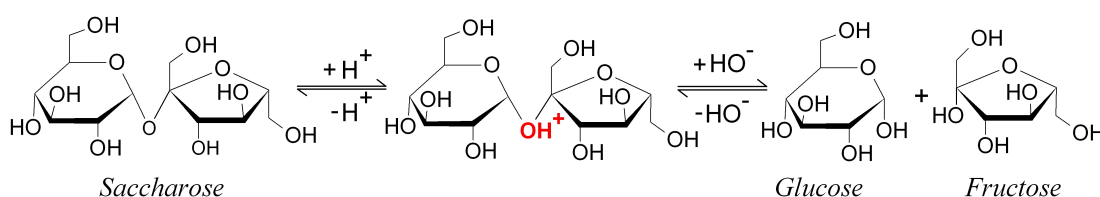


Reaction 7

The progression of Reaction (5) can be observed by the amount of accumulated N_2 -gas, that of Reaction (6) by the change in optical activity and the rate of Reaction (7) can be determined by the intensity of the luminescence. Here the reaction rate is a measure for the H^+ activity. This allows an extension of the measuring range, but the measuring time also grows exponentially.

As Nitrogen is a supercritical fluid at pressures above 3.4 MPa, it would be difficult to adapt a measuring system based on Reaction (5) to higher pressures (a possibility being to measure the accumulated gas after the pressure treatment, but dissolved Nitrogen will interfere with the equilibrium).

The adaptation of pH -measurements using Reaction (6) for high pressure was tried by some investigators (for an overview see LeNoble [151]). The measurements were not successful because they treated the reaction rate as being unaffected by pressure, but this reaction is influenced by pressure due to the charged transition state [151]:

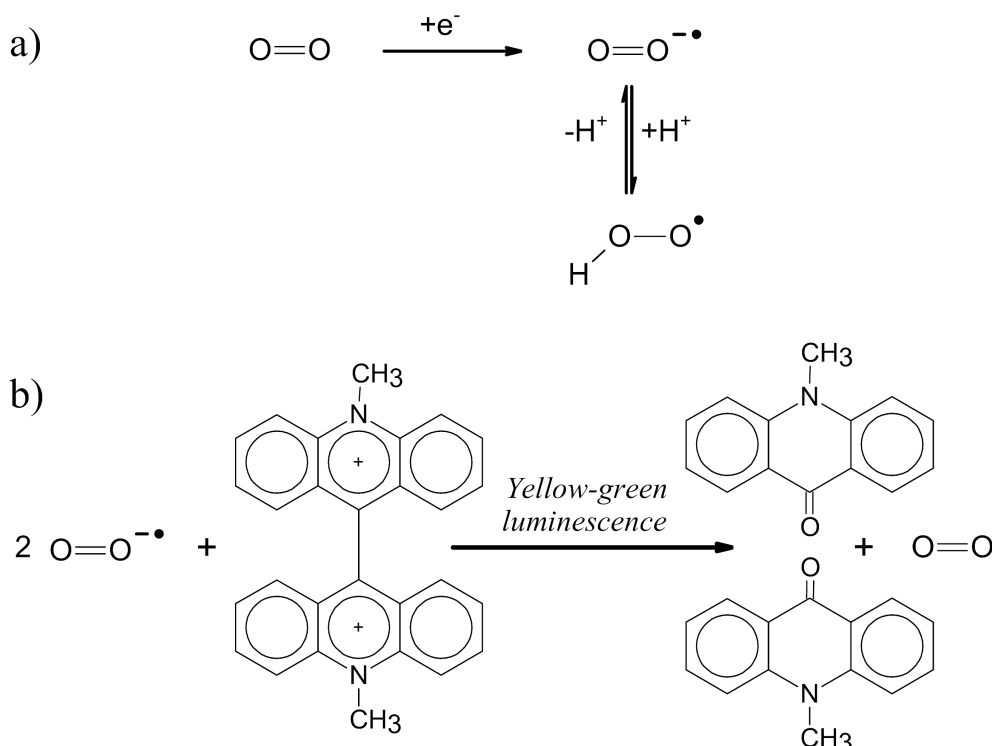
Reaction 8

But nevertheless, with a calibration at high pressure, a measurement based on this system would be possible over a limited range of pH -units.

Another reaction rate which depends on the pH -value is the oxidation of Lucigenin (Reaction (7)). Lucigenin is oxidised by the anionic oxygen radical $O = O^{\cdot -}$. This species is formed by an additional enzyme catalysed reaction (Reaction (9a)) and is in equilibrium with the Hydroxperoxyd radical. This

equilibrium is a function of the pH -value, as it is a reaction with H^+ . If an excess of Lucigenin is used, and the reaction forming the anionic oxygen radical has a constant rate, the reaction rate for the oxidation of Lucigenin is proportional to the amount of $O = O^{\cdot -}$. As Reaction (9b) is accompanied by an emission of light (luminescence) the rate is easy to detect.

Reaction 9



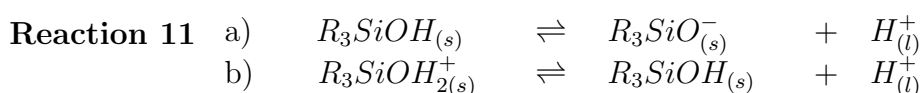
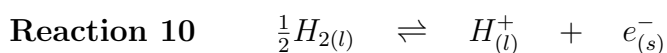
A measurement at high pressure is possible with such luminescence indicators, but a calibration at high pressure is necessary, as all concerned equilibria are functions of pressure.

Another way of measuring a large range of pH -values involves a characteristic trait of a special group of reactions: reactions with a charge transfer between two phases. This is the basis for numerous measurement methods to be discussed in the following section.

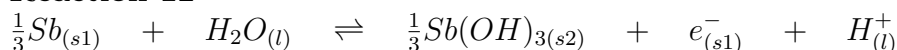
2.2 Determination of the *pH*-Value Using the Electrical Potential Difference Caused by Phase Boundary Reactions

Possible Reactions Used for Electrochemical *pH*-Measurements

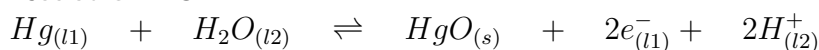
Some reactions at phase boundaries are able to transfer charge from one phase to the other (e.g. a liquid and a solid phase or two liquid immiscible phases). The following reactions will exemplify this.



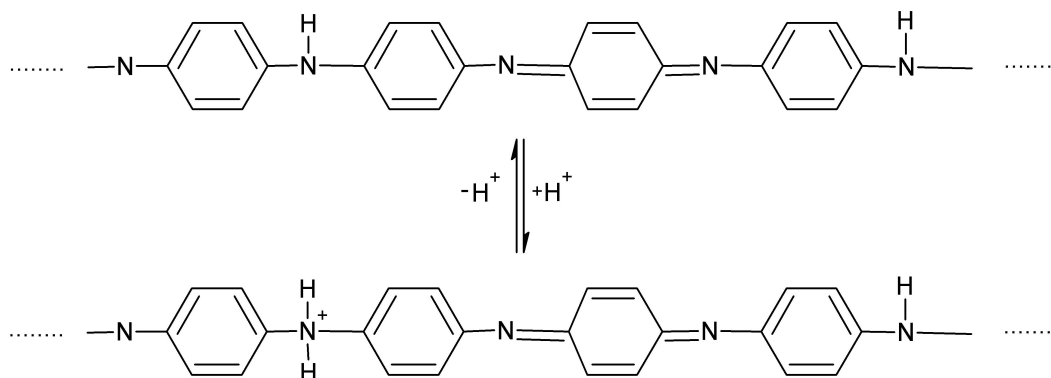
Reaction 12



Reaction 13



Reaction 14



The subscript $_{(s)}$ marks the solid phase and $_{(l)}$ the liquid. In Reaction (13) one solid and two immiscible liquid phases occur denoted by $_{(s)}$, $_{(l1)}$ and $_{(l2)}$. The analogous applies for Reaction (13) with one liquid and two solid phases denoted by $_{(l)}$, $_{(s1)}$ and $_{(s2)}$.

Reaction (10) describes an electrolytic dissociation of dissolved Hydrogen e.g. on Platinum electrodes and the Reactions (11) describe the occurrences on the surface of glass electrodes [152, 153], the most commonly used *pH*-measuring

system at ambient pressure. R_3SiOH represents a part of the glass-surface containing a Hydroxy group. Normally one of the Reactions (11a) and (11b) is predominant, depending on the pH -value of the solution and the electric potential difference between the solid and the liquid phase. If not explicitly stated, the glass-electrode is treated, for simplification, as if only Reaction (11a) would take place. Note that, in contrast to the other reactions in Reaction (11), no electrons are added or taken away. Inside the glass the electric potential is held constant by mobile ions. Similar reactions take place on the gate materials of **I**on **S**ensitive **F**ield **E**ffect **T**ransistors (ISFET) as described later.

Reactions (12) and (13) are examples of the huge variety of *metal|metal – oxide* electrodes. All of these are composed of a metal and its slightly soluble oxide or Hydroxide (the vertical dash | represents a phase interface).

Reaction (14) with reduced Polyaniline is an example of an electrode material made from conductive polymers. In addition to the electric potential, the conductivity and the colour of such polymers depend on Reaction (14) and therefore on the pH -value. Electrodes with conductive polymers as electrode material are described by Kaden et al. [154, 155] and by Jovanovic et al. [156]. The advantage of Reaction (14) is that the only reaction partners in the solution are Hydrogen ions. This leads to independence from other ingredients and from ionic strength. But until now no material has been found in which no other reactions such as ion-changing and redox reactions take place. Therefore methods based on such reactions have no practical use until now.

All of the above mentioned reactions have a similar electrochemical behaviour which will be discussed in the following section.

Calculation of the Electric Potential Difference between Phases Caused by pH -Dependent Reactions

The electric potential difference between two phases and the equilibria of reactions such as (10) to (14) influence each other. This relationship is described by the following equations as an example for Reactions (10) to (12):

$$U_{10} = U_{10}^* + \frac{RT}{F} \ln \frac{a_{H^+}}{\sqrt{a_{H_2}}}, \quad (2.5)$$

$$U_{11a} = U_{11a}^* + \frac{RT}{F} \ln \frac{a_{H^+} \cdot a_{(R_3SiO^-)}}{a_{(R_3SiOH)}}, \quad (2.6)$$

$$\begin{aligned} U_{12} &= U_{12}^* + \frac{RT}{F} \ln \frac{a_{H^+} \cdot a_{(Sb(OH)_3)}}{a_{H_2O} \cdot \sqrt[3]{a_{Sb}}}, \\ &= U_{12}^* + \frac{RT}{F} \ln \frac{a_{H^+}}{a_{H_2O}} \end{aligned} \quad (2.7)$$

where U_i is the electric potential difference between the liquid and the solid phase of Reaction (i) and the standard potential U_i^* is the value for U_i when all activities

are unity; F is the Faraday constant ($F = 96485.3415 \frac{\text{C}}{\text{mol}}$).

The activity of the pure solids $a_{\text{Sb}(\text{OH})_3}$ and a_{Sb} is constant and per definition unity. The activities of dissolved gasses (here only a_{H_2}) and of the groups on the glass surface $a_{\text{R}_3\text{SiO}^-}$ and $a_{\text{R}_3\text{SiOH}}$ are defined as follows:

$$\begin{aligned} a_{\text{H}_2} &\equiv \frac{p_{\text{H}_2}}{101300 \text{ Pa}}, \\ a_{(\text{R}_3\text{SiO}^-)} &\equiv \gamma_{(\text{R}_3\text{SiO}^-)} \frac{n_{(\text{R}_3\text{SiO}^-)}}{n_{(\text{R}_3\text{SiO}^-)} + n_{(\text{R}_3\text{SiOH})}}, \\ a_{(\text{R}_3\text{SiOH})} &\equiv \gamma_{(\text{R}_3\text{SiOH})} \frac{n_{(\text{R}_3\text{SiOH})}}{n_{(\text{R}_3\text{SiO}^-)} + n_{(\text{R}_3\text{SiOH})}} \end{aligned}$$

where p_{H_2} is the partial vapour pressure of Hydrogen and $n_{(x)}$ is the number of groups x per area of glass surface.

In Equations (2.5) to (2.7), the electric potential difference is a measure of the difference of "charge-concentrations" between the liquid and the solid phase.

Using Equation (1.10), Equations (2.5), (2.6) and (2.7) become:

$$pH_{10} = \lg \sqrt{a_{\text{H}_2}} + \frac{F \cdot \lg e}{RT} (-U_{10}^* + U_{10}), \quad (2.8)$$

$$pH_{11a} = \lg \frac{a_{\text{R}_3\text{SiOH}}}{a_{\text{R}_3\text{SiO}^-}} + \frac{F \cdot \lg e}{RT} (-U_{11a}^* + U_{11a}), \quad (2.9)$$

$$pH_{12} = \lg a_{\text{H}_2\text{O}} + \frac{F \cdot \lg e}{RT} (-U_{12}^* + U_{12}). \quad (2.10)$$

The last term $\frac{F \cdot \lg e}{RT} (-U_i^* + U_i)$ is identical for all reactions. For some reactions such as Reaction (10) (Equation (2.8)), all other terms can be kept constant (the activity of a_{H_2} can be held constant by saturation with a specific pressure of H_2). Such a behaviour is called *Nernstian*⁵. Electrodes with Nernstian behaviour have the advantage that the gradient angle in an electric potential difference/ pH -diagram depends on nothing other than the temperature⁶.

There is an interesting analogy between Equation (2.9) and the Henderson-Hasselbalch Equation (2.11) (and similarly, but not so obvious, between (2.8) and (2.11) or (2.10) and (2.11)).

$$pH = pK_a + \lg \frac{a_{(\text{HA})}}{a_{(\text{A}^-)}} \quad (2.11)$$

Reaction (11a) can be seen as an acid/base reaction with a pK_a -value dependent on the electric potential difference U_{11a} .

⁵In honour of Hermann Nernst (1864-1941), a German scientist who formulated the principles of thermodynamics from electric cells.

⁶But U_i^* is a function of pressure and temperature.

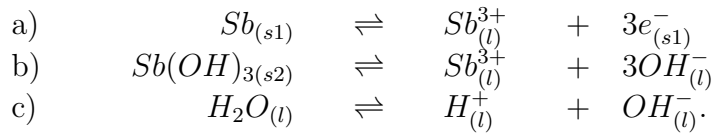
From a comparison between Equations (2.9) and (2.11) follows:

$$pK_{a(11a)} = + \frac{F \cdot \lg e}{RT} (-U_{11a}^* + U_{11a}). \quad (2.12)$$

The electric potential difference, U_{11a} , balances itself, as Reaction (11a) is followed by a charge transfer. This means a reaction with a "apparent equilibrium constant" changing with the process of the reaction. Therefore, such reactions can be used to measure across a broad pH -range. The analogous applies for Reactions (10) to (14).

Reaction (12) (and similarly Reaction (13)) seem to have Nernstian behaviour, as the change in the activity of water is in most cases negligible. But Equation (2.10) considers only the electrical potential arising from Reaction (12) and disregards the Antimony ions which dissolve. The number of dissolved Antimony ions is a result of the solubility product for Reaction (15b). To calculate the electric potential difference of a real $Sb|Sb(OH)_3$ -electrode, Reaction (12) can be divided into three parts:

Reaction 15



Even if Reactions (15a) to (15c) do not describe the actual single steps of reaction (12), the resulting electric potential difference must be the same according to Hess's law.

In the equation for the electric potential difference from Reaction (15a):

$$U_{15} = U_{15a}^* + \frac{RT}{3F} \ln a_{Sb^{3-}}. \quad (2.13)$$

the activity of the Antimony ion $a_{Sb^{3-}}$ can be expressed by the equilibrium constants K_{15b} and K_W from the Reactions (15b) and (15c) respectively:

$$pH_{15} = \lg \frac{1}{K_{15b}^3 \cdot a_{H_2O} \cdot K_W} + \frac{F \cdot \lg e}{RT} (-U_{15}^* + U_{15}). \quad (2.14)$$

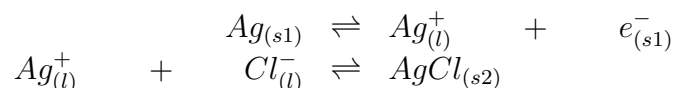
A detailed description of the computation is itemised in the appendix 5.1.1. Equation (2.14) shows that the electric potential difference of an Antimony electrode depends on the solubility of Antimony Hydroxide (Reaction (15b)) and the dissociation of water (Reaction (15c)). Nevertheless, this influence on the electric potential difference is in most cases small. Therefore the behaviour of electrodes such as $Sb|Sb(OH)_3$ are called "near Nernstian".

A near Nernstian behaviour is also observed for glass electrodes (Reactions (11)). Consequently, the activities $a_{R_3SiO^-}$ and a_{R_3SiOH} on the glass surface are nearly constant with changing pH -values (see Equation (2.9)). This is due to a

minimal change in the equilibrium (11a) which is followed by a strong change in electric potential difference. For example, a rise of 5 *pH*-units causes a decrease in electric potential difference of about 300 mV (at 101.3KPa/298 K). For a sphere with a diameter of 1 cm this change in electrical potential means a change of about 10^{-14} mol elementary charge (detailed calculations in [153]). A transformation of R_3SiOH to R_3SiO^- in this order of magnitude is in most cases small in relation to the total amount of R_3SiOH and R_3SiO^- . A further deviation from Nerstian behaviour occurs if surface reactions with different equilibrium constants take place simultaneously. For example if both Reactions (11a) and (11b) take place simultaneously or if different Hydroxy groups on the glass surface show different behaviour due to their position in the SiO_2 -structure. This causes a deviation of the slope with one inflection point in a graph U_i as function of *pH* [157].

All of the above mentioned electric potential differences are the differences between two phases. The electric potential of an aqueous solution is difficult to determine directly. For this reason in most cases a second liquid-solid reaction is used as antipole. Here, reactions which are not influenced by *pH*-value are used, e.g. Reaction (16).

Reaction 16



The amount of Ag^+ is held constant by addition of the hardly soluble $AgCl$. This reaction can take place in the same solution, but in most cases a second separate cell is used. To ensure the same electric potential in both cells an exchange of charge between the two liquids is necessary. Since charge transport in aqueous solutions is only possible with ions, it is necessary to allow an ionic migration between the two liquids. As only a small difference in the number of positive and negatively charged ions has a strong influence on the electric potential of a liquid, only a few ions are needed to migrate between the cells through small ports. Therefore only a small opening is necessary. This minimizes the pollution of both liquids by migration of ions between the cells. The viscosity of the solution in the reference cell can also be increased using a gel or a polymer resin which helps to minimize the diffusion.

The advantage of using two separate cells is that there are no additional chemicals in the test sample, such as Ag^+ , and no ingredients from the test sample can influence the reference electrode⁷. If two cells are employed, there it is possible to use the same reaction as a reference in a solution of known *pH*-value. This has the convenience that temperature and pressure affect both cells in the same manner.

⁷The electric potential difference of an $Ag|AgCl$ -electrode, for example, is influenced by Cl^- ions, heavy metals, anions forming hardly dissolvable salts with Ag^+ , such as S^{--} , and by the redox potential.

The disadvantage of liquid junctions is the appearance of diffusion potentials. A diffusion potential originates from charge separation due to different mobility of ionic species at the liquid junction between two electrolyte solutions of different type or concentration. The influence of diffusion of charged ions on the electric potential can be high. For example, the different mobility of H^+ and Cl^- and a concentration gradient of 1:10 between two HCl solutions causes a diffusion potential of 38 mV at 298 K. This leads to an error of more than half a pH -unit.

It is possible to minimize the diffusion potential by using a highly concentrated salt solution in the reference cell where the anion and the cation have nearly the same mobility (e.g. KCl or KNO_3). Therefore, the diffusion potential of both ions would be equal but with opposite algebraic sign. Due to the high concentration of the solution they will dominate the potential if the sample does not also contain mobile ions in high concentrations [158].

A possible way of avoiding the use of liquid junctions is a flow-through cell. The reference and sample solutions are fed with pumps into two tubes in which the reference and test electrodes are also fixed. After passing the electrodes the fluids are mixed to adjust their electric potential. Such cells were developed for experiments with supercritical aqueous solutions by Lvov et al. [159] and improved by Sue et al. [160, 161] enabling measurement at pressures of up to 29.8 MPa and temperatures of up to 666 K.

It must be mentioned that the diffusion potential of a liquid junction and the potential of a reference electrode are functions of pressure, as mobility of ions and solubility of $AgCl$ (if the $Ag|AgCl$ electrode is used) are also functions of pressure.

A further barrier for the migration of solutes between sample and reference is possible by using a third cell and two liquid junctions to both measuring and reference cell (see Figure (2.3a)). This so called *salt bridge* contains a highly concentrated salt solution in which the anion and the cation have nearly the same mobility (e.g. KCl or KNO_3). While such an arrangement reduces a diffusion between sample and reference cell it results in a pollution by the ions of the salt bridge.

Technical Construction of pH -Electrodes

Figure (2.3) shows some types of pH -electrodes. Hydrogen/Platinum electrodes ($H_2|Pt$) (a) are normally built as a pair of identical cells, one holding the sample solution, the other with a buffer solution of known pH -value. The two Hydrogen electrodes consist of freshly platinised Platinum surfaces⁸ in an open glass tube and are connected by a salt bridge. The junction between salt bridge and the cells is a barrier made of a porous material such as glass, ceramic, Teflon or sintered noble metal. A continuous supply of Hydrogen at a defined pressure (mostly

⁸Platinised means the electrolytic precipitation of Platinum to achieve a huge surface.

101.3 KPa) results in a constant Hydrogen activity in both cells.

When freshly prepared, $H_2|Pt$ cells are the most accurate cells, with good sensitivity and selectivity. Therefore, they are used for reference measurements, but suffer from complicated construction and handling, from redox reactions between Hydrogen and sample ingredients and from slow response as a long time is needed to reach equilibrium between the H_2 bubbles and the solved H_2 on the Platinum surface. Furthermore, the Platinum surface can become poisoned by complexing agents such as KCN , As_2O_3 , SO_2 and H_2S .

A problem in adapting this system to high pressure is the Hydrogen activity. It is not possible to maintain a constant activity by bubbling gas through the solution. Eklund et al. [162] solved this problem by pumping an external (at ambient pressure) Hydrogen saturated solution through the vessel. They described a method of measurement to obtain Henry's constant of Hydrogen up to supercritical conditions (298.15 - 723 K; 27.5 MPa) but this system can also be used for measuring the pH -value. As counter electrode a $Hg|HgO|ZrO_2(Y_2O_3)|$ electrode (described later) was used.

A simpler setup can be achieved if a Hydroquinone/Quinone mixture is used instead of Hydrogen. For such Quinhydrone electrodes, a wire of Platinum or Gold with a very small amount of Quinhydrone (an equimolar mixture of Quinone (left side in Reaction (17)) and Hydroquinone (right side in Reaction (17))), is added to the solution. As both are hardly soluble, a constant amount present in the solution is in equilibrium with the precipitation. Reaction (17a) takes place at the metal surface, resulting in a constant activity of H_2 on the metal surface. But in contrast to the $H_2|Pt$ electrode, the Quinhydrone electrode has no Nernstian behaviour. Using the same approach as for antimony electrodes the electric potential difference between solution and metal can be calculated as the electric potential difference of a $H_2|Pt$ electrode (Reaction (10)) with a H_2 activity resulting from Reaction (17b). Or in other words, Reaction (17a) can be treated as the sum of Reactions (17b) and (10). The activities from Hydroquinone and Quinone are a result of their solubility. The final electric potential difference is therefore, in addition to the pH -value, a function of the equilibrium constant of Reaction (17b) and the solubility of both species. A Quinhydrone electrode can be used in a pH -range of 0 to 9 at ambient pressure⁹. Above a pH -value of 9 the electrode accuracy breaks down, as the Quinhydrone becomes too soluble and easily oxidised. The solubility of Hydroquinone and Quinone are influenced by the ionic strength of the solution. Therefore the archived electric potential difference of a Quinhydrone electrode is also influenced by electrolytes. Nevertheless, before glass electrodes came into common use, such electrodes were customary for laboratory work at ambient pressure. Because of the pressure dependency of the solubility of Hydroquinone and Quinone and of Reaction (17a) such an electrode must be calibrated if it is to be applied at high pressure.

⁹No data is available for higher pressures.

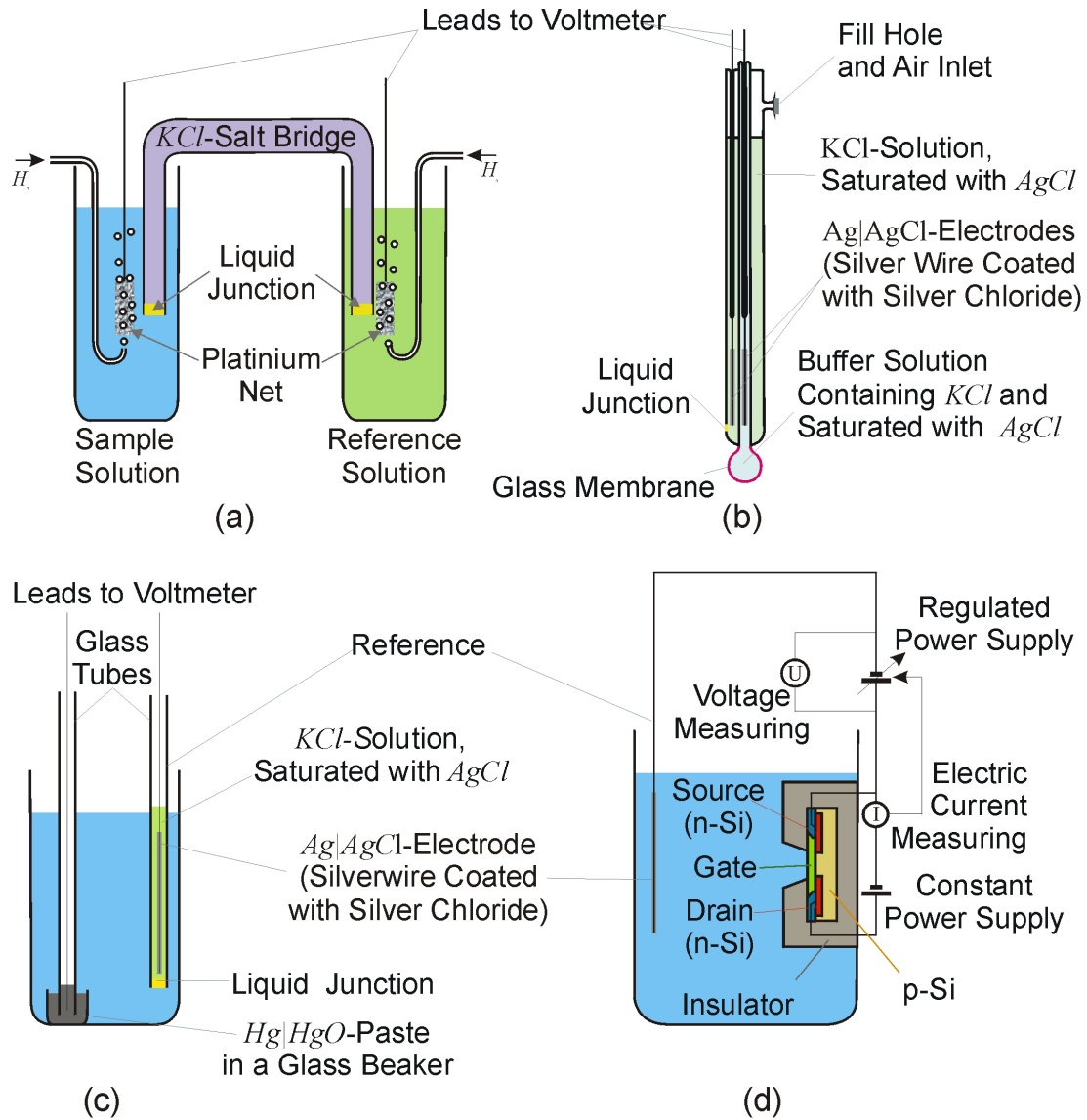
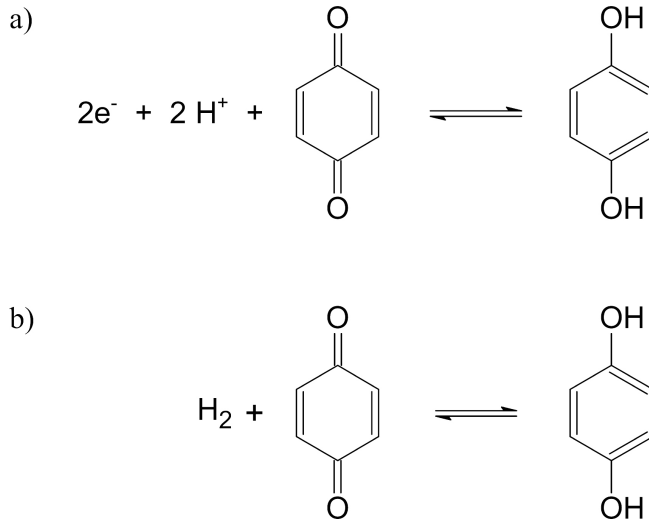
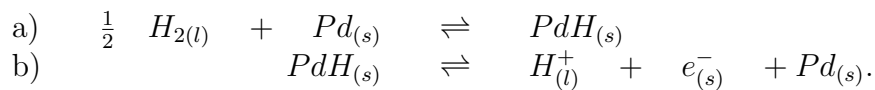


Figure 2.3: Setup using different kinds of *pH*-electrodes. (a) Hydrogen/Platinum electrode, (b) glass electrode, (c) Mercury electrode ($Hg|HgO$) and (d) ISFET. For the electrical connection between measuring and reference electrode different possibilities are shown: in (a) two identical cells are joined by a *salt bridge*, (b) and (c) have a single liquid junction and in (d) the reference electrode is placed directly in the sample solution.

Reaction 17

The reaction of a $H_2|Pt$ electrode (Reaction (10), Figure (2.3a)) can be divided into two steps. An intermediate step on the Platinum surface is the formation of Platinum Hydrid (PtH), the second the transformation to Pt , H^+ and e^- .

The same reactions happen with Palladium but here more Hydrid is formed [163]:

Reaction 18

Reaction (18a) will happen not only on the surface as Hydrogen is able to diffuse into Palladium. The interstitial in the lattice of Palladium allows a high degree of so called atomic solution in a solid. Therefore, it is possible to saturate the electrode cathodically with PdH at ambient pressure (the return Reaction (18b)). Afterwards, this electrode can be used without the need for additional H_2 . This is possible as only Reaction (18b) is linked with a change in charge and therefore only the H^+ -ions are responsible for the electric potential difference. Such an electrode was used by Macdonald et al. [164] (see also [165]) at pressures of up to 60 MPa and temperatures of up to 548 K.

To enable an electrical contact at the glass surface a metal can be coated by enamel glass. But as can be seen in Reaction (11) there are no formed or consumed electrons as found in the other reactions. Therefore, current conduction is not possible and the measured electric potential difference is a result of load attraction and rejection as in a capacitor. Enamel electrodes are used for rough industrial conditions (sometimes the complete coating of a reactor is used as an electrode) where no exact measurements are necessary.

A better electrical contact can be made by using a layer of conductive polymers between the glass and a metal surface. Ions from glass can move into or out of the polymer. By load attraction and rejection, electrons from the polymer can move between polymer and metal [154, 155].

Apart from these special cases, most applications of glass electrodes use a thin spherical glass membrane (pictured red in Figure (2.3b)), where both sides are immersed in aqueous solutions. The solution inside is a reference buffer with known pH -value. The electric potential is the same on both glass surfaces, the electric potential difference between the glass membrane and the liquids depends on their pH -value. Therefore the electric potential difference between the liquids depends on their pH -difference. These electric potentials are measured indirectly with the help of a pH independent internal element such as an $Ag|AgCl$ electrode (Reaction (16)).

$Ag|AgCl$ is the most common internal element, suitable for almost all applications. Another commonly used electrode is $Hg|Hg_2Cl_2$. Internal elements from $Cu|CuCl$ and Thalamid ($Tl|Hg|TlCl$) are also a possibility but are rarely used.

In most cases the reference electrode is separated in an additional cell by a liquid junction similar to those in $H_2|Pt$, the glass and the $Hg|HgO$ -electrodes (yellow in Figure (2.3)). Many applications for glass electrodes use combined electrodes with both half cells contained in one body as shown in Figure (2.3b). As for the $H_2|Pt$ cell in Figure (2.3a), there is the possibility of interfacing the sample solution with the reference cell by a double junction containing an electrolyte solution.

The construction of a glass electrode is easier than that of a H_2 -Platinum electrode and sensitivity, selectivity and stability are satisfactory for most applications. However, glass electrodes have several disadvantages due to the intrinsic nature of the glass membrane. For example, glass electrodes are easily affected by alkaline or HF solutions, the selectivity to alkali, silver and ammonia ions is poor at high pH -values, the fragility of glass confines their applications, they often exhibit a sluggish response and they are difficult to miniaturise.

For high pressure measurements with glass electrodes it is necessary to protect the glass membrane with a pressure balance to get the same pressure in all cells. This pressure equalisation can be realised by a membrane, an insulating fluid immiscible with water such as silicon oil [166, 168] or by moveable rubber stoppers [173, 59] or Teflon pistons [171]. The use of silicon oil was criticised by Withfield [171] because it pollutes the solutions and distorts the measurement. Measurements with glass electrodes at up to 300 MPa are described by several authors e.g. [59, 166, 167, 168, 169, 170, 171, 172, 173].

A further way to measure the electric potential of an insulating membrane is by using **Ion Sensitive Field Effect Transistors (ISFET)**. The surface consists of a small layer (gate electrode) made from a material such as Si_3N_4 , Al_2O_3 or Ta_2O_5 fixed on p-doped Silicon. This layer shows a similar behaviour to the

glass surface of a glass electrode (Reaction 11). The p-doped Silicon is enclosed by two n-doped Silicon electrodes. This electrodes are called drain (p-doped) and source (n-doped, see Figure (2.3d)). The electrical resistance between drain and source is influenced by the electric potential of the gate material. This potential depends on a reaction similar to Reaction (11) and the potential of the liquid. While Field Effect Transistors (FET) have a satisfying accuracy in only a small range of electric potential, the potential of the liquid is adjusted by a reference electrode with the help of an electric circuit. This electric circuit changes the electric potential of the reference electrode until a predetermined current between drain and source in the most sensitive range of the FET is reached. The electric potential difference measured on the reference electrode is consequently a measure for the pH -value. One of the advantages of ISFETs is the possibility to miniaturise them.

Until now, the technology of ISFETs has shown problems with the selectivity and long time stability of the gate materials. An adaptation for high pressure is in principle possible but has not been executed up to now.

A simple Antimony wire can be used as electrode, as Reaction (12) takes place when Antimony is submerged in an aqueous solution. pH -electrodes made this way exhibit problems with reproducibility and long time stability due to defects in the crystal structure of the generated $Sb(OH)_3$. This means that antimony electrodes must be compounded with a pure surface of monocrystalline Sb_2O_3 . Such electrodes are used, for example, for aggressive samples such as HF [174], in which glass electrodes corrode, or for in vivo measurements of blood and muscles [175] because of the possibility to miniaturise them. Unlike glass electrodes, *metal|metal – oxide* electrodes usually suffer from redox interference due to the fact that metal-oxides are mixed conductors, and electrons as well as ions may determine the electric potential. Furthermore, the solubility of Antimony Hydroxide is too high at pH -values smaller than about 3.

In addition to $Sb|Sb(OH)_3$ electrodes, Milazzo [182] describes electrodes made from $W|WO_3$ and $Mo|MoO_3$. Other *metal|metal – oxide* are made from $Ir|IrO_x$ [176] and $Bi|Bi_2O_3$ especially for concentrated KOH solutions [178] and $Pd|PdO$ for in vivo blood measurements [179, 180]. Fog at al. [181] studied various electrodes including $Pt|PtO_2$, $Ir|IrO_2$, $Ru|RuO_2$, $Os|OsO_2$, $Ta|Ta_2O_5$, $Rh|RhO_2$, $Ti|TiO_2$ and $Sn|SnO_2$. The results on pH -sensitivity, working pH -range, ion and redox interferences and hysteresis indicate that $Ir|IrO_2$ and $Ru|RuO_2$ are most useful at ambient pressure.

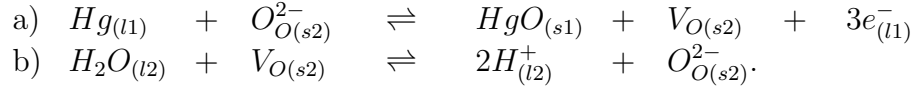
High temperature/high pressure measurements are described for $Pt|PtO_2$, $Ir|IrO_2$, $Rh|RhO_2$, $Zr|ZrO_2$ [183] and $W|WO_3$ [184] up to 523 K and 400 MPa and for IrO_2 up to 473 K and 26.6 MPa [165].

A Mercury electrode (Figure (2.3c)) is a special case of *metal|metal – oxyde* electrode because of the two liquid phases. In practical use the liquid Mercury is emulsified to a paste with the solid HgO and the reaction takes place on the Mercury surface. As the liquid Mercury is not crystalline, the electric potential

difference cannot be influenced by inhomogeneities in the lattice.

With a special construction it is possible to inhibit the solution of Hg^+ ions and therefore the solubility of HgO has no influence on the electric potential difference [185]. The $Hg|HgO$ -paste is enclosed by a Yttria-stabilised Zirconia ceramic membrane ($ZrO_2 + 9\%Y_2O_3$). This ceramic is a conductor for oxide ions because it has the crystal structure of Zirconia (ZrO_2) with some Zirconium ions being replaced by Yttrium. As Yttria (Y_2O_3) has a lower ratio between oxygen and metal, some spaces for oxygen in the crystal remain empty. These so called oxygen vacancies can be filled by oxide ions from the sample solution or from the mercury oxide on both interfaces of the ceramic. Inside the ceramic the oxygen moves by hole conductance. Whether more oxygen is moving from the aqueous solution to the $Hg|HgO$ paste or in the other direction depends on the following equilibria:

Reaction 19



where $V_{O(s2)}$ designates (in Kroger-Vink notation) an Oxygen vacancy in the Yttria-stabilised Zirconia lattice and $O_{O(s2)}^{2-}$ characterises an oxide ion in an anion site in the lattice. With this intermediate step the electric potential difference of a $Hg|HgO$ electrode is independent of the solubility of mercury oxide. Yttria-stabilised Zirconia electrodes show an "ageing" behaviour (decrease of slope and offset in the electric potential/ pH -diagram). This could be caused by surface reactions or by a further conduction mechanism with OH^- -ions. A further discussion is given in [165].

An advantage of such electrodes is the high mechanical and thermal stability of Yttria-stabilised Zirconia ceramics. Therefore, they can be used for measurements at high temperatures and at pressures of up to 40 MPa (673 K) (Ding and Seyfried [185, 186]; Macdonald et al.[162, 187, 188] up to 647 K/38 MPa). The oxide ion conduction increases with temperature [165]. This favours the above mentioned high temperature measurements, but at room temperature the membrane is almost an electric isolator which requires a complicated electric potential difference measuring device.

2.3 Determination of the pH -Value Using Indicator Dyes

There are indicators suited for many analytical fields. This work deals only with pH -(acid-base)-indicator dyes. Thus " pH -(acid-base)-indicator dyes" are here simply called "indicator dyes".

Determination of the pH -value with indicator dyes is one of the oldest measuring systems for the pH -value. As far back as 1909, Sørensen suggested using indicator dyes to distinguish between acids and bases [143]. In the years between 1915 and 1917 Lubs and Clark [189, 190, 191] reported some new indicator dye syntheses to complete a sequence of indicator dyes covering a pH -range from 1 to 14. In the following years, this series became the common way to determine the pH -value of solutions. A better accuracy was reached when spectroscopic methods were implemented.

2.3.1 Indicator Dyes

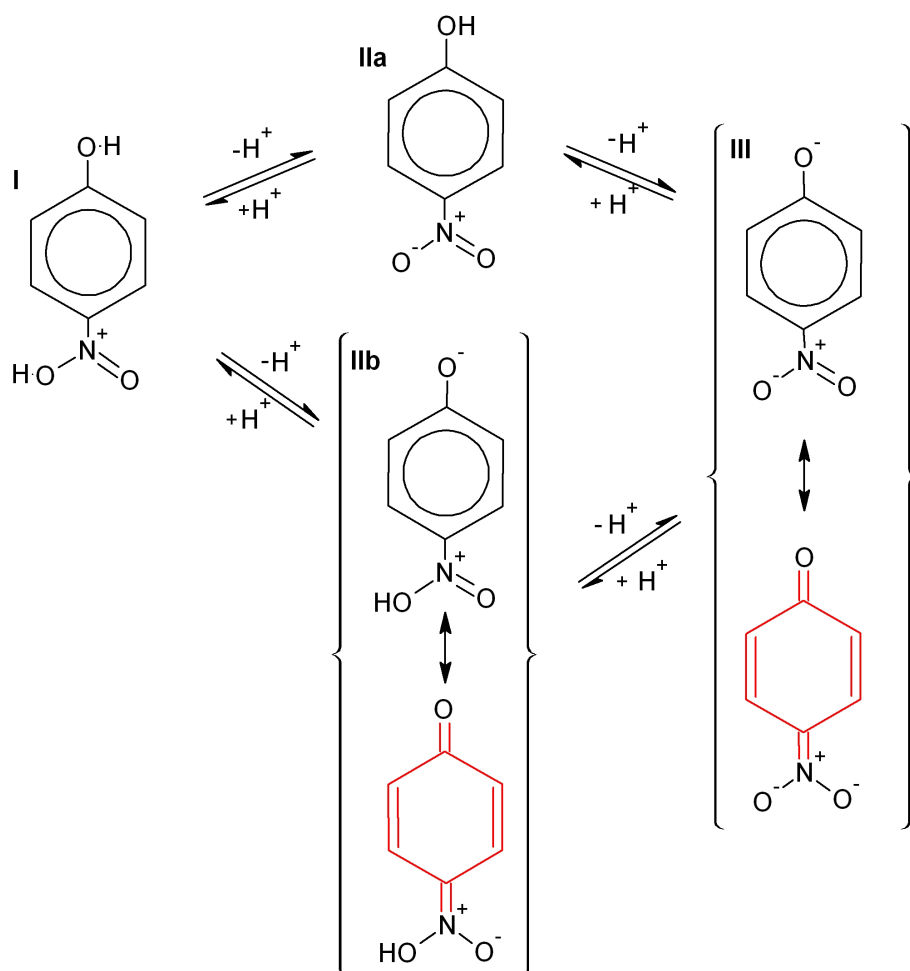
The purpose of an indicator dye is to indicate the pH -value by a specific colour. Therefore acid-base pairs are needed which vary significantly in their colour. To ensure that the influence of this indicator acid-base pair on the pH -value is minimal, the colour has to be intensive enough to be detected with small amounts. Other required properties of indicator dyes are minimal reactivity with sample components and stability against light.

The reactions of indicator dyes accompanied by a colour change will be discussed in the example of one of the simplest indicator dyes, namely p-Nitrophenol. These considerations will then be extended to cover most of the commonly used indicator dyes. The theory for following considerations is from Kolthof [192].

The acid-base reactions of p-Nitrophenol are based on a combination of the equilibria between four states of the indicator dye (Figure (20)). There is one protonated positive charged state (I on the left side of Figure (20)), two neutral isomeric states (IIa and the state marked by the two resonant structures IIb) and a deprotonated negative charged state (pictured by the resonant structures III on the right side). One of the neutral and one of the deprotonated resonant structures is quinoid¹⁰, the others are aromatic. The quinoid groups are marked red in Figure (20). As with most of the quinoid/aromatic resonance systems, states IIb and III absorb light in the visible range, appearing yellow.

¹⁰Quinoid denotes an electron configuration similar to that of Quinon; see Reaction (17) on the left side.

Reaction 20



The equilibrium between IIa and IIb is an intramolecular acid-base system between the resonance stabilized Hydroxy and the Nitro group. It tends mainly to side IIa, as the proton of the Nitro group is much more acidic¹¹. Therefore the indicator dye is colourless at low pH -values.

With the release of a further H^+ -ion, p-Nitrophenol has only the state described by the two resonance structures III. It is therefore coloured at high pH -values.

Nearly every commonly used indicator dye is based on such quinoid/aromatic resonance structures. Most of them are derivatives of two similar molecules: Phenolphthalein and Phenolsulfonephthalein. These base bodies are shown in Figure (2.4) and the possible variations caused by different substituents are given in Table (2.1). The possible reactions of Phenolphthalein are shown in Reaction (21).

¹¹The resonance stabilisation from the Nitro group decreases the pK_a value of the Phenol group from about 10 to 7, but this value is still much higher than that of a Nitro group.

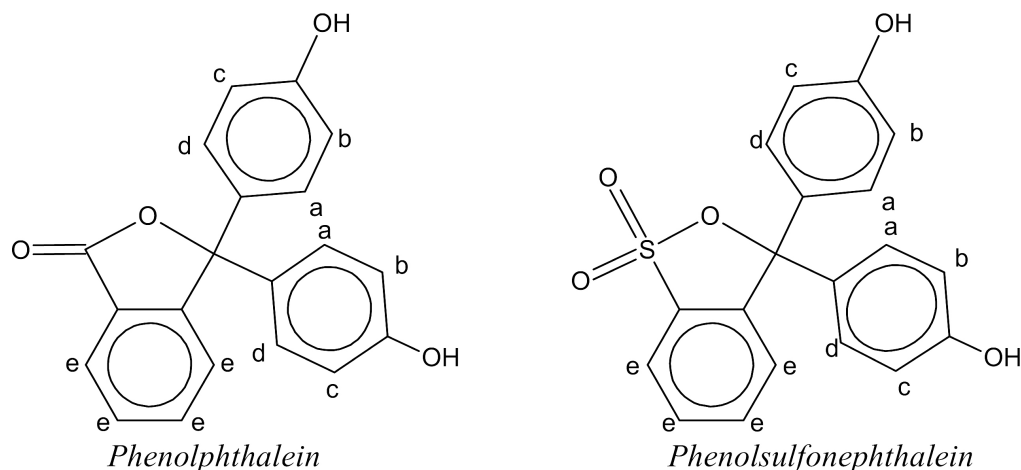


Figure 2.4: The indicator dyes Phenolphthalein and Phenolsulfonephthalein. Possible positions for substituents are marked with a letter (see Table (2.1)).

While Phenolphthalein has two Phenol groups which can react in the same way, the states Ia, IIa, IIb, IIIa and IIIb have another isomer or other mesomeric structures where the other Phenol group is quinoid or deprotonated, as indicated by the dots. Similar to Nitrophenol, every group of isomers with the same charge has a preferred state. Here it is Ic for the uncharged, IIb for the -1 charged state and IIIb for the -2 charged state. For the charge -3 only one state (III) is possible. The preferred state can change if Phenolphthalein receives substituents.

The analogous reactions take place for the Phenolsulfonphthaleins (see Figure (2.4)), but here state IIa is often more stable than IIb, and Ia more stable than Ib and Ic. Therefore, one can often find a greater number of differently coloured states at different pH -ranges for solutions of these indicator dyes. Furthermore the Phenolsulfonphthaleins are more acidic than the analogous Phenolphthaleins (see Table (2.1)).

As can be seen from Table (2.1), an increase in the number of aliphatic groups increases the pK_a -values slightly, whereas groups such as Oxygen or Halogens which attract electrons will greatly decrease the pK_a -values. Taking a closer look at the effects of alkyl substitution, it can be seen that meta- has a greater effect on the pK_a -values of the indicator dyes than ortho-substitution, that di-substitution has a greater effect than mono-substitution and that a combination of ortho and meta-substitution is more effective than di-ortho-substitution. Because of the great variety of possible substitutions with differing effects, it is possible to cover the whole range of pH -values with indicator dyes based on these substances. Most of those indicator dyes were first synthesised and described by Clark, Lubs and their co-workers [189, 190, 191, 193, 194].

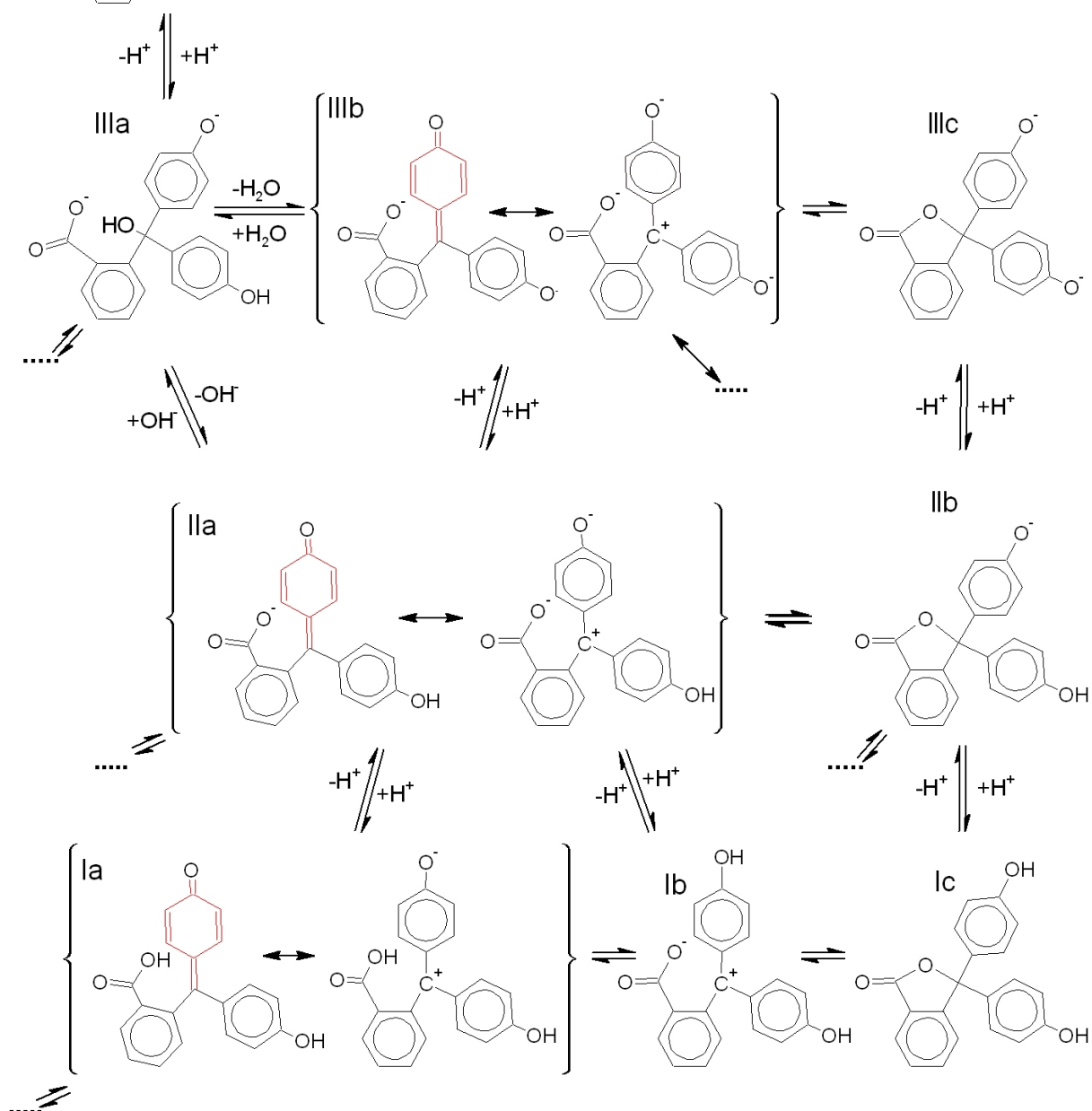
[O-]C(=O)c1ccccc1C(c2ccc([O-])cc2)C(c3ccc(O)cc3)c4ccccc4

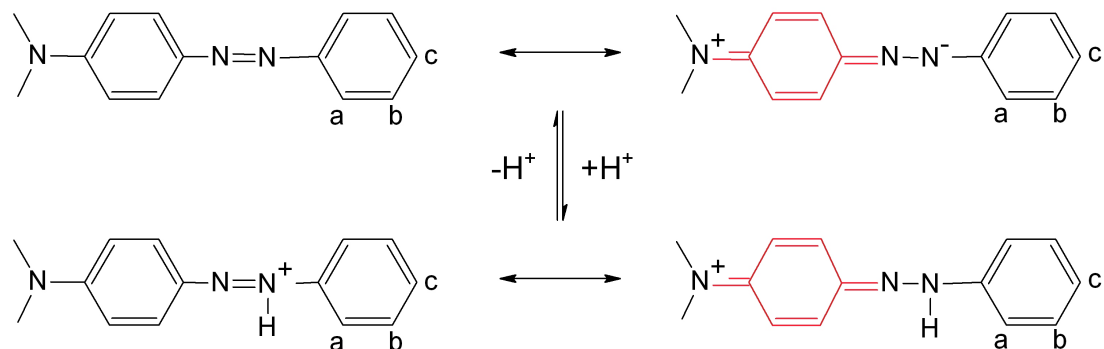
Table 2.1: Indicator dyes based on the bodies Phenolphthalein (**P**) and Phenolsulfonphthalein (**PS**) with various substituents (see Figure (2.4)).

<i>Substituent Position</i>					<i>Body</i>	<i>Name</i>	<i>pH-Range</i>
<i>a</i>	<i>b</i>	<i>c</i>	<i>d</i>	<i>e</i>			
H	H	H	H	H	P	Phenolphthalein	8-10; 12.5-14
H	H	H	H	H	PS	Phenol Red	6.5-8
CH ₃	H	H	H	H	P	Cresolphthalein	8-10
CH ₃	H	H	H	H	PS	m-Cresol Purple	1-3; 7.5-9.5
H	CH ₃	H	H	H	PS	o-Cresol Red	0-2; 6.5-8.5
CH ₃	H	CH ₃	H	H	PS	Xylenol Blue	1-3; 8-10
CH ₃	H	H	CH ₃	H	PS	2,6-Dimethyl Phenol Sulphophthalein	1-3; 7.5-9.5
CH ₃	H	CH(CH ₃) ₂	H	H	P	Thymolphthalein	9.5-10.5
CH ₃	H	CH(CH ₃) ₂	H	H	PS	Thymol Blue	1-3; 8-10
Cl	H	H	H	H	PS	Chloro Phenol Red	4.5-6.5
Cl	H	H	Cl	H	PS	Dichloro Phenol Sulphophthalein	3-5
Cl	CH ₃	H	Cl	H	PS	Chloro Cresol Green	3-5
Br	H	H	Cl	H	PS	Bromochloro Phenol Blue	3-5
Br	H	H	H	H	PS	Bromo Phenol Red	5-7
CH ₃	H	H	Br	H	PS	Bromo Cresol Purple	5-7
CH ₃	CH ₃	H	Br	H	PS	6-Bromo 2,3-Xylenol Sulphophthalein	6-8
H	Br	Br	H	H	PS	Bromo Phenol Blue	3-5
CH ₃	Br	CH(CH ₃) ₂	H	H	PS	Bromo Thymol Blue	6-8
Br	CH ₃	H	Br	H	PS	Bromo Cresol Green	4-6
H	H	H	H	H	P	Phenolphthalein	8-10; 12.5-14
NO ₃	CH ₃	H	NO ₃	H	PS	2,6-Dinitro Cresol Sulphophthalein	2.5-4.5
O ¹	H	H	H	H	P	Fluorescein	6.5-8
O ¹	I	I	H	H	P	Erythrosin B.	6.2; 5-4
O ¹	Br	Br	Br	Br	P	Eosin Yellowish	3-5
O ¹	Br	NO ₃	H	H	P	Eosin B.	1-3
O ¹	Br	Br	H	Cl	P	Phloxine B.	2-4
O ¹	Br	H	H	H	P	Solvent Red 72	5.5-7.5
O ¹	I	I	H	Cl	P	Rose Bengal	3.5-5.5
O ¹	OH	H	H	H	PS	Pyrogallol Red	1.5-3.5; 5.5-7.5

O¹: O-bridge between the two phenolic rings.

Other classes of indicator dyes are Azo-, Azine- and Triphenylmethan-dyes. As an example, the reactions of the base body of all Azodyes, Methyl Yellow (4-Dimethylaminoazobenzene), is shown in Reaction (22).

Reaction 22



Methyl Yellow is hardly soluble in water. However, by introducing polar groups into the molecule the solubility of indicator dyes in water can be increased. With a sulfonate group in position c the indicator dye Methyl Orange is obtained, and with a carboxy group in position a, Methyl Red.

The colour change of indicator dyes is mostly a consequence of a change in absorption, some fluorescence indicator dyes are also relevant (e.g. Fluorescein and Eosine B. in Table (2.1)). Some of these change both their absorption and their fluorescence spectra. This leads to a large number of measurement methods which are described in detail in Section 2.3.3.

Of less importance are chemiluminescent indicator dyes (see e.g. Reaction (7)). The reaction rate for the oxidation of the indicator dye depends on the *pH*-value. This rate is easily detectable as it is associated with the emission of light [195]. These indicator dyes are used for some applications with cloudy or strongly coloured solutions, but their redox dependence can be a problem.

A further group of indicators show no colour change but changes in their solubility [196]. These *turbidity indicators* are again acid-base pairs which are insoluble in their uncharged state, leading to opalescence or clouding. Turbidity indicators can be used for the determination of dead stops during titration processes, but the determination of the degree of turbidity is mostly too imprecise to obtain the exact *pH*-value.

2.3.2 Possible Errors in pH -Measurements using Indicator Dyes

Errors occurring during pH -measurements using indicator dyes can have three reasons: side reactions of the dyes, changes in the equilibria of the reactions with H^+ and inaccuracies in the measuring setup such as noise from the light source. In the following paragraphs the errors caused by the different possible reactions of the indicator dyes are discussed. The errors caused by the setup of the measuring instrument will be dealt with in Chapter 2.3.3.

Influence of Temperature, Pressure and Ionic Strength on the Chemical Equilibria of Indicator Dyes

Using optical methods one is able to determine the *concentration* (but not the *activity*!) of one or more states of the indicator dye. The pH -value is obtained from the concentration by the Law of Mass Action (Equation (2.2)). For the example Reaction (4) and AH as the detectable form one obtains:

$$pH = pK_a + \lg \left\{ \frac{\gamma_{(A^-)} (c_{\Sigma} - c_{(HA)})}{\gamma_{(HA)} \cdot c_{(HA)}} \right\}. \quad (2.15)$$

While the Equation (2.15) is exact, some errors result from neglecting the temperature [192, 197] or pressure [69, 80, 81] dependency of pK_a and γ_i , and from neglecting the influence of other ingredients of the solution on γ_i . Here particularly, dissolved ions play a role [158, 192, 193, 195, 197, 198, 199]. The influence of ions on the deviation of Equation (2.15) is known as the *salt error*. These errors can be avoided if the calibration takes place at the same temperature, pressure and ionic strength as the measurement. The areas in which the errors are smaller than 0.05 pH -units is roughly: $\Delta T \approx 25$ K, $\Delta p \approx 10$ MPa and $\Delta I \approx 0.05$. If the difference in temperature, pressure or ionic strength between the calibration and the measurement is great or more accurate determinations are required, thermodynamical corrections are necessary (analogous to the calculations in Chapter 3.1).

The pressure dependency of equilibrium constants is given in Chapter 1.1.2 (Equation (1.1)) and the temperature dependency is given by the following equation, which also was developed by Planck [49]:

$$\left(\frac{\partial \ln(K)}{\partial T} \right)_p = -\frac{\Delta H}{RT^2}. \quad (2.16)$$

Here, ΔH is the molar enthalpy change of the reaction, the other symbols are the same as in Chapter 1.1.2. Both ΔV and ΔH are functions of temperature and pressure. Note that for most indicator dyes several equilibria are relevant (see for example Reaction (21)).

For such calculations not many values can be found in literature. Most of the ΔV data available for indicator dyes is tabled in [69, 71]. ΔH and ΔS ($= \frac{\partial \Delta H}{\partial T}$) values can rarely be found. Kordatzki [158] lists temperature coefficients (which are proportional to the enthalpy change) for many indicator dyes and the book by Kolthof [192] contain tables with crossover areas of some indicator dyes at different temperatures.

ΔH is mostly negative and about 0 to $-10 \frac{\text{KJ}}{\text{mol}}$. ΔV depends on the charge of the indicator acid, for neutral indicator acids ($HA \rightleftharpoons H^+ + A^-$) it is always negative and about -10 to $-20 \frac{\text{cm}^3}{\text{mol}}$. Negatively charged indicator acids ($HA^- \rightleftharpoons H^+ + A^{--}$) always have a negative ΔV of about -15 to $-30 \frac{\text{cm}^3}{\text{mol}}$ and positively charged indicator acids ($HA^+ \rightleftharpoons H^+ + A$) have small volume changes ($10 \geq \Delta V \geq -5 \frac{\text{cm}^3}{\text{mol}}$).

For the correction of the influence of the ionic strength some publications contain tables with correction factors for different indicator dyes [192, 193, 200]. A correction according to the thermodynamic relations described in Chapter 3.1 requires the Debye radii of the indicator dye, but not many values are listed in literature. One exception is the early publication from Kielland [201] containing the Debye radii of the Congo Red anion (3.5 nm).

Changes in the Spectra

In addition, a change in the spectra of each form of the indicator dye can appear when the temperature or pressure is changed. For example Tsunda et al. [80] reported experiments with the indicator dyes p-Nitrophenol and Cresol Red at pressures of up to 600 MPa. They observed a small shift in the absorption bands of both indicator dyes to a higher wavelength. To avoid errors caused by such a change in spectra, again a calibration at temperatures and pressures at which the measurement takes place is necessary. These changes are small compared to the changes in pK_a so therefore a calibration is in any case sensible.

Indicator Error

Another error takes place because Reaction (4) can accept or donate protons and therefore influence the pH -value of the solution [195]. While the added amount of indicator dyes is in the order of magnitude $10^{-5} \frac{\text{mol}}{\text{kg}}$, this error is only important with weakly buffered solutions. Here again, thermodynamical corrections are possible in order to calculate the pH -value the solution would have without added indicator dye. It is also feasible to estimate the pH -value with a preliminary test and add a mixture of the indicator dye and its salt in the same composition as in a solution of the evaluated pH -value [158]. Another possibility is to work with minimal quantities of indicator dyes but at the same time with a long optical pathway through the sample [158] (see also the remarks on Equation (5.7) in the appendix).

Apart from the above mentioned points describing the influence on the equilibria, there are some reactions of indicator dyes with ingredients which can influence the results. The most important of these reactions are the interactions with proteins, alcohol and some special ions.

Protein Error

Charged forms of indicator molecules can accumulate on protein chains on groups which have the opposite charge. This influences the equilibrium between the forms of the indicator dyes, as one of them is stabilised by the bonding. Therefore the *pH*-range of the colour change can vary for some *pH*-units [143, 158, 192, 193, 195, 198]. In some cases this effect is so pronounced that the reactions between proteins and indicator dyes are used for the analytical determination of proteins (e.g. [202]). Here, the fact that only some specific proteins react with some indicator dyes is problematic. Therefore it is not possible to be sure that an indicator dye is insensitive to all proteins if it is proven only with some proteins.

Alcohol Error

The name *alcohol* error is imprecise, as this expression is also commonly used for other organic substances. The addition of organic materials to aqueous solutions can alter both the pK_a -values and the colour of indicator dyes [158, 195, 203, 204]. For measurements in such solvents, or mixtures of organic substances with water, a calibration with the same composition is necessary or a correction made according to empirical tables (e.g. in [192]). For a rough approximation, Kordatzki [158] suggested a correction of + 0.1 *pH*-units at 10% alcohol or similar organic solvents to +1.5 at 70% if the indicator acid is neutral ($HA \rightleftharpoons H^+ + A^-$). For positively charged indicator acids ($HA^+ \rightleftharpoons H^+ + A$) the required correction is smaller and has the opposite algebraic sign.

Interaction with Specific Ions

Some specific ions can react with indicator dyes in a similar way to Hydrogen ions leading to a similar colour change [195]. Examples are the indicator dye Morin (sensitive to Ga^{3+} and In^{3+}), Pyrogallol Red (sensitive to Bi^{3+} , Pb^{2+} , Co^{2+} , Ni^{2+} and rare earth metal ions) and 3-Hydroxy-2-naphtholic acid (sensitive to Al^{3+}). While such interactions are rare, the substitution of such indicator dyes with others is for the most part possible.

The reactions of all these examples can be used for the determination of the fore-mentioned metals.

Besides the reactions with dissolved ions, some interactions take place with the surface of precipitates, especially with those of the Halogenides and Pseudo-halogenides of silver. While these reactions depend on the charge of the surface

which changes at the neutralisation point, such indicator dyes can be used for the titrimetric determination of Halogenides and Pseudohalogenides with Ag^+ or the determination of Ag^+ with Br^- . Examples are Fluorescein (Cl^- , Br^- , I^- and SCN^- with Ag^+), Eosin Yellowish (Br^- and I^- with Ag^+) and Rhodamine 6G (Ag^+ with Br^-) [195].

Again, a substitution of such indicator dyes with others is the best solution for such problems.

In conclusion, it must be noted that all the above mentioned reactions with sample ingredients depend again on temperature, pressure and ionic strength. As the thermodynamical parameters for such reactions ($\Delta V, \Delta H, \dots$) are rarely known, it is once again advisable to calibrate at the same conditions as the measurement if no substitution with other indicator dyes is possible.

2.3.3 Methods for pH -Measurements using Indicator Dyes

During the first decades of the 20th century, the pH -value was determined by the comparison of the colour of an indicator dye in a sample solution with the colours of the same indicator dye in an array of buffer solutions. A similar method is still used with indicator papers and a printed colour scale.

The technological advances in spectroscopy lead to an enhanced accuracy and a simpler operating procedure. The absorbed, fluorescent or emitted light can be measured and from this the concentration of one or more forms of the indicator dye can be determined. The fraction of the different forms is a measure for the pH -value.

Methods using absorption indicator dyes are indirect methods, which means that the measured value for the *absorption* cannot be determined directly, but by the difference between the intensities of a light beam passing through a solution with and without added indicator dye.

For luminescence measurements, the absolute intensity of light emitted by an indicator dye is a direct measure of the fractions between the different forms.

Fluorescence is the absorption of light energy at a specific range of wavelengths and the emission of a part of this energy with another range of wavelengths. Because the emitted energy is lower than the absorbed energy, the absorption wavelength is higher than the emitted wavelength, the remainder of the energy being converted to thermal heat. Emission occurs after the absorption with a half-life period characteristic for the respective dye. Similar to absorption indicator dyes, fluorescence indicator dyes occur in two or more forms, whose distribution depend on the pH -value. The different forms vary in absorption wavelength, emission wavelength and half-life period. The variation in these three parameters is the reason for there being a large number of different methods, as every change can be used for a detection of the fraction between the different forms.

Some components of the measuring device can be found in nearly every setup: the light source¹², the optical system, the sample cell and the detector.

Light Source

The light source can be one that covers a large range of wavelengths (a so called broad band light source) or one emitting light at only one or a very small range of wavelengths. Examples for broad band light sources are Halogen Tungsten light sources (see Figure (2.5)); examples for small ranges are laser or Sodium vapour lamps. Additional light sources such as those with Mercury vapour or Deuterium have both: one or more strong peaks at discrete wavelengths and a band of continuous light over a range of wavelengths. LEDs have a limited range of wavelengths with a full width at half maximum of about 50 nm. Therefore, they lie between broad band light sources and sources with very small peaks. The spectra of some selected light sources are shown in Figure (2.5).

Broad band light sources are used, for example, when the whole spectra is needed or if different measurements (e.g. with different indicator dyes for selected *pH*-ranges) are made with the same setup. A simpler setup for measurements needing only one wavelength is possible if a light source can be found with only this specific wavelength, but the variety of available light sources of this type is limited. An exception is the dye-laser where a wavelength can be selected from a broad range, but such lasers are too expensive for most applications.

For fluorescence measurements, light sources with a small range at the exciting wavelength are common (most of the fluorescence indicator dyes can be excited with blue and/or ultraviolet light).

If the half-life period is to be measured, a light source with a fast response time is needed. Here, LEDs are common and some lasers can also be used. Two methods are possible: an exciting light flash and a direct detection of the emitted light decay or an alternating light exciting an emission with the same frequency but a phase shift. This phase shift is a measure for the half-life period.

Selection of Wavelength

If a broad band light source is chosen, an optical system must be used which can select the required wavelength (the same is true for light sources with more than one discrete peak). This selection can take place before and/or after the light passes through the sample. The arrangement with selection of a wavelength before the sample has the advantage that the sample is not exposed to the broad range of light energy. This energy can interfere with the sample ingredients by inducing reactions and/or inducing fluorescence. A wavelength selection before the light passes the sample cannot fully negate such interference, but can limit it

¹²An exception is found in luminescence measurements, where the light is generated by the dye.

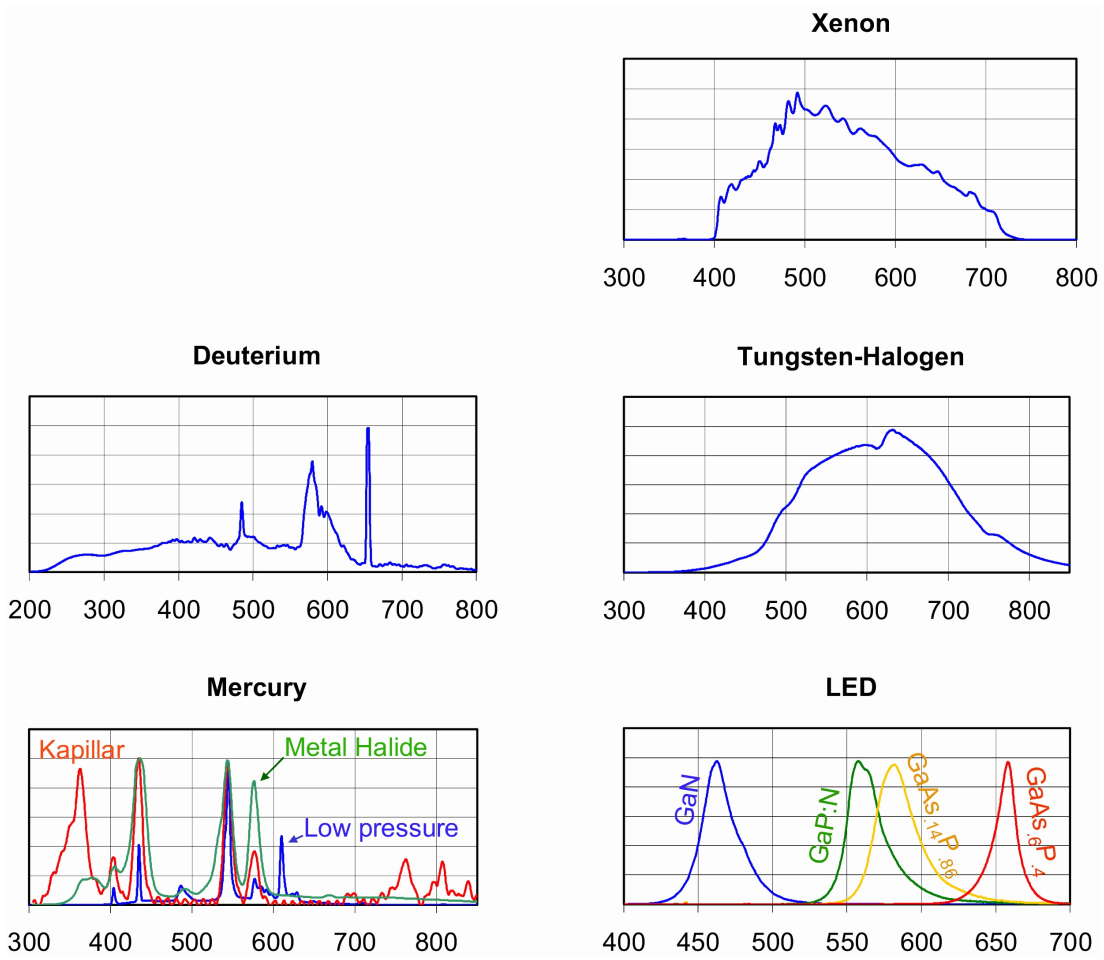


Figure 2.5: Spectra of different light sources. A Xenon light source (ILC 402B from ILC Technology, California), a Deuterium light source (Deuterium part of DH-2000-S from Mikropack Avantes, Germany), a Tungsten Halogen lamp (Tungsten Halogen part of DH-2000-S from Mikropack Avantes, Germany), three Mercury light sources (low pressure Mercury (blue): L58 W/25 from Osram, Germany for room illumination; high pressure capillar (red) (CPG 2-1 from Seefelder Meßtechnik) and a Metal Halide lamp (green) (a high pressure Mercury with added metal Halogenide to enlarge the spectra) (MHL 150 from ABV, Germany)) and four different standard LEDs. The spectra of the metal Halide and the capillar Mercury lamp were taken from the spectrometer MMS1 from tec5; all other spectra were taken with a SQ 2000 #1-UV2-L2-SLIT-50 from Mikropack Avantes. The intensity at the Y-axis is a value proportional to the electrical current from the detector, it depends on the light intensity, the sensitivity of the sensor at this wavelength and the properties of the optical fibres and is normalised for all spectra. Both spectrometers used have Si-sensors with low sensitivity in the UV-range which accounts for the low readings at low wavelength. Note that there are different ranges on the X-axis.

to reactions and fluorescence excitings caused by light at the selected wavelength. The interference of fluorescence can be eliminated by using two optical systems which select the same wavelength before and after the sample. A selection of the wavelengths only after the sample is sensible only if a detecting system is used in which all wavelengths are determined at the same time.

Three systems are commonly used to select the wavelength: filters, prisms and gratings. The easiest setup is with filters and a variation is possible by using a set of interchangeable filters. Also available are *linear variable filters* in which the wavelength which is allowed to pass through depends on the place on the filter (see Figure (2.6)). Here the wavelength can be adjusted by moving the filter in a slide carrier with a slit.



Figure 2.6: Picture of a linear variable filter (Type LVF from Ocean Optics). This filter is positioned in a carrier with a variable slit. The position of the slit on the filter determines the wavelength, the width of the slit determines the range of wavelengths.

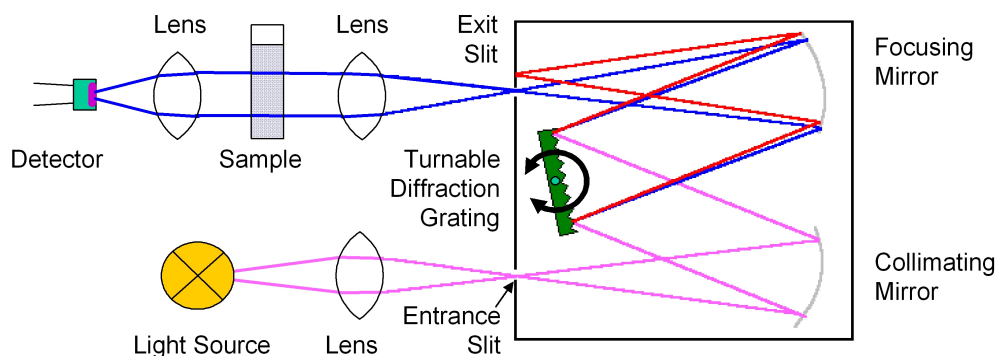
The filters normally consist of a glass plate coloured with dyes. Also used are interference filters. Interference filters consist of multiple thin layers of dielectric material which have different refractive indices (mostly metallic layers). Interference filters are wavelength-selective by virtue of the interference effects that take place between the incident and reflected waves at the thin-film boundaries.

By using prisms and gratings it is possible to select a wavelength by changing the angle between the light beam and the prism (or grating). Prisms and gratings are used in a similar way (see Figure (2.7)): the light is aligned parallelly. This beam passes through the prism or grating (or is reflected by the grating) and is split into different colours. The wavelength can be chosen by the position of the slit. The width of this slit has to be chosen as a compromise between light intensity and width of the wavelength range. For organic dyes –like indicators– with broad peaks it is better to use broad slits. It is almost the same compromise with the width of the inlet light beam: the smaller the light beam, the better the dispersion, but the lower the light intensity.

The selection of the wavelength can be made by moving the slit or by moving the prism/grating. The latter is the common way as it makes it possible to obtain a light beam from the optical system which does not change direction. To obtain a spectra the whole range has to be scanned. Therefore such instruments are called *scanning spectrometers*.

Another possibility is to detect the whole range of wavelength at once. Advances in micro-electronics allow the ordering of a linear array of up to 2048 photodiodes on one microchip. This microchip can be placed in the position where the spectra is to be mapped. A picture of such an arrangement can be seen in the upper part of Figure (2.7).

a) Scanning Spectrometer



b) Diode Array Spectrometer

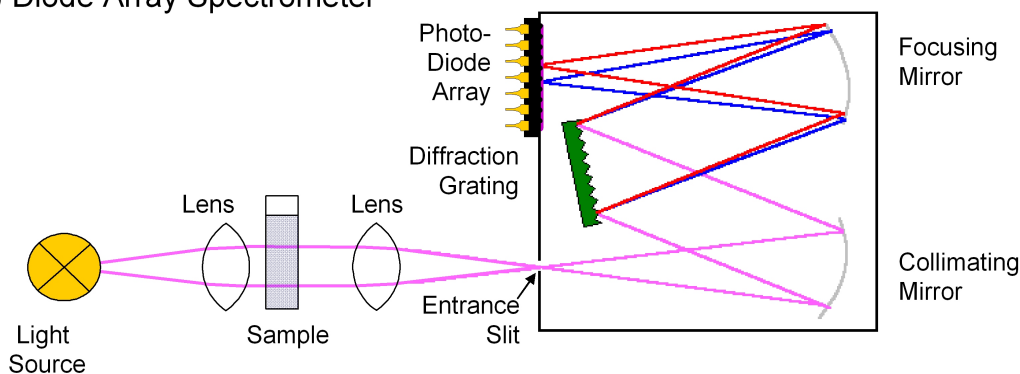


Figure 2.7: Schematic setup of an absorbance spectrometer with grating monochromator; (a): scanning version with rotatable grating, (b): version with diode array detector.

The main advantage of such an array is the possibility of faster measurements. If the light is intense enough, it is possible to measure the whole spectra in less than one second. A further benefit is that no moveable parts are included, enabling a very small and robust setup which avoids elaborate fine mechanics to position the prism or grating.

Detectors

Different types of photodiodes and phototransistors are commonly used as detectors. As they are small, robust and cheap elements they have displaced the former commonly used tubes. For very low light intensities photomultipliers are useful with which even single photons can be detected, but for measurements using indicator dyes it is easier to provide adequate light from a strong light source. Photodiodes are reverse-biased semi-conductor diodes which become conductive when illuminated. Photons provide the energy to raise electrons from the valence band (filled orbitals) to the conduction band (unfilled orbitals) creating an electron - hole pair, causing an increase in conductance. The energy of the stimulating photons must be in the same order of magnitude as the distance between valence and conducting band. Therefore every type of material for semiconductors can be stimulated by photons in a specific range of wavelength. Table 2.2 lists the different materials used for photodiodes and the range of wavelength in which they can be used.

Table 2.2: Materials for photodiodes and their useable wavelength range.

<i>Detector Type</i>	<i>Wavelength Range [nm]</i>
Si	200 - 1100
Ge	400 - 1800
GaAs	500 - 850
InGaAs	800 - 1600
InAs	1000 - 3800
InSb	1000 - 7000
InSb	1000 - 5600
HgCdTe	1000 - 25000

While the stimulation of electrons in order to raise them from the valence band to the conducting band can be by thermal energy, a better signal-to-noise ratio is reached when the detectors are cooled.

Phototransistors are a combination of a photodiode and a transistor in one component. It is made by placing a photodiode in the base circuit of an NPN transistor with the result that the current flowing through the diode is directly amplified by the transistor (see Figure (2.8)). Therefore, a phototransistor is much more sensitive to light.

To enhance the range of the photo detectors it is possible to connect the photodiode (or the phototransistor) to a capacitor. This so called **Charged Coupled Device (CCD)** detector stores the charge passing through the photo element. At the end of a controlled time-interval (integration time), the remaining charge on

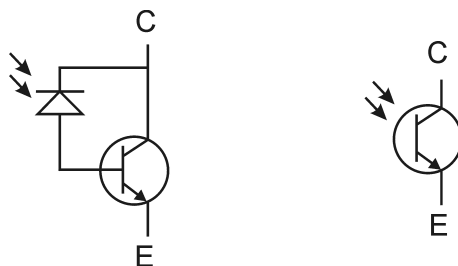


Figure 2.8: Phototransistor, Connecting Diagram and Symbol.

the capacitor is transferred to a buffer and this signal is then transferred by an AD converter. CCD detectors have an enormous dynamic range limited only by the dark (thermal) current of the photodiode and the speed of the AD converter.

Optical Pathway

The light path can be conducted through the instrument only by lenses and mirrors as pictured in Figure (2.7). A minimum of optical components means also a minimum of sources of error. But for complex sample cells, such as those for high pressures and/or high temperatures, optical fibres are used. The use of optical fibres is based on the phenomenon of total internal reflection. The fibres consist of two materials with different optical densities. A core with higher optical density is surrounded by a cladding of lower refractive index (see Figure (2.9)).

Incidental light is transmitted through the fibre if it strikes the cladding at an

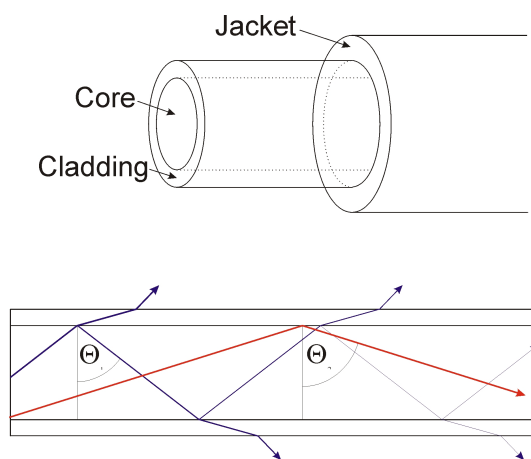


Figure 2.9: Multimode optical fibre: setup and pathway of two light beams with different angles. If the angle Θ is smaller than the critical angle, total reflection takes place (red beam). Otherwise a part of the light exits the fibre (blue beam). The jacket has no optical function, but is used as mechanical protection.

angle greater than a critical one, so that it is totally reflected by the core/cladding interface. Most fibres are covered with a protective jacket which has no effect on the wave-guiding properties.

While all common methods for measurements with absorption and luminescence indicator dyes are similar, a variety of methods using fluorescence indicator dyes exist. Indeed, Gottwald wrote in his book about spectroscopy [205] that in fluorescence spectroscopy nearly as many possible methods are known as there are scientists working with them, and even for the small domain of pH -measurements with fluorescence indicator dyes several different methods are described. These will be introduced in the following section.

Methods for pH -Measurement Using Fluorescence Indicator Dyes in Solution

In contrast to absorption measurements where the light passes through the sample cell, fluorescence measurements use mostly an angle other than π between the light from the primary source and the detected fluorescent light. This is to avoid superposition of the signal and the primary light source. Most common is an angle of $\frac{\pi}{2}$. Another difference with absorption measurements is the use of two monochromators, one before and one after the sample cell or the use of a light source with a limited range.

Reasons for the diversity of methods are the possible variations in both the change of the wavelength of stimulated and emitted light and the possibility to detect intensities and half-life periods. The basic principle of the different methods with fluorescence indicator dyes are:

1. Measurement of the change in light intensity at a fixed emitted wavelength with one fixed exciting wavelength.
2. Measurement of an emission spectra with a fixed exciting wavelength. The spreading of the light into different wavelengths as a measure for the spreading of the different forms of indicator dyes contains less sources of error than measuring the intensity of one fixed wavelength.
3. Variation of the exciting wavelength and measurement of the change in intensity at a fixed wavelength.
4. Variation of the exciting wavelength and measurement of the changes of the emission spectra.
5. Alternating intensity of a fixed exciting wavelength and measurement of the phase angle of the emitted light. This value is a measure for the half-life period and less sensitive to interferences.

Method 1 has the simplest setup with satisfying results when suitable indicator dyes are used. Fluorescein for example shows strong changes in the emission when excited with blue light (intense yellow-green fluorescence in neutral and alkaline solutions and no fluorescence in acidic solutions).

Variation of the exciting wavelength (Method 4) is sensible if the different forms of the indicator dye vary in the absorption wavelength. But this method is chosen primarily if the indicator dye has two fluorescence mechanisms, one of them being independent from the *pH*-value. Here, the fluorescence at the exciting wavelength which is not influenced by *pH*-value is a measure for the amount of indicator dye in the path of the light beam. The ratio of fluorescence between two exciting wavelengths is therefore a measure for the fraction between the protonated (or deprotonated) form and the sum of both forms of indicator dye. This procedure is useful if there are difficulties in adjusting the amount of indicator dye. It is used, for example, to measure the internal *pH*-value of microorganisms (see for example [13]). In this case, the method used to insert the indicator dye into the cells is not precise and leads to a varying amount of indicator dye in the single cell. Furthermore, the number of microorganisms in the light beam can vary. While the intensity of the emitted light is strongly affected by these fluctuations, the ratio of the fluorescence at the different wavelength is not influenced.

If the whole emission spectra is taken instead of the intensity at one wavelength (Methods 2 and 4) interferences can be identified if, for example, the form of the peak is not as expected. Furthermore, properties such as the area below a peak are less susceptible to noise than if the intensity at a single wavelength is used. There is also the possibility to detect the fluorescence spectra of both forms of the indicator dye if there is a dye with different fluorescence spectra for the different forms.

A variation in decay time (Method 5) can be the result of different reasons which are discussed below.

A detection of the *pH*-value from the decay time of one fluorescence indicator dye would be possible if both forms of the indicator dye emit light with different excited-state lifetimes, but such indicator dyes are rare. Furthermore, the decay time of most fluorescence dyes is a matter of nanoseconds. Thus sophisticated and expensive instruments are required.

An influence on the decay time can be recorded using a combination of a *pH*-insensitive lumiphore (fluorescence or phosphorescence dye) with a long lifetime (in the order of magnitude of 1 ms) and a *pH*-sensitive quencher [206, 207]. This *pH*-sensitive quencher is nothing more than an absorption indicator dye with an absorption spectra similar to the emission spectra of the fluorescence dye. Energy transfer takes place without the emission of a photon if an excited fluorescence dye has contact to an absorption dye. This is more likely to happen with lumiphores which have longer excited state lifetimes. For a detailed mathematical description see [206]. Errors can occur because the probability of a collision of the fluorescence

dye and the quencher is, in addition to their concentration, a function of viscosity and temperature. Furthermore, there are also other molecules which can quench the lumiphore, primarily oxygen.

The third possibility is to use a pair of luminophores with different decay times and similar excitation spectra [208]. A pH -insensitive phosphorescence dye with short lifetime (a few μs) is combined with a fluorescence pH -indicator dye with a lifetime of a few ns . The reference phosphorescence dye gives a constant background signal (black in Figure (2.10)) while the intensity of the fluorescence signal of the indicator (blue) depends on the pH -value. The phase of the exciting LED is nearly the same as that of the indicator dye because of its short excited-state lifetime. The average phase shift, Φ_m , as a combination of both signals (red) directly reflects the intensity of the indicator dye and, consequently, the pH -value.

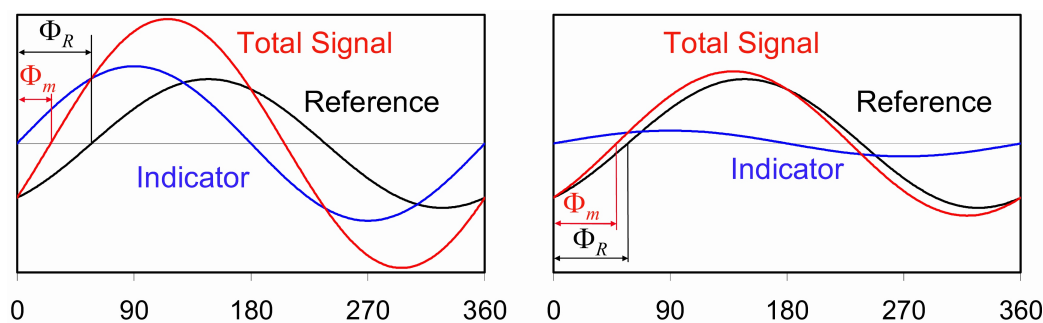


Figure 2.10: Phase shift of the total luminescence (Φ_m , red), the reference (Φ_R , black) relative to the exciting light (which is nearly in phase with the fluorescence of the indicator dye ($\Phi \approx 0$, blue)). Left graph: the indicator dye is in the form with intense fluorescence. Right picture: indicator dye is in the form with weak fluorescence [208].

Methods of pH -Measurements Using Immobilised Indicator Dyes

To avoid interactions between sample ingredients and indicator dyes, to be able to measure strongly coloured and/or cloudy samples and to simplify the measuring device, optical sensors (optodes) have been developed in which the indicator dye is immobilised on a window in the sample cell or on an optical fibre (see Figure (2.11)).

The light does not have to pass through the sample, it interacts only with the immobilised indicator dye then is reflected on the interface between immobilising matrix and sample and exits with a similar pathway as it arrived. Therefore, if the indicator dye is immobilised on the interface, the interaction between sample and indicator dye takes place at this interface.

If the immobilising matrix contains the indicator dyes the H^+ and the OH^- -ions must be able to diffuse into it. As it is rarely possible to find materials which

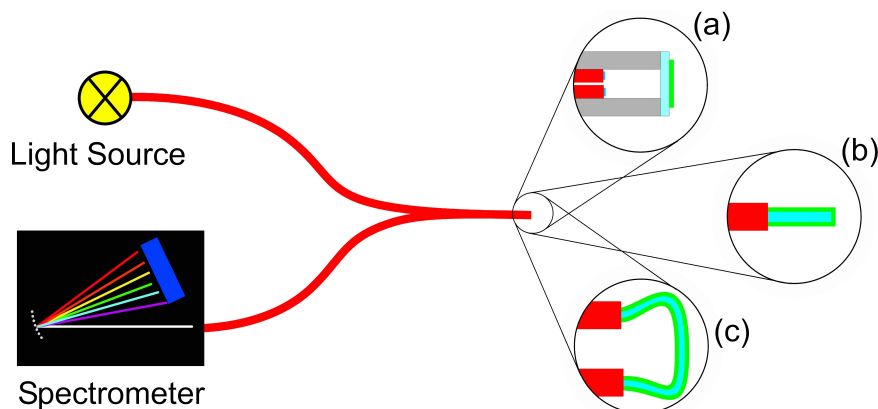


Figure 2.11: Possible setups for measuring devices with pH -optodes. All have in common a light source and a light detector connected to the optode by optical fibres (red). In version (a) a tube (grey) with a glass window coated with the immobilised indicator dye (green) is used. Both fibres are fixed in the tube (it is also possible to use a bundle of fibres for the connection to the detector wrapped around the fibre from the light source). The tube can be filled with air or an optical material like Silica and the window can be inclined to avoid interfering reflections. In versions (b) and (c) indicator coatings directly on the fibre are used. Since in (b) this fibre ends in the sample a beam splitter is necessary. In version (c) the indicator is coated on a de-cladded part of the fibre. The light passes this sensitive part of the fibre and is fed to the detector. Devices like (a) are described by [211, 213, 217, 226, 227], (b) by [219, 220, 221, 228] and (c) by [214, 215, 216, 218].

have a total reflection on the interface between immobilising matrix and sample this method leads to a loss of light. To solve this problem an additional reflective layer such as a thin metal film made from vacuum-metallisation or reflective particles can be used, but they reduce the required diffusion of H^+ and OH^- -ions. If fluorescence indicator dyes are used, the reflection must be minimized to ensure that mainly the light emitted by the dye is thrown back.

The difficulty when making optodes is to find an immobilising matrix which is permeable enough for a fast diffusion of H^+ and OH^- -ions from the sample to the indicator dyes, but which is impermeable to the dye and sample ingredients such as proteins. Further requirements are an adequate adhesion on the fibre (or window), optical transmittance and, depending on the application, the possibility to clean and sterilise the sensor. A detailed overview of optodes is given by Wolfbeiss [207], recent developments are reviewed by Lin [209].

Materials for the immobilising matrix are polymers such as Polyacrylamides [210], ion-exchange resins [211, 212, 213] and Sol-gels [214, 215, 216, 217, 218, 219, 220, 221]. Most promising is the immobilisation using Sol-gels, particularly as all other materials fail to retain the dye in the matrix. An overview of immobilising with Sol-gel is given by Wolfbeiss et al. [222] and Lin and Brown [223].

***pH*-Measurements Using Indicator Dyes at High Pressure**

Spectroscopic measurements of *pH*-values at high pressure have been described by several authors. Neumann et al. [81] and Tsuda et al. [80] used only one indicator dye at a time in standard solutions of a selected buffering agent with the purpose of extracting the acid-base ionisation constant that describes the chemical equilibrium at pressures of up to 650 MPa. Hayert et al. [224] described a similar system for pressures of up to 250 MPa. They used a fluorescent indicator dye, neglecting the pressure dependency of its dissociation constant. Lippard and Jost [225] used the indicator dye Alizarin Yellow to observe fast reactions corresponding with a *pH*-change at pressures of up to 150 MPa. Similar experiments were described by Grant [229] for pressures of up to 300 MPa. In order to measure the *pH*-value of seawater at depths of up to 9 km Hopkinsa et al. [230] described the pressure behaviour of the indicator dye Thymol blue. Hamann and Linton [231] determined the dissociation constants of various Phenols by their absorption spectra at pressures of up to 200 MPa, finding among them some Phenols which can be used as indicator dyes (e.g. Phenolphthalein).

2.4 Comparison of the Different Methods

In principle, several of the above described methods are applicable at high pressure. All of them have advantages and disadvantages. Table (2.3) summarises the pros and cons of the different methods.

For every method based on electric potential difference there is the possibility to choose between a reference element (e.g. $Ag|AgCl$) directly inside the sample or separated by a liquid junction. A reference element inside the sample gives a better accuracy and easier setup, but stronger interactions with sample ingredients. Therefore, in Table (2.3), rows are listed for all these systems both with and without a liquid junction.

Most of the methods which give a satisfying accuracy need a difficult setup. Glass electrodes which usually comprise of three cells need pressure equalisation between all cells. Further difficulties are caused by the fragile glass membrane which has to be fixed and sealed. Thus, an elaborate and error-prone setup and large volume is necessary. But a large volume is rare in high pressure applications. Nevertheless, if these problems are solved, the glass electrode offers a satisfying accuracy and marginal interactions with sample ingredients.

Pressure balance between cells is a necessity for all methods based on electric potential difference if a separated reference cell with liquid junction is to be used. Without such a liquid junction, the electric potential will depend, apart from the *pH*-value, on the molality of other ions (for example Cl^- if a $Ag|AgCl$ reference electrode is used directly inside the sample). The molality of Cl^- can be determined by additional analytical methods, which are laborious but lead to

Table 2.3: Advantages and disadvantages of the different methods for the determination of pH -values and their adaptability to high pressure. $Me|Me_nO_m$ summarises all Metal|Metal oxide sensors, except Mercury which has an additional line ($Hg|HgO$) due to its different behaviour. All methods which deal with electric potential differences are listed with and without a liquid junction (labelled LJ). The rating ranges from ++ for very positive characteristics to - - for very negative ones. *Complication of Setup* deals with the difficulties which occur when building the setup; *Complication of Processing* denotes the difficulties a laboratory worker would have while measuring. *Interaction System→Sample* describes reactions in which the measuring device interacts with the sample e.g. a reaction of H_2 with sample ingredients for a $H_2|Pt$ -cell and *Interaction Sample→System* describes errors in the pH -value caused by the interference with sample ingredients e.g. the alkaline error for glass electrodes. *Width* deals with limitations caused by properties of the sample e.g. the inability to measure nontransparent media with absorption indicator dyes.

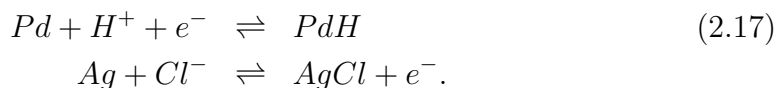
Method	Reaction	Figure	Complication		Interaction		Width	Accuracy	pH -Range
			of Setup	of Processing	System ↓ Sample	Sample ↓ System			
Glass Electrode - - + LJ	11		-	++	±	+	-	++	++
		2.3 b	- -	++	++	+	++	±	++
ISFET - - + LJ		2.3 d	++	++	±	-	++	-	+
			±	++	++	±	++	- -	+
$Me Me_nO_m$ - - + LJ	12		++	++	-	- -	++	++	++
			±	++	±	-	++	±	++
$Hg HgO$ - - + LJ	13		-	-	±	±	+	++	++
		2.3 c	- -	-	++	++	++	±	++
$Pt H_2$ - - + LJ	10		- -	- -	-	-	±	++	++
		2.3 a	- -	- -	±	±	±	+	++
$Pd H_2$ - - + LJ	18		++	++	±	±	±	++	++
			-	-	+	+	±	+	++
Chinhydrone - - + LJ	17a		++	++	-	±	±	-	+
			±	++	±	++	±	- -	+
Sucrose Inv.	6		++	++	-	±	-	++	- -
Absor./Fluor. Indicator Dyes	20, 21	2.7	++	++	++	-	-	++	++
Luminescence Indicator Dyes	9		++	++	±	±	±	±	-
Immobilised Indicator Dyes	20, 21	2.11	±	++	++	++	++	±	++

a good accuracy. Another possibility is a correction using the difference of pH -values detected at ambient pressure with both a commonly used glass electrode and the high pressure measuring system without a liquid junction.

Further problems are caused by the influence of Ag^+ -ions on the sample. As the molality of Ag^+ is fixed by the solubility of $AgCl$, the redox potential is predetermined. Furthermore, even small amounts of Ag^+ can influence microorganisms by inhibiting important enzymes. Something similar also occurs with other reference electrodes, as all commonly used reference electrodes contain chlorides of heavy metals (see Chapter (2.2)). The problem with heavy metal contamination is also an issue with commonly used measuring electrodes, as most of them are made from heavy metals and their oxides (see Chapter (2.2)). But if all of these interactions can be avoided or allowances made, a system such as $Ir|IrO_2|sample|AgCl|Ag$ would be the easiest setup as the IrO_2 and $AgCl$ can be electrochemically made directly onto Ir or Ag wires, and as an adaption to high pressure only two electrical connectors to the high pressure vessel are necessary.

A system based on a $Hg|HgO$ electrode will have all of the above mentioned advantages and disadvantages of Metal|Metal oxide electrodes but a better accuracy as there is no influence of a crystal lattice. But the setup and measurement with a high pressure system containing an interface between sample and liquid mercury would be difficult. In addition, routine work with such a measuring device would be more problematic due to safety regulations for working with mercury.

The complexity of the most accurate $H_2|Pt$ electrodes is only warranted for experiments where the highest accuracy is required. The possibility to saturate Palladium electrodes with Hydrogen at ambient pressure allows a measuring routine with moderate operating expense and excellent accuracy, but, like the metal|metal oxide electrodes, problems are caused by the reference electrode and by side reactions (here, above all, the reduction of sample ingredients with Hydrogen). As with a $Ir|IrO_2|sample|AgCl|Ag$ electrode, an easy setup is possible for a $PdH|sample|AgCl|Ag$ electrode. The electrodes can be prepared before the measurement by using diluted HCl in the sample cell and applying voltage to force the following reactions:



In this way both electrodes will be reconditioned in one step. Additional work is necessary as Palladium electrodes must be coated electrochemically once in a while with new Palladium layers to ensure a large surface¹³.

Quinhydrone electrodes allow for the same easy setup. It is not necessary to prepare the electrodes, but the presence of Quinon and Hydroquinon allow

¹³Electrochemically secreted Palladium forms porous, spongy distributed structures.

some additional side reactions, leading to both inaccuracies and influences on the sample.

The setup for most optical systems is easy, as high pressure cells with sapphire windows are readily available and optical components such as light sources, spectrometer, optical fibres, lenses and polariser are available as construction kits. Exceptions are the methods using immobilised indicator dyes which are discussed below.

Sucrose inversion (see Reaction (6)), in which the rate is proportional to the Hydrogen ion activity, has an excellent accuracy with weak acid concentrations, but the reaction becomes too fast with low pH -values and very slow with high pH -values leading to inaccuracies or a long measuring procedure respectively. Interference is possible from other reactions which cause a change in optical activity at high pressure or by mechanisms for the decomposition reaction of saccharose other than Reaction (8) e.g. by enzymes. The addition of saccharose also leads to a modification of the sample, particularly with regard to microorganisms for which it is a foodstuff, can have baroprotective characteristics [232, 233, 234], and can also be an inhibitor due to its influence on osmotic pressure.

As with the saccharose inversion, single indicator dyes give good accuracies in only a small pH -range, but the huge variety (especially of absorption indicator dyes) makes it possible to find dyes for every pH -value and mixtures of dyes for every possible pH -range. The influence of the indicator dyes on the sample is small due to the small concentration used and the low reactivity of the dyes. Problems can only occur with unbuffered solutions and the influence of the alcohol used to dissolve the dyes. But unbuffered solutions are rare in food science, and if interference with alcohol occurs there is the possibility to dissolve the dyes directly in the sample. More difficult to compensate for is the influence of sample ingredients on the dyes, e.g. protein errors, which are discussed in Chapter 2.3.2. Hence a good knowledge of sample ingredients is required to avoid or to correct such errors. If the sample is non-transparent or intensely coloured at wavelengths used for the detection, measurements with absorption indicator dyes are impossible. Even so, for cases in which these problems can be avoided or corrected, there is the possibility of an easy setup and a measuring procedure with a satisfying accuracy.

Fluorescence and luminescence indicator dyes have a somewhat larger application range than absorption indicator dyes as the sensitivity to turbidity and coloured ingredients is less troublesome as the light emitted near the surface can be detected. While several indicator dyes are available for fluorescence measurements, not many luminescence indicator dyes are known. This luminescence indicator dyes are usually associated with a redox reaction which can interfere with other redox reactions in the sample. Therefore, both a disruption of the measurement by sample ingredients as well as an influence of the oxidant on the sample can occur. Thus, measurements using luminescence indicator dyes are less suitable than those using fluorescence or absorbance dyes.

One possibility of avoiding most problems concerning measurements with indicator dyes is the immobilisation of the dyes in a matrix, ideally only permeable for H^+ and OH^- -ions. Here, a method to immobilise the indicator dyes inside a window of an optical cell or on an optical fibre leading to a high pressure cell must be developed. Such a setup can lead to breakages if linked materials have different compressibilities. Linked materials with which such problems can occur are the window and the immobilising matrix, reflecting materials and dye-binding materials in the immobilising matrix and core, the cladding and the immobilising matrix if the fibre is fed into the vessel. Further development is necessary as immobilising techniques which ensure long term stability are not fully developed even at normal pressure.

To recap, it can be said that there is no possibility of making an explicit decision in favour of one method as all of them show their advantages and disadvantages, but measurement with indicator dyes seems to be the best compromise between setup, accuracy and interferences.

Therefore the choice was made to use an optical system with absorption indicator dyes. A mixture of indicator dyes was used in order to cover the whole range of possible pH -values of food.

Furthermore, some preliminary tests were made with immobilised indicator dyes due to their better width and fewer interactions with the sample.

Chapter 3

Performance of Experiments

3.1 Calculation of the pH -Value of the Calibration and Validation Buffer Solutions

The choice was made to use a system in which calibration takes place at the same pressure as the measurement. The pH -value of buffer solutions varies with pressure due to their equilibrium constants and activity coefficients changing. This chapter describes the method used for calculating these pH -values at high pressure. These calculations can be divided into three parts: the method of calculating the equilibrium constants, the method of calculating the activity coefficients and the path of calculations to account for the interactions of equilibria and activity coefficients and the interaction of multiple reactions if an acid such as H_3PO_4 , which can form several bases, is used as buffer.

Equation (1.1) (Chapter 1.1.2) is the basis for the calculation of the changes in the equilibrium constant. It can be converted and integrated to give:

$$pK_a = pK_a^o + \frac{\lg e}{RT} \int_{p^o}^p \Delta V(p) dp. \quad (3.1)$$

In order to solve this equation, the pressure dependency of the volume change ΔV must be known. This pressure behaviour is discussed in Chapter 1.1.2. As is shown there, Equation (1.9) from Hamman and Él'Yanov [96] shows the best agreement with experimental data.

A good approximation for activity coefficients as a function of ionic strength and temperature is the early equation from Debye and Hückel [235]

$$\lg \gamma_i = -\Omega \cdot (\epsilon T)^{\frac{3}{2}} z^2 \cdot \frac{\sqrt{I}}{1 + \frac{\Lambda}{\sqrt{\epsilon T}} r_i \sqrt{I}}, \quad (3.2)$$

with the coefficients $\Omega = 1.82 \cdot 10^6 K^{-\frac{3}{2}}$, $\Lambda = 503 \frac{\sqrt{K}}{nm}$, the Debye radius r_i of the ion

i , the number of elementary charges z_i of the ion i , the density ρ of the solution and the dielectric permittivity of the solvent ϵ .

The definition of the ionic strength I is:

$$I = \frac{1}{2} \sum_{i=1}^{N_{ions}} \frac{c_i \cdot z_i^2}{c_o} \quad (3.3)$$

where c_i is the concentration of the ion i , $c_o = 1\text{mol/dm}^3$ and z_i is the number of elementary charges of an ion.

Equation (3.2) is based on a theory from Born [102] and has been well proven at ambient pressure and temperature and ionic strengths of up to about 0.5. For higher ionic strength the values obtained using Equation (3.2) are smaller than experimental data, as the approximation of Debye and Hückel neglects the ability of ions to arrange themselves with a lower energy level. Equation (3.4), which shows a better agreement with measured data, is an extended form of the Debye Hückel equation incorporating an empirically determined term linear in I [236]:

$$\lg \gamma_i = -\Omega \cdot (\epsilon T)^{\frac{3}{2}} z^2 \cdot \frac{\sqrt{I}}{1 + \frac{\Lambda}{\sqrt{\epsilon T}} r_i \sqrt{I}} + CI. \quad (3.4)$$

The additional constant C has a value of 0.2. As the term CI becomes very small in comparison with $\Omega \cdot (\epsilon T)^{\frac{3}{2}} z^2 \cdot \frac{\sqrt{I}}{1 + \frac{\Lambda}{\sqrt{\epsilon T}} r_i \sqrt{I}}$ if the ionic strength is small, both Equations (3.4) and (3.2) become almost the same with an ionic strength smaller than 0.5. Therefore Equation (3.4) is valid for the full range of ionic strength used here.

While Equation (3.4) shows a good agreement with measurements at ambient pressure it fails when applied to higher pressure [237].

Hamann [237] found the best agreement with measurements for the change of γ_i with pressure using the following equation¹:

$$\ln \gamma_i(p) = \ln \gamma_i^o + \sqrt{\frac{\rho(\epsilon^o)^3}{\rho^o \epsilon^3}}. \quad (3.5)$$

Hamann found no reason why Equation (3.5) shows a better agreement than (3.2) and (3.4). Note that the influence of the ionic strength is determined by the activity coefficient at ambient pressure γ_i^o . This value can be obtained by Equation (3.4). A combination of the Equations (3.4) and (3.5) results in:

$$\ln \gamma_i(p) = -\Omega \cdot (\epsilon^o T)^{\frac{3}{2}} z^2 \cdot \frac{\sqrt{I^o}}{1 + \frac{\Lambda}{\sqrt{\epsilon^o T}} r_i \sqrt{I^o}} + CI^o + \sqrt{\frac{\rho(\epsilon^o)^3}{\rho^o \epsilon^3}}. \quad (3.6)$$

¹He found a better agreement for the equation: $\gamma_{(H^+)}\gamma_{(A^-)}(p) = \gamma_{(H^+)}^o\gamma_{(A^-)}^o \cdot \exp\left\{\frac{\Delta V^o(p-p^o)}{RT(1+b(p-p^o))}\right\}$ [231], but with this equation one gets only values for ion pairs. b and ΔV^o are the same as in Equation (1.9).

The equations describing the change in equilibria (2.1) and those describing the influence of ionic strength (3.6) are connected to each other, as Equation (2.1) contains the activity coefficients and the ionic strength which are used in Equation (3.4). This equation depends on the ionic reactions described by the equilibrium constants from Equation (2.1). An iterative computation was considered to be the best solution.

The following values must be known:

- The pH -value of the buffer solution at ambient pressure (here measured with a glass electrode).
- The ΔV° and pK_a -values at ambient pressure for all reactions.
- The equilibrium constant K_W and the volume change ΔV_W° for the dissociation of water.
- The sum of the molalities $m_{\Sigma,B}$ of all components of the buffering agents (in the example of Phosphoric acid:
 $m_{\Sigma,PO_4} = m_{H_3PO_4}^\circ + m_{H_2PO_4^-}^\circ + m_{HPO_4^{2-}}^\circ + m_{PO_4^{3-}}^\circ$)
- The Debye radii r_i of all involved ions.

Figure (3.1) shows the flow schema for the iterative calculation.

The molality of H_3O^+ at ambient pressure is calculated by the pH -value and the activity coefficient $\gamma_{H_3O^+}$ at normal pressure. The calculation of the pH -value at high pressure is based on the changes of the pK_W and the pK_a -values and the balance of H_3O^+ ions. The balance of H_3O^+ ions is considered by the following equations:

$$\Delta H_{A_l}^+ = \sum_{j=0}^J j \cdot m_{H_j A} - \sum_{j=0}^J j \cdot m_{H_j A}^\circ \quad (3.7)$$

$$0 = \sum_l^L \Delta H_{A_l}^+ \quad (3.8)$$

where $\Delta H_{A_l}^+$ is the number of moles of H^+ per kg solution changing with all reactions of the acid $H_J A$ and J is the number of H atoms in the acid. The number of involved acids is L and the corresponding index is l ($l = 1, 2, \dots, L$). Water is treated like an acid. The sum of the all changes must be zero.

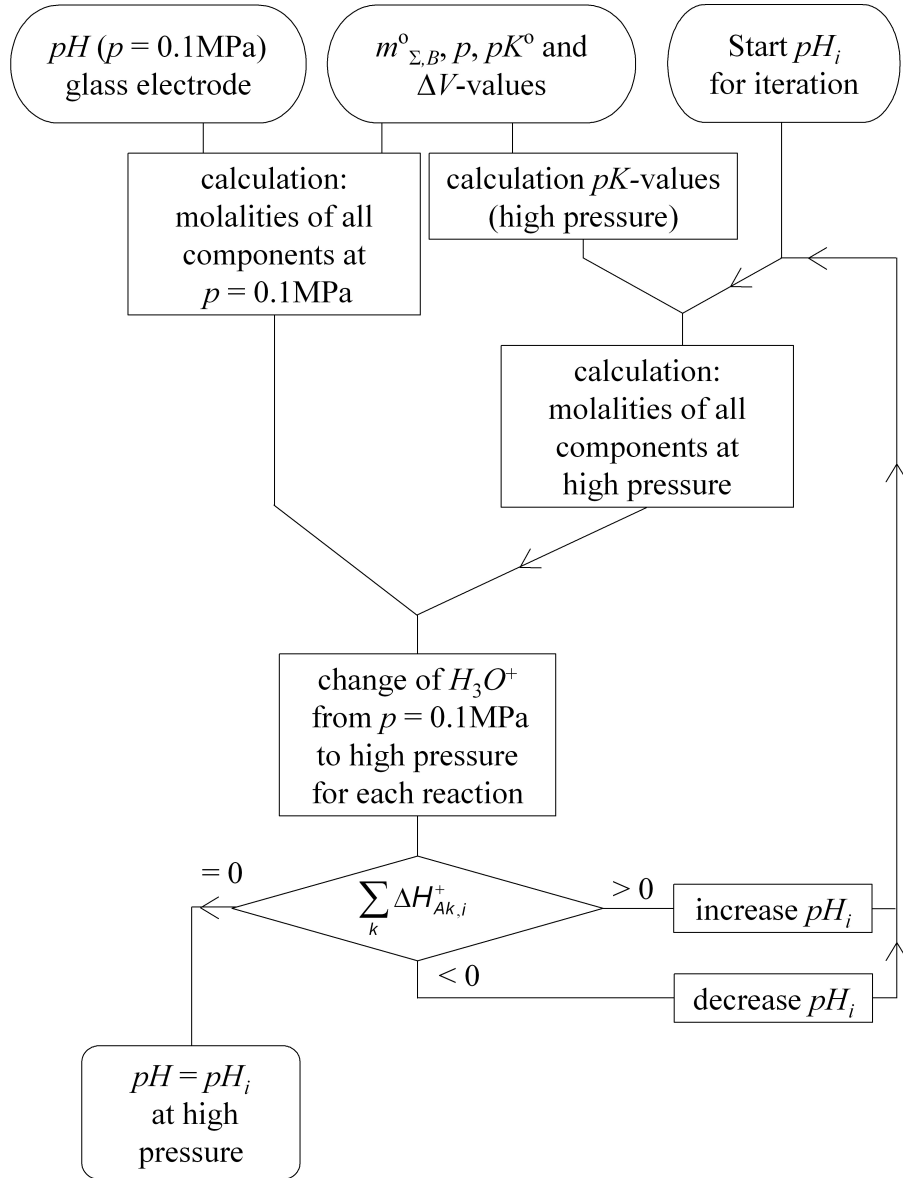


Figure 3.1: Flow diagram for the iterative calculations of pH -values under pressure.

As an example, Equation 3.7 is applied for the reactions of a Phosphoric acid buffer (Equation (3.9)) and for the reactions of water (Equation (3.10)):

$$\Delta H_{(PO_4)}^+ = 3 \cdot m_{H_3PO_4}^0 + 2 \cdot m_{H_2PO_4^-}^0 + m_{HPO_4^{2-}}^0 \quad (3.9)$$

$$- 3 \cdot m_{H_3PO_4} - 2 \cdot m_{H_2PO_4^-} - m_{HPO_4^{2-}}$$

$$\Delta H_{(H_2O)}^+ = 3 \cdot m_{H_3O^+}^0 + 2 \cdot m_{H_2O}^0 + m_{OH^-}^0 \quad (3.10)$$

$$- 3 \cdot m_{H_3O^+} - 2 \cdot m_{H_2O} - m_{OH^-}.$$

Equation (1.9) can be used to calculate the pK_W and pK_a -values at high pressure. For a starting pH_i -value (subscript i for the number of iteration steps) the molalities of all components are calculated based on the Law of Mass Action. From the change of these molalities, the number of H^+ -ions formed or abolished by a reaction is calculated. The iteration has converged if the predicted sum of H^+ formed by individual dissociation reactions is zero. If the sum $\sum_l^L \Delta H_{A_l,i}^+$ is negative the calculation must be started with a smaller value of pH_i , and vice versa.

3.2 Measurement of pH -Value Using Solved Absorption Indicator Dyes

3.2.1 Experimental Setup for pH -Measurements Using Solved Absorption Indicator Dyes

Figure (3.2) shows the experimental setup. By opening the valves, either a sample or a rinsing solution is pushed through the system by a low-pressure piston pump. A tubing pump was proved to be not appropriate, as a part of the indicator dye was absorbed by the silicon tube. After closing the valves, the pressure can be increased up to 450 MPa by means of a hand-operated piston. The actual measuring cell has a volume of approximately 2.5 ml and is fitted with two sapphire windows. It has an optical pathway of 14 mm and an optical width of 6 mm (total width 10 mm). The temperature is held constant at 298 K by a thermostat bath (not shown in Figure (3.2)). A combined Deuterium/Tungsten-halogen light source is connected to the cell by a fibre-optic cable. The light is parallelly aligned using a lens. On the other side of the optical cell, a further lens focuses the light into another fibre-optic cable which transmits it to the spectrometer. As no spectrometer exists which covers the whole range from 250 to 1150 nm, two spectrometric units were used, covering the ranges from 250 to 800 nm and from 500 to 1150 nm. To provide both spectrometers with light the fibre-optic cable has a Y-junction. The fibre-optic cable from the light source has also a y-junction and a third y-branched fibre-optic cable connects the light source to a second pair of spectrometric units in order to correct fluctuations. The connection between the fibre-optic cable from the light source and that to the reference spectrometers is pictured in Figure (3.3).

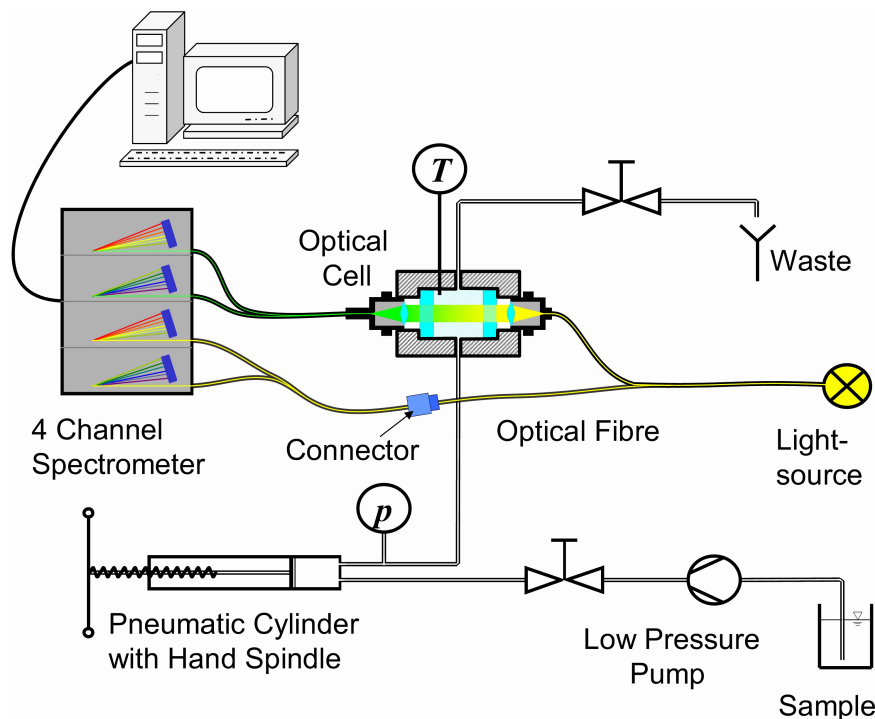


Figure 3.2: Experimental setup for the optical determination of pH -value at high-pressure.

Due to the ability to vary the angle and the distance of parts A and B it is possible to regulate the light intensity arriving at the reference spectrometers. This is necessary because all spectrometric units are centralised in one housing, sharing one A/D converter and it is not possible to use different settings such as integration times. Thus it is necessary to have the same light intensities in each spectroscopic unit. Both pressure and temperature inside the cell are measured using commercial measuring devices.

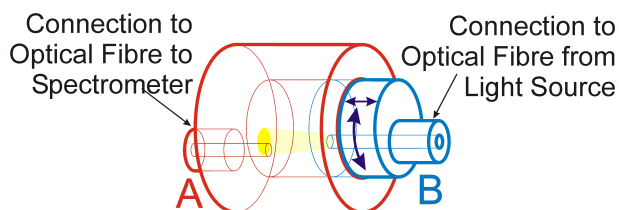


Figure 3.3: Connection of the fibre-optic cables between light source and reference spectrometer. It is possible to move part B (blue) in the part A (red) in an axial and a rotational direction to adjust the fraction of the light from the optical fibre from the right connection into the left one. Note that the connections to the optical fibres are not centred. Part B can be fixed by screws into A (not pictured).

3.2.2 Selection of Indicator Dyes

An indicator mix consisting of 16 different indicator substances was used. Indicator dyes are most sensitive when the pH -value is in the vicinity of their pK_a (see Equation (2.4), (5.7) and Figure (2.2)). To achieve an appropriate sensitivity over the whole pH -range, the pK_a -values of the indicator dyes are evenly distributed. Thus the distance from the pK_a -value of one indicator dye to the next is around 0.5 units. The indicator mix covers the range from about pH 1 to 10 at ambient pressure to allow for the changing equilibrium constants of both indicator dyes and ingredients of samples and buffers. The criteria for the selection of the indicator dyes are (see the remarks in the Appendix to Equation (5.7)):

- high absorption of light at small concentrations (high α -values),
- absorption at a wavelength at which most of the other indicators have no absorption (high I°),
- absorption at wavelengths of high system sensitivity (high I°),
- low reactivity, and
- stability against light.

Table (3.1) shows the composition of the indicator mix used. The amount of indicator dye was chosen to agree to the condition $\frac{I}{I^\circ} = 0.35$ from the Appendix (Notes to the Equation 5.7). As mentioned in the appendix the sensitivity is

Table 3.1: Composition of the indicator-mix. The indicator dyes were solved in Ethanol.

<i>Indicator</i>	<i>g/250 ml Ethanol</i>	<i>Indicator</i>	<i>g/250 ml Ethanol</i>
Alizarin	0.15	Alizarin Red S	0.075
Bromocresol Green	0.04	Bromo Thymol Blue	0.04
Congo Red	0.04	Ortho-Cresol Red	0.03
Methyl Orange	0.04	Methyl Red	0.02
2-Naphthol	0.7	2-Nitrophenol	0.6
4-Nitrophenol	0.12	Phenolphthalein	0.025
Phenol Red	0.03	Quinaldine Red	0.2
Thymol Blue	0.4	Thymolphthalein	0.03

proportional to I° . For different wavelengths, varied system sensitivities are achieved due to the different intensity of the light source, different sensitivity of the photodiodes and losses of light by absorption, reflection and so on in the fibre-optic cable, sapphire windows etc. To illustrate the differences in I° as a function of the wavelength λ , Figure (3.4) shows the spectra recorded with water in the sample cell.

The intensity can be regulated by the integration time of the spectrometer, but it is only possible to set one value for all spectrometers and all photodiodes. Values which are too high result in an overload of the A/D converter as can be seen in the spectra at the top of Figure (3.4) for the range of wavelengths between 575 and 600 nm. Nevertheless, this spectra shows a typical adjustment of the measurements as this range of wavelength is in an area where both spectrometric units overlap.

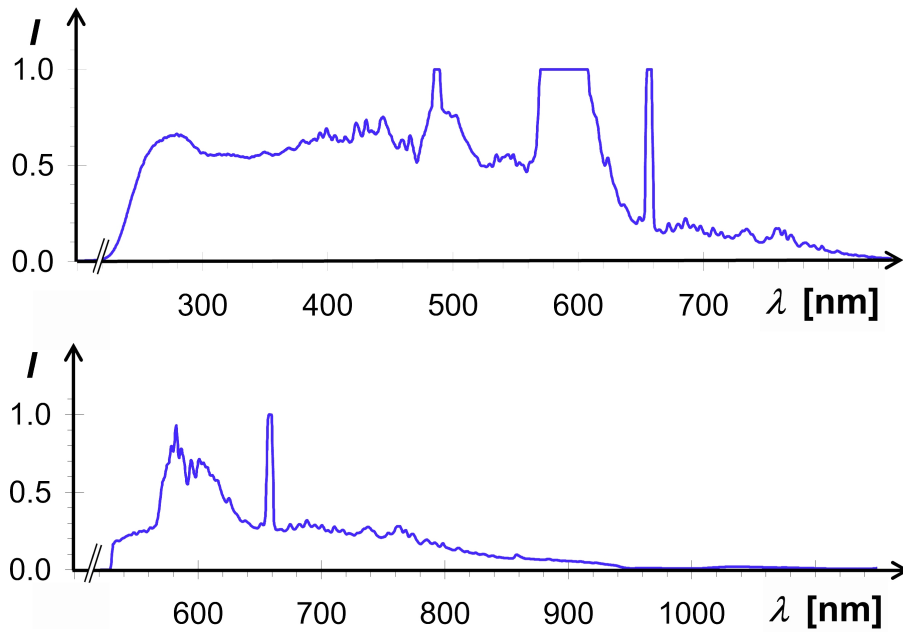


Figure 3.4: Spectra obtained with water in the sample cell with adjustments typical for measurements. The top spectra was taken with the spectrometer unit SQ 2000 #1-UV2-L2-SLIT-50, the other with SQ 2000 #4-OF-1-L2-Slit-50, both spectra are an average of 200 spectra taken with an integration time of 6 ms. The intensity at the Y-axis is a value proportional to the electrical current from the detector, it depends on the light intensity, the sensitivity of the sensor at this wavelength and the properties of the optical path. It is normalised using the maximum value which can be detected by the A/D converter.

The values for the wavelength 485 to 490 nm and 655 to 660 nm where there are intense peaks of the Deuterium light source are always overamplified. But as peaks of indicator dyes are always wider than 20 nm there is not much loss of information if this part of the spectra is omitted. Short integration times lead to a weak signal resulting in a poor signal-to-noise ratio.

No adequate means have been found to avoid ranges of wavelength where the signal is very low. In the ranges below 230 nm and above 950 nm the signal is too low to get any practical information, the ranges 230 to 250 nm and 640 to 950 nm are useable but show a worse signal-to-noise ratio compared with the values between 250 and 640 nm. An improvement can be made by taking more measurements at different integration times e.g. with 6 ms for the values between 250 to 640 nm and 20 ms for the values in the ranges 230 to 250 nm and 640 to 950 nm. The intensities below 230 nm and above 950 nm were too small to get any usable signal (a longer integration time can minimize the signal-to-noise ratio of the A/D converter, but not that of the photo diodes). This method was not practised as the available indicator dyes change their colour at wavelengths of between 250 and 700 nm. In this range the signal is adequate with an integration time of 6 ms (there are also changes above 1000 nm, but these changes have proven to be not significant).

Measuring Procedure

Some of the adjustments were only made before the first calibration measurement and kept unmodified for all calibration and sample measurements (an exception is when there were repairs made to the cell or if the recorded spectra showed that the settings had markedly changed). These adjustments refer to the distance between lenses and the end of the optical fibres, the relation between the intensities of the Tungsten/Halogen and the Deuterium part of the light source and the settings of the spectrometer.

The lens situated at the end of the optical fibre from the light source was adjusted from outside the high pressure cell by changing the distance until the light beam was parallel. The other lens was adjusted to achieve the highest possible signal to the spectrometer with water in the optical cell. It was possible to control the intensity of the Tungsten/Halogen part of the light source to adjust the ratio between both light sources (see the spectra in Figure (2.5)). This ratio was optimised to reach an intensity which is as uniformly distributed as possible.

The integration time and the connector between the optical fibres to the reference spectrometers were adjusted before each measuring procedure.

After rinsing the system with demineralised water, sample solution was pumped through the optical cell. The first 10 ml were discarded to be sure that all rinsing water was replaced. Spectra measurements are taken when the temperature is constant. The integration time of the spectrometer is chosen to obtain a spectra similar to that shown in Figure (3.4), with a signal strength of

over 50 % at wavelengths of between 250-640 nm and overload only in a range where both spectra overlap or at the intense lines of the Deuterium light source. An integration time of 6 ms was appropriate for most cases. The spectrometer software provides an opportunity to take an average over a number of successive spectra readings and this number was set to 200 as an increase in the number of readings leads to no noticeable increase in the signal-to-noise ratio. Afterwards, the connector between the optical fibres and the reference spectrometer is adjusted if necessary. A setting is chosen in which the reference spectra are similar to the measurement spectra.

Spectra measurements were taken when the desired pressure was reached and the temperature was constant. The same procedure was repeated with a mixture of 25 ml of the sample solution containing 100 μ l of the indicator mix. For evaluation, the difference between the spectra with and without indicators was used. The spectra without indicator dyes were required in order to make allowance for the colour of the solutions and effects such as changing cell geometry or changing refractive index under pressure. The calibration was performed using buffer systems and the pressure dependency of their *pH*-values was calculated as described in Chapter 3.1. The graduation between each individual test buffer was about 0.25 *pH*-units. 0.2 M solutions of Citric acid (*pH* 2.5 - 6.25), Acetic acid (*pH* 4.75 - 5.5), TRIS (*pH* 8.0), CAPS (*pH* 10.0) or Potassium Dihydrogen Phosphate (*pH* 2.0-2.5 and 6.25-7.5) were mixed with 1 M NaOH or HCl solutions until the desirable *pH*-value was reached. Then, demineralised water was added to make a 0.1 M solution. Before each measurement, the *pH*-value of the buffer was checked in a thermostat bath (298 K) using a glass electrode. The buffer solutions covered a range from *pH* 2 to 8 at ambient pressure, corresponding to a range from 1.2 to 8.3 at 450 MPa. The spectra of calibration buffer solutions were recorded in 50 MPa steps up to 450 MPa.

3.3 Measurement of *pH*-Value Using Immobilised Indicator Dyes

As discussed in Chapter 2.3.3 and 2.4, immobilised indicator dyes show some advantages compared with dissolved indicator dyes, but the immobilising technique is still poorly conceived. Therefore, some immobilising techniques described in literature were tested at ambient pressure and the most promising ones were tested at high pressure. Besides the immobilising techniques, two different ideas of possible measurement setups were investigated: the immobilisation of indicator dyes directly on the fibre and the immobilisation on a window inside the high pressure cell. High pressure experiments were performed only with immobilisation on the window because of the easier adaption of the existing setup for measurements with solved indicator dyes. Following, the different immobilising techniques de-

scribed in literature are briefly introduced and afterwards the procedure for the techniques actually used are described in more detail.

3.3.1 Techniques Used for Immobilising Indicator Dyes

In literature, three basic types for immobilising indicator dyes are described: absorption, covalent bonding and embedding in a porous matrix [209].

Immobilisation of Indicator Dyes by Covalent Bonding

A covalent bonding of indicator dyes is described with cellulose as the matrix by Wolfbeiss et al. [93] and two patents [238, 239] describe methods of fixing indicator dyes onto paper (originally for use as non-bleeding indicator papers). Another method is described by Kosch [206]. She used an Azzo dye fixed onto the Polyurethane Hydrogel by a dehydration reaction between the Vinylsulfonyl group of the dye and a Hydroxy group of the polymer. While these methods result in consistent bondings between matrix and dye they are limited by the small number of indicator dyes which can be used for such an immobilisation and the difficulty of fixing cellulose on glass fibres or on windows. Therefore such experiments were not carried out in this work.

Immobilisation of Indicator Dyes by Absorption

This method uses the hydrophobic or the electrostatic interaction between the dye and the matrix. The method is simple, but the binding is not durable as the interaction between matrix and dye is not much stronger than the interaction between water and dye.

For an electrostatic absorption, ion exchanger resins are usually used [209, 211]. The loaded ion exchanger resin can be fixed using a polymeric layer of Polyvinyl Chloride [211]. Other materials were also developed, e.g. Sulfonated Polystyrene and Polyelectrolyte-containing Silica and a hydrophobic absorption of indicator dyes on organic polymers such as Amperlite was described by Motellier et al. [240].

Immobilisation of Indicator Dyes by Entrapment

Embedding of the indicator dyes was first described with cellulose as the matrix (e.g. [207]). Later publications describe mainly Sol-gel as an embedding material (e.g. [206, 215, 216, 220, 222, 223, 241, 242]). The company PreSens uses Polyurethane Hydrogels as the H^+ and OH^- transmissible matrix.

Like glass, the main structure of Sol-gel is formed by Si-O-Si bridges, but in contrast to glass it also contains organic groups. The advantage of Sol gel compared to glass is the possibility to synthesise it at low temperatures. Like glass, Sol-gels are transparent over a wide range of wavelengths from UV to NIR

and resistant to most chemicals. By varying the preparation conditions it is possible to obtain a wide variety of porosity and pore sizes.

3.3.2 Manufacture of Optodes

Production of Optodes on Glass Plates with Ion Exchanger Resin

These optodes are produced in a similar manner to those described by Vishnoi et al. [211]:

- Wash the ion exchanging resin IRA 400 with demineralised water.
- Wash the ion exchanging resin with Acetone.
- Dry for four hours at 353 K.
- Pulverise with mortar and pestle.
- Add this powder to a saturated solution of BTB (Bromo Thymol Blue) in demineralised water.
- Stir for twelve hours at ambient temperature.
- Filtrate, thoroughly wash with demineralised water and dry.
- Pipette some drops of a PVC-solution (50 mg PVC in 5 ml THF (Tetrahydrofurane)) onto a glass plate (cover slip for microscopy).
- Partially dry in THF atmosphere.
- Before the PVC is completely dry disperse the dye loaded ion exchange resin onto it.
- Dry for 24 hours at 333 K.

Optodes made this way are called *ion exchanger optodes* in the following text.

Manufacturing of Optodes on Glass Plates by Absorption of Indicator Dyes in Polyamide

The production of these optodes was similar to that described by Wollenweber [243]. To obtain a better adhesion of the polyamide matrix on the glass plate, the glass was first silanised:

- Dissolve 1 ml 3-Methacryl-oxypropyl-trimethoxysilan in 50 ml of 50% Ethanol.
- Stir for 25 minutes.
- Immerse the cleaned glass plates in this solution.
- Dry the glass plates at 353 K.

The actual immobilisation was performed as follows:

- Dissolve 4.25 g Acrylamid and 0.75 g BIS (N,N-Methylene bisacrylamide) in 10 ml demineralised water.
- Admix 350 μl of a 0.01 molal aqueous solution of BTB and 15 μl 4-N-TEMED (N,N,N',N'-Tetramethylethylenediamin) to 150 μl of this solution.
- Pipette 10 μl of this solution and 3 μl of an aqueous Ammonium Persulfate solution (132.5 g/l) on the silanised glass plate.
- Dry for 10 minutes at ambient temperature.
- Wash with water.

Optodes made this way are referred to as *polyamide optodes* in the following text.

Production of Optodes on Glass Plates with a Sol-gel Matrix

The procedure used for the immobilisation in Sol-gel is largely the same as described by Kosch ([206] Chapter 5.2.1).

- Dissolve 3 mg BTB in 1 ml Methanol.
- Add 200 μl TMOS (Tetramethyl Orthosilicate) and mix.
- Add 100 μl HCl (0.1 M) and mix in ice water.
- Store for 6 Days in a sealed tube.
- Dip the glass plate fixed on an adhesive strip into the solution.
- Slowly pull out (≈ 1 cm/s) the glass plate.
- Dry for a short time.
- Repeat the dipping, pulling out and the drying between 2 and 4 times.
- Dry for one day.

Optodes made this way are referred to as *Sol-gel plate optodes* in the following text. Different optodes made according to the same instructions vary greatly in the thickness of the layer. The adhesion of the Sol-gel was weak and as a consequence the layer sometimes peeled away.

Production of Optodes on Optical Fibres with a Sol-gel Matrix

The procedure used for the immobilisation in Sol-gel on fibres is derived from that described above for glass plates.

- Solve 3 mg BTB in 1 ml Methanol.
- Add 200 μ l TMOS and mix.
- Add 100 μ l HCl (0.1 M) and mix in ice water.
- Store for 6 Days in a closed tube.
- Prepare the fibre by removing the outer jacket with a knife and the inner polyamide jacket with a Bunsen burner.
- Etch the glass cladding by dipping the first centimetre of the fibre in a saturated *KOH/NaOH* solution and heating it with a Bunsen Burner (repeat this step until the fibre tip appears cloudy).
- Wash with demineralised water, Acetone and again with demineralised water.
- Dry.
- Dip the fibre in the BTB/TMOS solution.
- Pull slowly out (1 cm/s) the fibre.
- Dry short.
- Repeat the dipping, pulling out and the drying 2 to 3 times.
- Dry for one day.

Optodes made this way are referred to as *Sol-gel fibre optodes* in following text.

For the first tests it was attempt to make such optodes without the fibre etching step. These trials failed as the Sol-gel did not adhere stably onto the fibre. A further advantage of the etching is that the cladding of the fibre is partially removed, resulting in a larger illuminated surface which can be coated by the indicator-containing Sol-gel.

A variation of the fibre preparation was tested: a small glass ball (diameter about 2 mm) was melted from the tip of a Pasteur pipette (Duran) onto the etched end of the glass fibre. This ball was etched again in the same way. Afterwards it was treated in the same way as the etched fibre. Optodes made this way are referred to as *Sol-gel ball optodes* in later text.

3.3.3 Experimental Setup for pH -Measurements with Optodes

Figure (3.5) shows the setups for different versions of the tested optodes. The optodes on glass plates were tested in both an ambient pressure setup using a cuvette and with a sapphire window which can be placed into a high pressure cell.

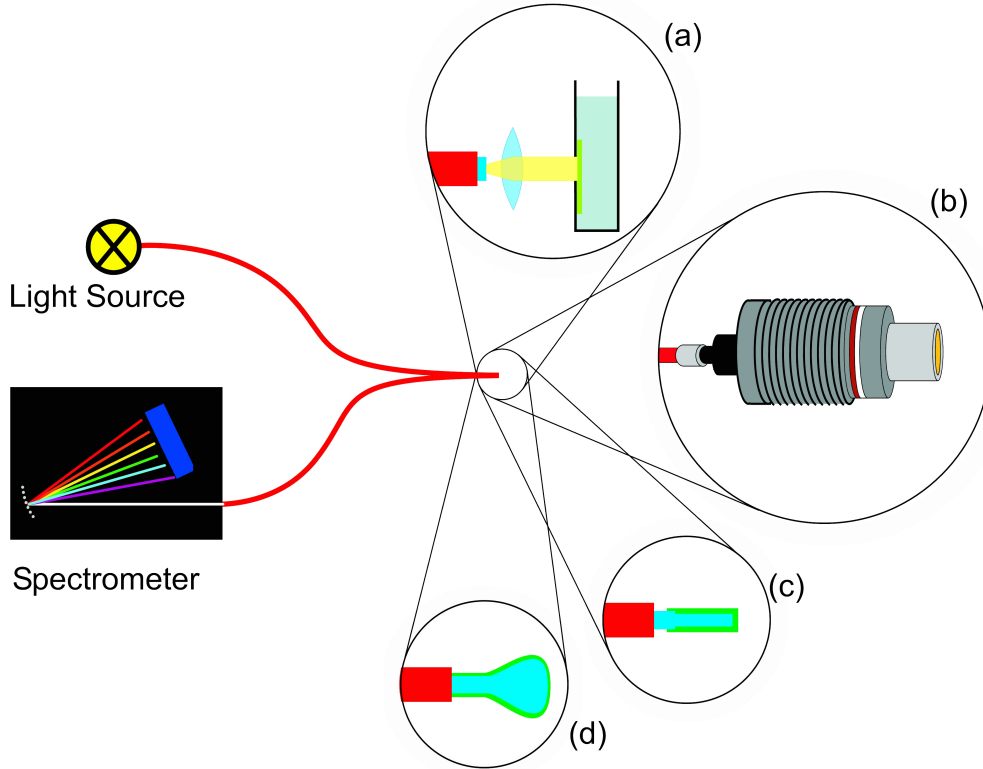


Figure 3.5: Different types of optodes tested in this work. (a) is a measuring device to test the optodes at ambient pressure. The optodes on glass plates are attached inside a cuvette. The light from the optical fibre is aligned parallelly using a lens. The same lens focuses the reflected light onto the fibres and a Y-junction in this fibre leads the light to the spectrometer. Setup (b) is similar, but instead of the cuvette a sapphire window from a high pressure cell was used which enables measurements at both high and ambient pressure. (c) shows the setup for optodes with the pH -sensitive layer directly on the fibre and (d) the version with a glass ball melted onto the end of a fibre.

3.4 Investigations of pH -Inhomogeneities in High Pressure Vessels

The build up of pressure is associated with the generation of inhomogeneities in several physical parameters, among them the pH -value. For planning and interpreting high pressure experiments it is necessary to know the extent of such inhomogeneities.

The time necessary to adjust imbalances in the pH -value depend mainly on the convection in the vessel. If there is only a little convection the homogenisation results from diffusion. Here, the mobility of ions belonging to H^+ and OH^- -ions are the rate-determining step, as H^+ and OH^- -ions are very mobile, but cannot move without a counter-ion because otherwise an electric field would be generated which detains the H^+ and accordingly the OH^- -ions.

To investigate pH -inhomogeneities in a high pressure cell special experiments were made. The setup for these experiments is a variation of that for the absorption measurements with the solved indicator dyes and is shown in Figure (3.6).

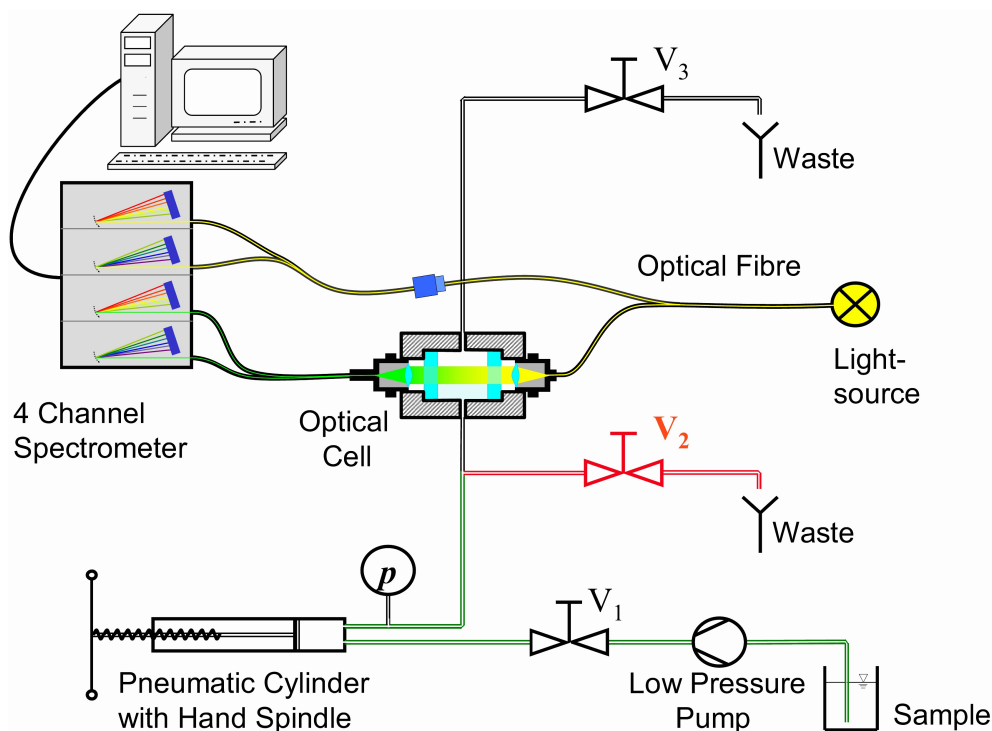


Figure 3.6: Setup for the experiments to show pH -inhomogeneities in a high pressure vessel. The differences to the setup for the pH -measurements with solved indicator dyes (Figure (3.2)) are marked red.

The difference to the setup for absorbance measurements (Figure (3.2)) is a branching out in the inlet pipe and a third valve (red in Figure (3.6)). This gives the possibility of filling the cell via valves V_1 and V_3 with an indicator dye/buffer solution. After closing valve V_3 and opening V_2 , the pneumatic cylinder and the pipes which are marked red and green in Figure (3.6) can be rinsed and filled with another indicator dye/buffer solution. While building up the pressure with the pneumatic cylinder both buffer solutions come together in the optical cell and the homogenisation can be observed by the colour change of the indicator dye. The spectra contains only an average value over the whole window, but this value contains enough information to estimate the time of homogenisation.

A further variation of the setup allows viewing at the allocation of the pH -value directly (see Figure (3.7)). The light of a blue LED (GaN , $\lambda_{max} = 470 \text{ nm}$, see Figure (2.5)) is fed through a third window into the measuring cell at an angle of $\frac{\pi}{2}$ to the two other windows. One of these windows is connected to the spectrometer as in the previous experiments, the other window is equipped with a camera.

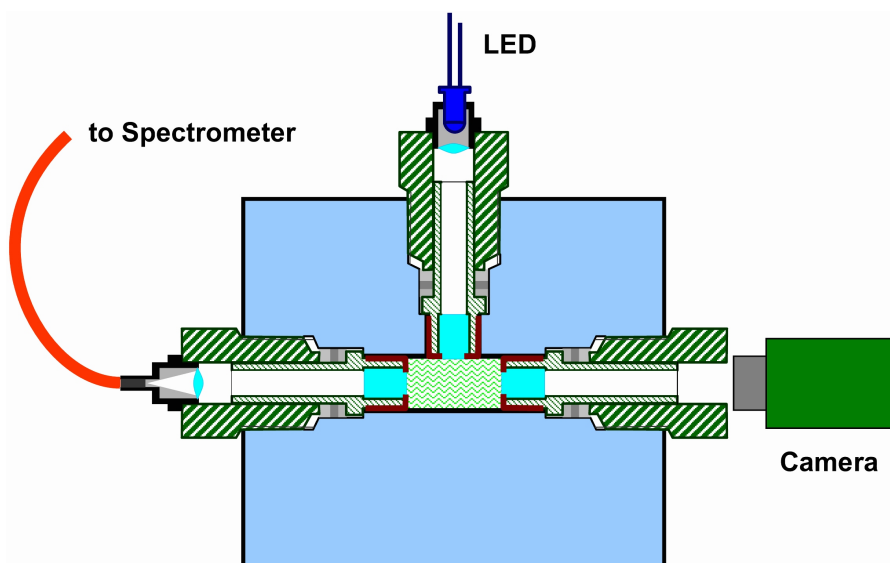


Figure 3.7: Setup for the experiments to show pH -inhomogeneities in a high pressure vessel with fluorescent indicator dyes. In- and outlet are below and above the pictured layer and the armatures are the same as in Figure (3.6).

Fluorescein is used as indicator dye and has a yellow-green fluorescence with a maximum light intensity at about 518 nm in alkaline solutions and no fluorescence in acidic solutions ($pK_a(0.1 \text{ MPa}) \approx 6$). Thus it is possible to simultaneously measure the development of the intensity at 518 nm and to see with the camera the areas in which the pH -value is below 6 and where it is above.

3.5 Sources of Chemicals and Equipment

Chemicals

2-Nitrophenol, Quinaldine Red, Potassium Dihydrogen Phosphate, Sodium Hydroxide, Hydrochloric Acid, EPPS (3-[4-(2-Hydroxyethyl)-1-Piperazine] Propane-Sulfonic acid), Disodium Hydrogen Phosphate Dihydrate and Ethanol 5% v/v Ether

from Fischer Scientific GmbH (Germany).

Citric acid Monohydrate, Acetic acid, CAPS (3-(Cyclohexylamino)-1-Propanesulfonic Acid) and Fluorescein

from Fluka (Germany).

Alizarin, Alizarin Red, Bromocresol Green, Bromo Thymol Blue, Congo Red, Ortho-Cresol Red, Methyl Orange, Methyl Red, 2-Naphthol, 4-Nitrophenol, Phenolphthalein, Phenol Red, Thymol Blue, Thymolphthalein

from Omikron GmbH (Germany).

Polyvinyl Chloride of high molecular weight (K-value 6), Tetrahydrofuran (stabilised), ion exchanging resin: Amperlite IRA 400 (Cl) strong alkaline

from Sigma-Aldrich (Germany).

Acrylamid (Research Grade), Ammonium Persulfate (PA), 3-Methacryloxypropyltrimethoxysilan (Purum), N,N'-Methylenbisacrylamid (PA), N,N,N',N'-Tetramethylethylenediamin (Research Grade)

from Serva Electrophoresis GmbH (Germany).

Hexadecyltrimethylammonium Chloride (99 %), Methanol (99,8 %), Tetramethyl Orthosilicate (99 %), Acetone (99+ %)

from Acros Organics (Belgium).

Silicon for the splicing of the optodes:

Rhodia Elch

from Rhodia Silicon GmbH (Germany).

Equipment

High Pressure Equipment

Optical cell: Type 740.2064,
Hand-operated piston: Type 750.1700,
Thermocouple: Type 791.99.0098-J,
Valves: Type 710.6310,
T-Junctions: Type 720.1633,
Tubes: Type 730.2350 and
Tube Connections: Type 720.0310 and 720.0320
from SITEC (Switzerland).

Pressure transducer: Type 501-7000-1
from Dunze (Germany).

Optical Equipment

Spectrometer UV-VIS: SQ2000 #1-UV2-L2-SLIT-50,
Spectrometer VIS-NIR: SQ2000 #4-OF-1-L2-SLIT-50,
AD converter: ADC-1000,
Light source: DH 2000 MC,
Fibres: FCB-UV600-2-SR,
Lens: COL-UV and
Cuvette holder: CUV-UV
from Micropack/Avantes (Germany).

Cuvettes: Plastibrand PMMA, optical path: 1 cm; volume 2.5 ml
from Brand (Germany).

Cover slip round diameter 10 mm, thickness 0.13-0.17 mm
from Laborhandel Krumpholz (Germany).

Phase detection device (incl. fibre-optic): PDD-470 and
Dual-lifetime referenced optode: SF-pH-HP2
from PreSens (Germany).

Other Equipment

Low-pressure piston pump: ETS15-E/C-230-50-M
from Eckerle Industrie-Elektronik GmbH (Germany).

Thermostat bath: F8-C40
from Thermo Haake GmbH (Germany).

Chapter 4

Presentation and Discussion of Results

4.1 Discussion of the *pH*-Measurements Using Solved Indicator Dyes

4.1.1 Data Analysis of the *pH*-Measurements Using Solved Indicator Dyes

During measurements, some changes in the spectra occurred which were not a result of the absorption in the sample but a consequence of the changing geometry of the optical cell during pressurisation. These changes were not always the same. A possible reason for this are changes in the geometry of the measuring cell during pressure supply. The resulting change in spectra was mainly a general stretch in direction of the Y-axis uniform over all wavelengths. As there are wavelengths in which the indicator dyes used show no absorption, the intensity in this range is a measure of the stretch factor. Therefore a correction was possible by dividing each transmission spectral value by an average of selected values in this range:

$$\left(\frac{I_{\lambda}}{I_{\lambda}^o}\right)_{\text{corr}} = \frac{\frac{I_{\lambda}}{I_{\lambda}^o}}{\frac{1}{5} \cdot \sum_{i=1}^5 \frac{I_{\lambda i}}{I_{\lambda i}^o}} \quad (4.1)$$

where $\frac{I_{\lambda}}{I_{\lambda}^o}$ is the absorption at the wavelength λ (I_{λ} and I_{λ}^o are the intensities at the wavelength λ with and without indicator mix, respectively) and $\frac{I_{\lambda i}}{I_{\lambda i}^o}$ are the absorptions at the above mentioned wavelengths of between 700 and 980 nm. Both spectrometric units showed a different stretch and were separately corrected. For the UV/VIS-spectrometer the values $\frac{I_{\lambda i}}{I_{\lambda i}^o}$ are the absorptions at 700, 710, 715, 720 and 725 nm and for the VIS/NIR-spectrometer absorptions at 700, 730, 900, 950 and 980 nm.

Figure (4.1) shows the measured calibration spectra at 450 MPa before and after this correction.

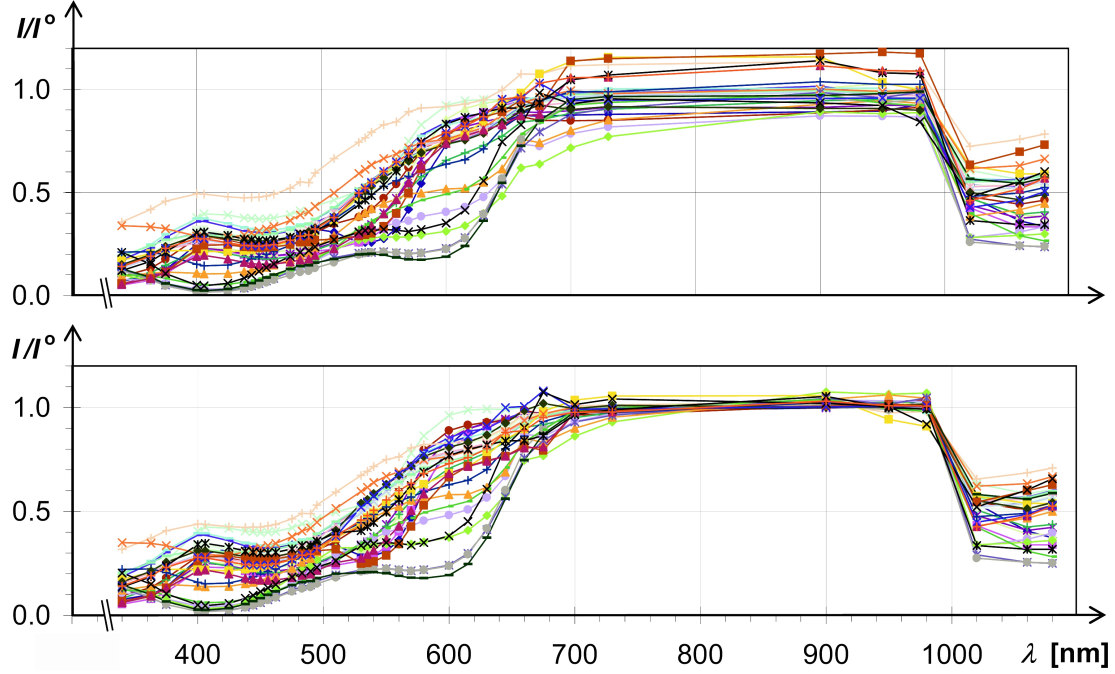


Figure 4.1: All calibration transmission spectra taken at 450 MPa. Top: before correction. Below: after correction according to Equation (4.1). Only the data points are displayed at the wavelengths which were originally used for calibration and correction according to Equation (4.1).

If there is an anomaly in the transmission spectra which indicates changes other than a linear stretch, such as the inclined curve between 700 and 980 nm in Figure (4.2) these spectra were not used.

Additionally, a correction was made for fluctuations of the light source by means of a second spectroscopic unit. This correction was made by the spectroscopy software according to the following equation:

$$I_{m(\lambda)} = I_{mm(\lambda)} \frac{I_{mr(\lambda)}(t = 0)}{I_{mr(\lambda)}}. \quad (4.2)$$

The direct value from the AD converter connected to the photodiodes is $I_{mm(\lambda)}$, $I_{mr(\lambda)}$ is the same as $I_{mm(\lambda)}$ using the reference spectroscopic unit and $I_{mr(\lambda)}(t = 0)$ the value recorded by the spectroscopic unit at a time determined by the laboratory worker (this is usually when the first "white" spectra (buffer without indicator dye) was taken).

Spectra from diode array spectrometers contain a large amount of information. The spectrometer used provides absorption values at around 2000 wavelengths

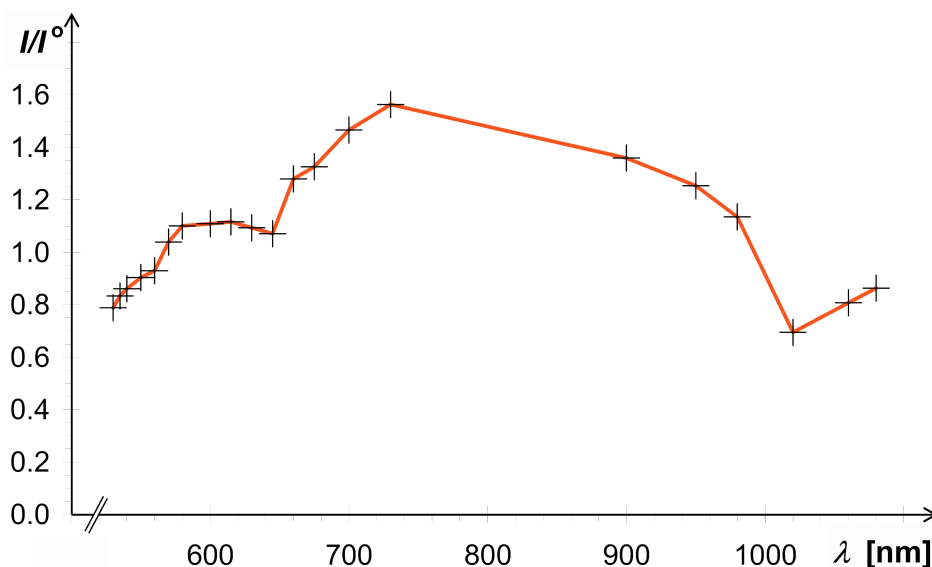


Figure 4.2: Transmission spectra of the indicator mix in a calibration buffer of Imidazol ($pH=6.98$) at 0.1 MPa. The inclined course between 700 and 980 nm is a sign that the measuring cell has changed its geometry compared to the geometry when the "white" spectra was recorded (the spectra of the buffer without indicator mix). Spectra with such a course were discarded.

for each spectra and more than 350 spectra were used for calibration. This huge amount of data would overstrain the calibration calculations.

A data reduction without too much loss of useful information is possible because of two characteristics of the spectra obtained from organic dyes like the indicators used: in some ranges of wavelength there is no absorption (see, for example, in Figure (4.1) the range between 700-900 nm) and the absorptions at different wavelengths show multi-colinearity. Two wavelength readings which are adjacent to one another by and large contain the same information, and one of the wavelength reading is therefore superfluous. If the absorption at the wavelength of 350 nm rises, for example, then the absorption values will also rise at the wavelengths of 349 and 351 nm. But not only absorptions in neighbouring wavelengths show these linear dependencies, the spectra of the indicator mix is a linear combination of the spectra of the different forms of the indicator dyes. Multi-colinearity also means that much of the information in the spectra is redundant. It is possible to describe with some selected wavelengths the same as with the whole spectra. Spectra can therefore be compressed using suitable methods, without information regarding the sample being lost.

The following ways to reduce data were chosen:

26 wavelengths were selected in which significant changes in absorption take place. For each wavelength an average value for all diodes of ± 1 nm was taken.

As the distance between the wavelength of two neighbouring diodes is about 0.3 nm an average of values from between 5 and 7 diodes was used. The chosen wavelengths are pictured in Figure (4.1) as dots. To select the single values from the original data files and find the average in the way described a PASCAL program was written whose source code is attached in Appendix 5.1.2. Special calibration procedures, namely PCR (**P**roincipal **C**omponent **R**egression) and PLS (**P**artial **L**east **S**quares), were used in order to account for the linear dependencies of the spectra. Excellent overviews of these methods are given by [210, 244, 245]. Therefore, in this text only the most significant characteristics of these methods relevant to the aim of the present work are explained.

The basis for both calibration methods was a data matrix containing the absorption values of 26 selected wavelengths (in columns) of all calibration measurements. The selected wavelengths are mainly in areas where significant effects were observed (see the points in Figure (4.1)). In addition, it was tested to see if the accuracy rises if the data matrix was expanded with an additional column containing the pressure levels used. Each column was normalised by dividing the values by the highest value of the respective column.

Principal Component Regression

With PCR, the spectral data was analysed for linear dependencies to find virtual variables (or Principal Components (PCs)) [245]. These virtual variables are linear combinations of the absorption data and contain most of the spectral information, even though the number of PCs is less than the number of original data. This so called **P**roincipal **C**omponent **A**nalysis (PCA) can be regarded as a transformation into a new orthogonal coordinate system. PCA is a spectral decomposition with an inverse least square regression method which creates a quantitative model for the complex spectra. The criteria for choosing the new axes is the variance of the projection of the data points on the axes: the first new axis, the principal component 1 (PC1) is the vector parallel to the greatest variance of the measured values, the next axis, PC2 is the vector with the greatest variance perpendicular to PC1, PC3 is the vector with the greatest variance perpendicular to both previous axes and so on. Therefore, principal components are linearly independent, unlike the measured data. It is possible to obtain as many principal components as the primary matrix has dimensions, but generally only the first principal components are relevant. The PCs represent the spectral variations of all spectroscopic calibration data. Therefore, using this information to calculate a regression equation produces a robust model for predicting the *pH*-value in such complex samples as a mixture of different forms of different indicator dyes.

The factors between the absorption values from the original matrix and the PCs are called loadings. They are a measure for the importance of the chosen wavelengths. Omitting columns with small loadings can lead to a better model.

This was the case for the wavelengths in the NIR-range.

A decrease in the variance of the PCs means also a decrease in information. The actual calibration was performed using the first principal components. Calibrations were tested using a different number of principal components and the best agreement was reached with a validation data set for the calibration with the first 3 principal components. For the actual calibration the method of inverse least squares was used.

A disadvantage of the PCR calibration model is that in the first step, the PCA, the absorptions at selected wavelengths, are calculated independently of any knowledge of the pH -value. They merely represent the largest common variations among all the spectra in the training set. Presumably, these variations will be related mostly to changes in the pH -values, but there is no guarantee that this is always true.

A direct consideration of the target value, the pH , takes place in another calibration procedure, the already mentioned Partial Least Squares (PLS) described in the next subsection. Both methods, PCR and PLS, were tested and the findings are given in Chapter 4.1.2.

Partial Least Squares

With PLS, linear combinations of the measured values were used, but here the criterion in selecting weights was to reach maximal covariance with the pH -values. The factors are presented during the calculation in such a way that the variation of the pH -value can be explained as well as possible by the PLS factors which are to be determined. Or in other words: it is not only the spectral variance which is taken into account, but also the variance of the pH -value. This can lead to a better significance, as the factors are oriented in accordance with the target value. Unlike PCR, PLS is a one-step process as the obtained factors describe directly the relationship between spectral data and pH -value.

4.1.2 Results of the pH -Measurements Using Solved Indicator Dyes

Figure (4.3) shows a section of the transmission spectra of the indicator mix at 450 MPa for selected pH -values.

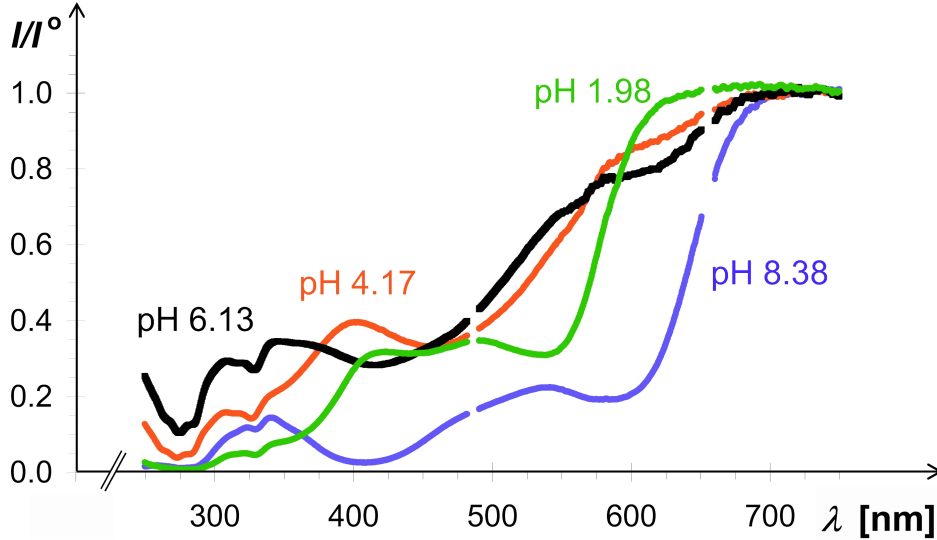


Figure 4.3: The UV-VIS transmission spectra of the indicator mix at a pressure of 450 MPa for selected pH -values. There is no data for the wavelengths 485-490 nm and 653-660 nm, as the lines from the Deuterium light source are so strong in this area that the values are out of range.

As can be seen, the spectra differ significantly with pH -values. This observation represents a presupposition of an accurate measurement. To test the stability of the indicator dyes at high pressure, before and after every calibration measurement a spectra was recorded at ambient pressure. The comparison of these pairs of spectra showed no irreversible changes during pressure treatment. In order to illustrate this, Figure (4.4) shows as an example the transmission spectra of the indicator mix in a 0.1 molal Phosphate buffer before treatment, at 450 MPa and after treatment.

Different pressures produce different spectra for the same pH -value due to both the changing absorption spectra of each form of indicator dye and changing dissociation constants. There are three ways of compensating for this:

1. to calibrate each pressure step individually,
2. to treat the pressure as an additional input, or
3. to calibrate with data over the full range of pH and pressure.

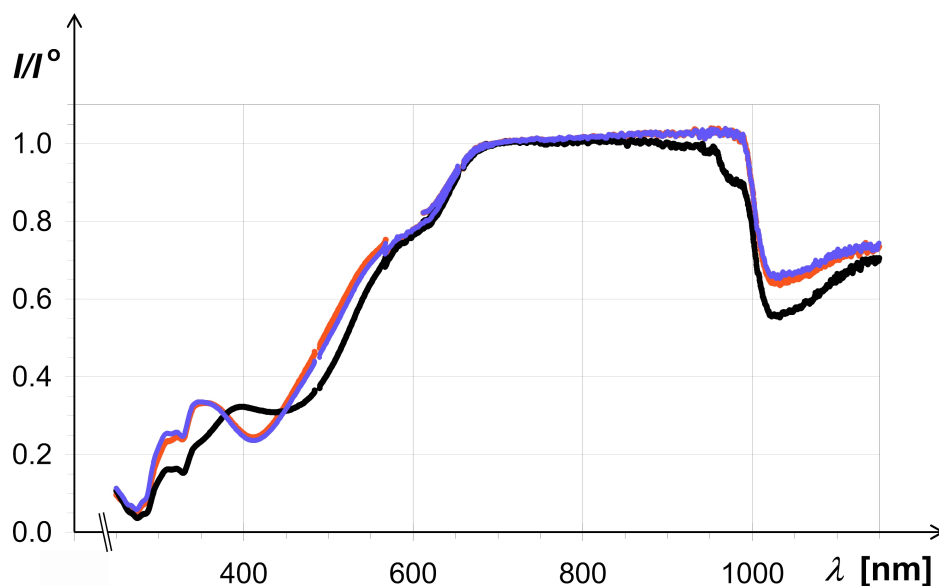


Figure 4.4: Transmission spectra of the indicator mix in a 0.1 molal Phosphate buffer at ambient pressure/ pH 6.99 before pressure treatment (red); at 450 MPa/ pH 5.58 (black) and after pressure treatment 0.1 MPa/ pH 6.99 (blue). As in Figure (4.3), there is no data for the wavelengths 485-490 nm and 653-660 nm, because of the lines from the Deuterium light source. For the range between 570 and 700 nm, values from both spectrometric units are pictured.

The first method leads to a great additional operating cost for both calibration and measurement without the prospect of a noticeable increase in accuracy. Therefore, only methods 2 and 3 were tested.

To test the accuracy of the system, spectra of eight buffer solutions at different pressures evenly distributed over the pH and pressure range were used for validation. The test buffer solutions were prepared in the same way as the calibration buffers. Figure (4.5) shows a comparative parity plot and the corresponding data is given in Table (4.1).

The reference values are shown in relation to the values calculated from the spectroscopic data using PCR and PLS. The reference values are computed in the same way as the calibration buffers. Similar accuracies and comparable results were produced using PLS (with 2 factors) and PCR (with 3 principal components). The empirical variance ΔpH was 0.34 (PLS) and 0.39 (PCR) pH -units.

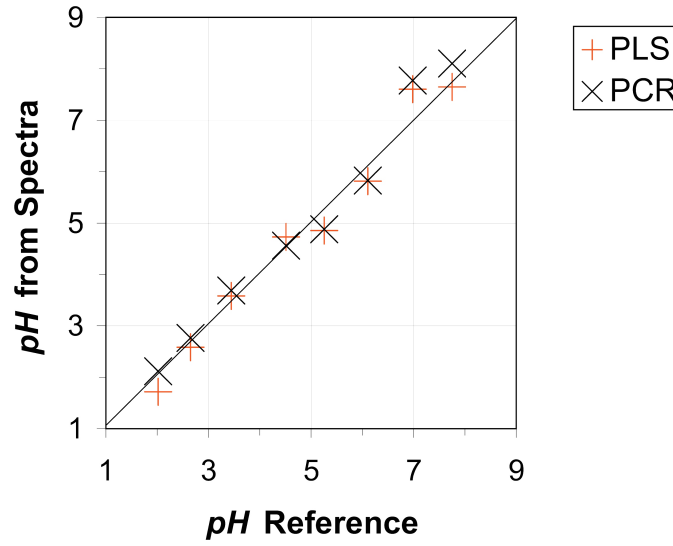


Figure 4.5: Parity plot of the calculated data from thermodynamic (pH_{Ref}) and spectroscopic data using two different methods; PLS: Partial Least Squares and PCR: Principal Component Regression. The measuring points cover the whole range between 0.1 and 450 MPa. For additional information about these measurements see Table (4.1).

Table 4.1: pH -values of the validation buffer solutions (pH_{Ref}) at different pressures and the findings achieved with PLS (pH_{PLS}) and PCR (pH_{PCR}) from the spectroscopic data. pH_{Ref}^0 is the pH -value of the buffer at ambient pressure. The data of the last three columns is pictured in Figure (4.5) above.

Buffer	p [MPa]	pH_{Ref}^0	pH_{Ref}	pH_{PLS}	pH_{PCR}
Phosphate	450	2.63	2.02	1.72	2.12
Citrate	200	2.84	2.65	2.58	2.76
Citrate	400	4.04	3.45	3.58	3.69
Acetate	0.1	4.51	4.51	4.73	4.56
Citrate	300	6.06	5.26	4.85	4.88
Phosphate	350	7.28	6.11	5.81	5.82
Phosphate	100	7.39	6.98	7.61	7.77
Phosphate	50	7.96	7.75	7.65	8.10

Figure (4.6) compares the results of PCR including and excluding pressure as additional input (the normalized pressure p/p_{max} ($p_{max} = 450$ MPa) was used as an additional variable). The corresponding data is displayed in Table (4.2).

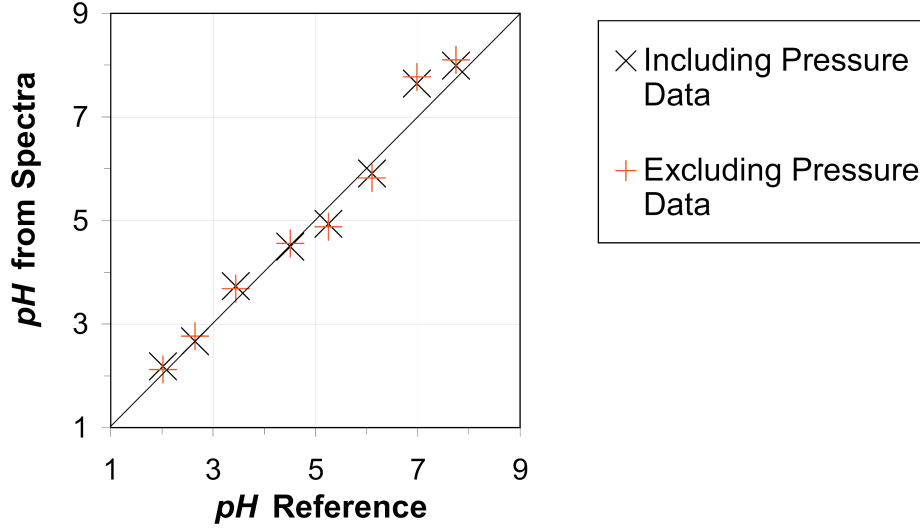


Figure 4.6: Parity plot of the calculated data from thermodynamic ($pH_{Reference}$) and spectroscopic data using PCR including and excluding the pressure as an additional input. The measuring points cover the whole range between 0.1 and 450 MPa. For additional information about these measurements see Table (4.2).

Table 4.2: pH -values of the validation buffer solutions (pH_{Ref}) at different pressures and the findings achieved with PCR including (pH_{incp}) and excluding (pH_{excp}) pressure as an additional input. pH_{Ref}^o is the pH -value of the buffer at ambient pressure. The data of the last three columns is pictured in Figure (4.6) above.

Buffer	p [MPa]	pH_{Ref}^o	pH_{Ref}	pH_{incp}	pH_{excp}
Phosphate	450	2.63	2.02	2.18	2.12
Citrate	200	2.84	2.65	2.66	2.76
Citrate	400	4.04	3.45	3.73	3.69
Acetate	0.1	4.51	4.51	4.49	4.56
Citrate	300	6.06	5.26	4.94	4.88
Phosphate	350	7.28	6.11	5.91	5.82
Phosphate	100	7.39	6.98	7.64	7.77
Phosphate	50	7.96	7.75	7.99	8.10

As can be seen, there is no great difference in the findings of both methods. When including pressure data as an additional input, the empirical variance was

0.35 pH -units, not much more accurate than without. A similar behaviour can be observed for PLS ($\Delta pH = 0.33$).

Indicator dyes are influenced by the ionic strength (see, for example, Galster [177]). To test the system for sensitivity to ionic strength, two Phosphate buffers, one with a high ionic strength (2.80 at 0.1 MPa) and one with a low ionic strength (0.0015 at 0.1 MPa) were used. The calibration buffer and all other validation buffers had an ionic strength of between 0.03 and 0.70. The results of the measurements are shown in Figure (4.7) and Table (4.3).

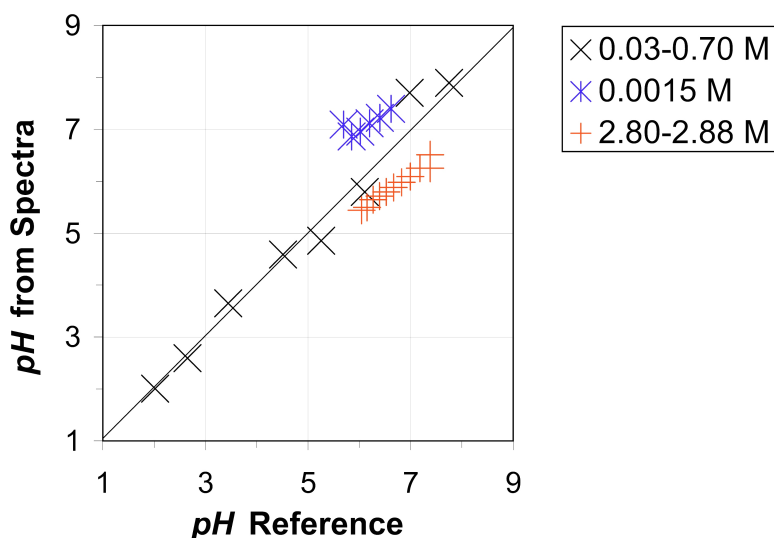


Figure 4.7: Parity plot of the calculated data from thermodynamic (pH Reference) and spectroscopic data using PLS, including pressure data over the full pressure range with different ionic strengths. For additional information about these measurements see Table (4.3).

As can be seen, the deviation increases with the difference between the ionic strength at calibration and the ionic strength at validation (or measurement). Because the ionic strength of a food sample is often unknown, it is not sensible to calibrate with the ionic strength as an additional input. But there are two ways to gather information about ionic strength from the spectroscopic data: one method is to use the different effects of various indicator dyes on ionic strength, which can be measured if there is an overlapping pH -range between adjacent indicator dyes. The other way is to observe the difference between the pH -value measured using the above-described system and the pH -value measured with a glass electrode, both at ambient pressure. The advantage of the first method is that all of the information is contained in the spectra, but calibration measurements over the full range of ionic strength are necessary. Although an array of indicator dyes with overlapping pH -ranges over the full pH -range is required, each pair of adjacent indicator dyes has significant differences in their sensitivity to ionic strength. The

Table 4.3: pH -values of the validation buffer solutions (pH_{Ref}) at pressure p , ionic strength I and the results achieved with PLS (pH_{PLS}) from the spectroscopic data. pH_{Ref}^o is the pH -value of the buffer at ambient pressure. The data of the last two columns is pictured in Figure (4.7).

Buffer	I	p [MPa]	pH_{Ref}^o	pH_{Ref}	pH_{PLS}
Phosphate	0.093	450	2.63	2.02	2.01
Citrate	0.060	200	2.84	2.65	2.60
Citrate	0.228	400	4.04	3.45	3.65
Acetate	0.041	0.1	4.51	4.51	4.59
Citrate	0.581	300	6.06	5.26	4.85
Phosphate	0.267	350	7.28	6.11	5.79
Phosphate	0.267	100	7.39	6.98	7.70
Phosphate	0.289	50	7.96	7.75	7.90
Phosphate	0.0015	0.1	6.62	6.62	7.39
Phosphate	0.0015	50	6.62	6.40	7.22
Phosphate	0.0015	100	6.62	6.20	7.12
Phosphate	0.0015	150	6.62	6.02	6.96
Phosphate	0.0015	200	6.62	5.85	6.86
Phosphate	0.0015	250	6.62	5.70	7.09
Phosphate	2.80	0.1	7.38	7.38	6.51
Phosphate	2.82	50	7.38	7.18	6.25
Phosphate	2.83	100	7.38	7.00	6.09
Phosphate	2.84	150	7.38	6.83	5.98
Phosphate	2.85	200	7.38	6.67	5.88
Phosphate	2.86	250	7.38	6.53	5.80
Phosphate	2.87	300	7.38	6.39	5.72
Phosphate	2.87	350	7.38	6.27	5.64
Phosphate	2.88	400	7.38	6.15	5.50
Phosphate	2.88	450	7.38	6.04	5.44
Phosphate	2.80	0.1	7.38	7.38	6.25

second method used to adjust for changes caused by ionic strength is much easier, but some approximations are needed. Neglecting the change of ionic strength with increasing pressure and approximating that the influence of the ionic strength is the same at different pressures, one can measure the pH -value at ambient pressure with both the above-described system and using a glass electrode, on which the influence of the ionic strength is small.

Therefore, the pH -value can be calculated by Equation (4.3):

$$pH_p = pH_{s,p} - (pH_{s,o} - pH_{g,o}) \quad (4.3)$$

where the subscripts denote the pressure (high pressure: p , ambient pressure: o) and the measuring system (spectrometric: s , glass electrode: g). With this correction, the values from Figure (4.7) reach a better agreement with the reference data as can be seen in Figure (4.8) and Table (4.4).

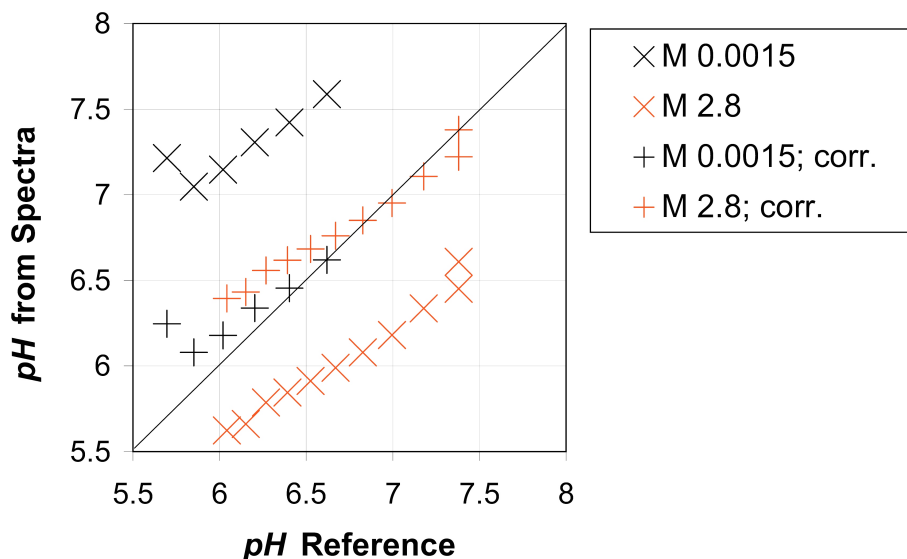


Figure 4.8: Parity plot of the calculated data from thermodynamic (pH Reference) and spectroscopic data over the full pressure range. The values for the buffers with an ionic strength of 0.0015 and 2.80 M (at ambient pressure) are shown with and without correction. The correction of the vertical black and red crosses (+) has been carried out using Equation (4.3). For additional information about these measurements see Table (4.4).

The improvement in accuracy afforded by this simple correction is enormous: the empirical variance for the validation with buffers with an ionic strength of 0.0015 and 2.80 M improves from 0.94 to 0.24 pH -units, a more accurate value than that reached at calibration and validation with a similar ionic strength of between 0.03 and 0.70. A small trend is detectable: a fit of the measured values seems to have a smaller gradient as the plotted bisecting line. This is presumably a characteristic of changes in ionic strength with pressure caused by the dissociation of Phosphate. A calibration which accounts for this is impossible, as changes in ionic strength with pressure are not predictable for samples with unknown ingredients. The influence of buffering agents on the changes in ionic strength are not predictable if the composition of the buffering substances remain unknown.

Table 4.4: pH -values of the validation buffer solutions (pH_{Ref}) at pressure p , ionic strength I and the results achieved with PLS with ($pH_{PLS,corr}$) and without (pH_{PLS}) correction according to Equation (4.3). All buffers are made of Phosphoric Acid. pH_{Ref}^o is the pH -value of the buffer at ambient pressure. Only those buffers are listed here in which the ionic strength at calibration and that at validation differ significantly. The data of the last three columns is pictured in Figure (4.8).

I	p [MPa]	pH_{Ref}^o	pH_{Ref}	pH_{PLS}	$pH_{PLS,corr}$
0.0015	0.1	6.62	6.62	7.59	6.62
0.0015	50	6.62	6.40	7.42	6.45
0.0015	100	6.62	6.20	7.31	6.34
0.0015	150	6.62	6.02	7.15	6.18
0.0015	200	6.62	5.85	7.05	6.08
0.0015	250	6.62	5.70	7.22	6.25
2.80	0.1	7.38	7.38	6.61	7.38
2.82	50	7.38	7.18	6.34	7.11
2.83	100	7.38	7.00	6.18	6.95
2.84	150	7.38	6.83	6.08	6.85
2.85	200	7.38	6.67	5.99	6.76
2.86	250	7.38	6.53	5.91	6.68
2.87	300	7.38	6.39	5.85	6.62
2.87	350	7.38	6.27	5.79	6.56
2.88	400	7.38	6.15	5.66	6.43
2.88	450	7.38	6.04	5.62	6.39
2.80	0.1	7.38	7.38	6.45	7.22

Figure (4.9) shows the course of the pH -value with pressure of a sample of yoghurt centrifugate.

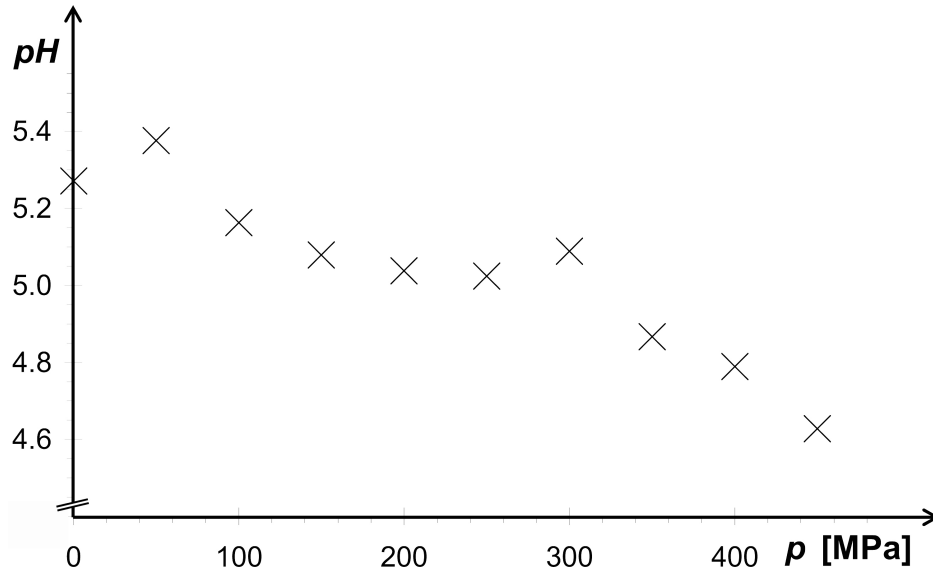


Figure 4.9: Course of the pH -value with pressure of a sample of yoghurt centrifugate.

The values at 50 and 300 MPa do not fit as they are higher than surrounding values, but the deviation is in the range of the accuracy of measurement. What is interesting is that the gradient $\frac{\partial pH}{\partial p}$ seems to increase with increasing pressures. This behaviour is not to be expected as buffering agents in yoghurt centrifugate should behave according to Equation (1.9) (Chapter 1.1.2). But the accuracy of measurement is too low in comparison to the observed effect so that one cannot be sure that yoghurt centrifugate shows an exception.

4.2 Discussion of the pH -Measurements Using Immobilised Indicator Dyes

4.2.1 Data Analysis of the pH -Measurements Using Immobilised Indicator Dyes

As in the high pressure experiments with dissolved indicator dyes, a shift along the Y-axis is noticeable in the range of the spectra where there is no absorption (see Figure (4.11)). Possible reasons for this could be changes in the position of the cuvette during cleaning or changes in the connections between light source/fibre, fibre/optode, or fibre/spectrometer. A correction method similar to the one applied to the absorption spectra of the dissolved dyes was again used with the wavelengths for which no absorption occurred. For the optodes where BTB was used as the indicator dye, the range which shows no absorption is between 750 and 850 nm .

$$I_{\lambda} = I_{m(\lambda)} \cdot \frac{\bar{I}_{m(750-850)}}{\bar{I}_{m(750-850)}(pH3)} \quad (4.4)$$

Here $\bar{I}_{m(750-850)}$ is the average of the intensity between 750 and 850 nm and $\bar{I}_{m(750-850)}(pH3)$ is the same as $\bar{I}_{m(750-850)}$ for the reference measurement at a pH -value of 3. The values labelled with an m are the measured values.

Similar to the measurements with dissolved indicator dyes, a correction is made for fluctuations of the light source according to Equation (4.2).

With the exception of the DLR-optodes from PreSens, all optodes contained BTB as an indicator dye and the spectra of these BTB-optodes were all analysed in the same manner. In the following paragraphs, the derivation of the function that was used to fit the spectral data to the pH -values is given.

In Figure (4.10) the transmission spectra of the alkaline and the acidic form of BTB are shown, as well as the spectra of the Sol-gel plate optode and the Sol-gel fibre optode made with this indicator dye in alkaline buffers. The basic difference between spectroscopic measurements with optodes and solved absorption dyes is that with optodes it is not possible to take a reference spectra without indicator dye. Therefore, these spectra are related to the spectra obtained at a pH -value of 3. As BTB has a pK_a -value of about 7.1, the dye is nearly completely in an acidic form at a pH -value of 3.

The basis for the following calculations is the Lambert and Beer law:

$$\lg \frac{I_{\lambda}}{I_{\lambda}^0} = -\alpha_{(\lambda)}dc. \quad (4.5)$$

Here $\alpha_{(\lambda)}$ is the absorption index for the wavelength λ , c the concentration, and d the length of the sample through which the light beam passes. The length d is unknown for optodes but has the same value for all wavelengths. I_{λ} is the

intensity of light with the wavelength λ after passing through the sample and I_λ^0 is the intensity of light at λ without indicator dye which can only be determined if a form of the indicator dye is colourless at a specific wavelength, for example when $\lambda > 590$ nm for BTB as indicator dye (see Figure (4.10)).

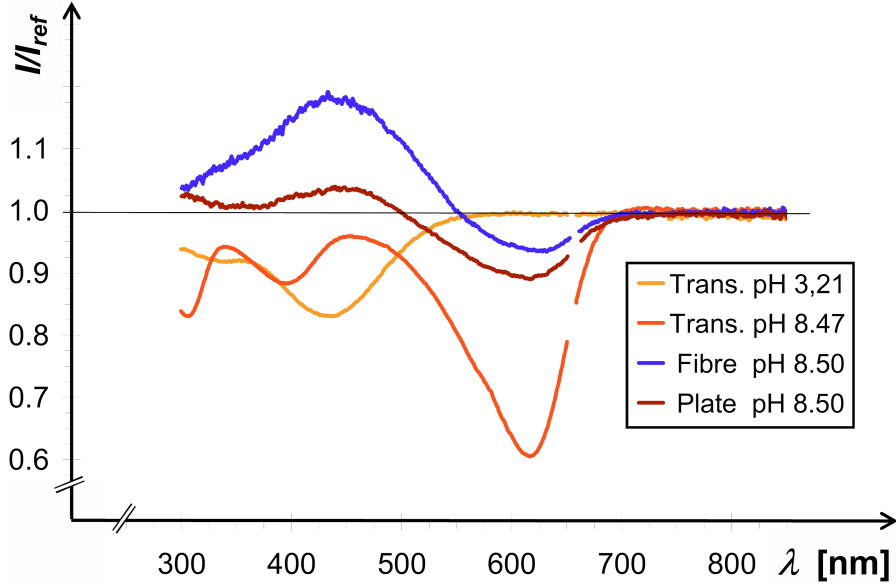


Figure 4.10: Spectra of the indicator dye BTB. The orange and red curves show the transmission spectra of the alkaline and the acidic form (0.1 ml of an indicator solution (0.1004 g BTB/100 ml Ethanol) in a 1 ml TRIS or respectively a Citric acid buffer solution; cuvette: 1 cm/2.5 ml; integration time: 10 ms, average of 100 records); the blue curve shows the signal of the Sol-gel fibre optode in an alkaline buffer and the brown curve the signal of the Sol-gel plate optode (measuring details are described above). As the signals of the optodes are relative to the signals of the same optode at a pH -value of 3, this spectra shows the changes in the absorption, based on the first measurement at this pH -value. There is no data for the wavelengths 653-662 nm because of the intense lines from the Deuterium light source.

In order to obtain a relationship between the spectral data and the pH -value, the ratio of intensity values from a range of wavelengths where only the alkaline form absorbs light (590-652 nm) and from a range of wavelengths where both the alkaline and the acidic form of the indicator dye absorb light with nearly the same α -value (366-391 nm) is taken:

$$\begin{aligned} \frac{\lg \frac{I_{600}^0}{I_{600}^s}}{\lg \frac{I_{375}^0}{I_{375}^s}} &= \frac{-\alpha_{600}dc_{(A^-)}}{-\alpha_{375}dc_\Sigma} \\ &= \frac{c_{(A^-)}}{c_\Sigma} \cdot \frac{\alpha_{600}}{\alpha_{375}}. \end{aligned} \quad (4.6)$$

The values labelled with $_{600}$ are the averages of the range of wavelengths between 590 and 652 nm, and those labelled $_{375}$ correspond to the range of 366-391 nm. $c_{(A^-)}$ is the concentration of the alkaline form of the indicator dye and c_{Σ} is the total concentration of the indicator dye (the sum of the concentrations of the alkaline and the acidic form).

The intensities I_{600} and I_{375} are the measured values (with the correction from Equation (4.4)), $I_{600}^o = I_{600, (pH=3)}$ as the acidic form of the indicator dye does not absorb at wavelengths higher than 590 nm. The parameter I_{375}^o had to be fitted to the measured values (see below). The single values of the concentrations $c_{(A^-)}$ and c_{Σ} are not required as it is possible to find a relation between the fraction $\frac{c_{(A^-)}}{c_{\Sigma}}$ and the pH -value based on the Henderson Hasselbach equation (compare to (2.2)):

$$\begin{aligned}
 pH &= pK_a^* - \lg \frac{c_{(HA)}}{c_{(A^-)}} \\
 &= pK_a^* - \lg \frac{c_{\Sigma} - c_{(A^-)}}{c_{(A^-)}} \\
 10^{(pK_a^* - pH)} &= \frac{c_{\Sigma}}{c_{(A^-)}} - 1 \\
 \frac{1}{10^{(pK_a^* - pH)} + 1} &= \frac{c_{(A^-)}}{c_{\Sigma}}.
 \end{aligned} \tag{4.7}$$

To formulate Equations (4.6) and (4.7) as functions of the fraction $\frac{c_{(A^-)}}{c_{\Sigma}}$ has the further advantage that the system is independent of changing indicator dye concentration, e.g. bleeding out.

The combination of Equations (4.6) and (4.7) leads to:

$$\frac{\lg \frac{I_{600}}{I_{600}^o}}{\lg \frac{I_{375}}{I_{375}^o}} \cdot \frac{\alpha_{375}}{\alpha_{600}} = \frac{1}{10^{(pK_a^* - pH)} + 1} \tag{4.8}$$

$$pH = pK_a^* - \lg \left(\frac{\lg \frac{I_{375}}{I_{375}^o}}{\lg \frac{I_{600}}{I_{600}^o}} \cdot \frac{\alpha_{600}}{\alpha_{375}} - 1 \right). \tag{4.9}$$

In order to determine I_{375}^o Equation (4.8) can be converted to:

$$I_{375}^o = I_{375} \cdot \left(\frac{I_{600}}{I_{600}^o} \right)^{\frac{\alpha_{375}}{\alpha_{600}} (10^{(pK_a^* - pH)} + 1)}. \tag{4.10}$$

For a better possibility of a good fit, Equation (4.8) can be divided into two parts:

$$Y_l = \frac{\lg \frac{I_{600}^o}{I_{600}^o}}{\lg \frac{I_{375}^o}{I_{375}^o}} \cdot \frac{\alpha_{375}}{\alpha_{600}} \quad (4.11)$$

$$Y_r = \frac{1}{10^{(pK_a^* - pH)} + 1}. \quad (4.12)$$

The symbols Y_l and Y_r stand for the left and the right side of Equation (4.8). Ideally they are the same, but if errors in the measurement and in the fit function are accounted for, the following equation is obtained:

$$Y_l = Y_r + e \quad (4.13)$$

with the error e , which has to be minimized by the fit. Y_l is a function of the measured values containing the unknown value I_{375}^o . Y_r is a function of the pH -value and the unknown value pK_a^* . For each set of entered data (I_{375} , I_{600} , pH), one data point of I_{375}^o was reached. Among the range of these values, the value that showed a minimum for e in Equation (4.13) was ascertained. The same applies for the pK_a^* -value of BTB, which depends on the immobilisation matrix. It is possible to calibrate both values, I_{375}^o and pK_a^* independently from each other as the pK_a^* -value only effects a translational displacement along the X -axis and the range of Y_r (Equation (4.12)) must always be between zero and one. Therefore, I_{375}^o can be varied until all points of Equation (4.11) lie on a sigmoidal curve between zero and one and afterwards the pK_a^* -value can be fitted to give a good agreement between Y_l and Y_r . In order to visualise this, Y_l and Y_r are plotted against the pH -value for different optodes in Figures (4.12), (4.19) and (4.20).

4.2.2 Results of the pH -Measurements Using Optodes

Results with Glass Plate Optodes in Cuvettes

The measuring setup for these experiments is given in Figure (3.5a). The optodes were fixed inside a PMMA (Poly(Methyl Methacrylate)) cuvette using a PVC-solution (50 mg PVC in 5 ml THF (Tetrahydrofuran)) as adhesive. The cuvette was placed in a cuvette holder with connector pins for optical fibres and integrated lenses (originally used for transmission measurements). The spectra were recorded in transmission mode, with a reference "white" spectra at a pH -value of 3. The measurements were averaged over 50 records with an integration time of 30 ms.

Before each measurement the cuvette was cleaned with deionised water and rinsed twice with the buffer solution which was used for the measurements. Figure (4.11) shows the spectra obtained using a Sol-gel plate optode. The value on the

Y-axis is the intensity relative to that achieved at a pH -value of 3. As BTB has a pK_a -value of about 7.1, the dye is almost completely in the acidic form at this pH -value.

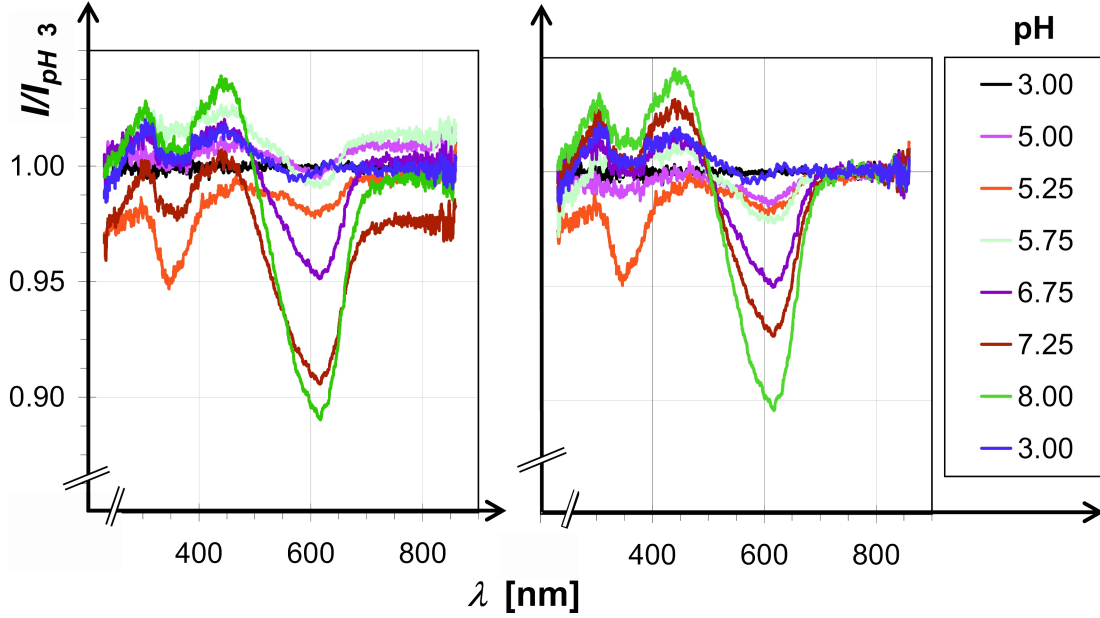


Figure 4.11: Spectra obtained using a Sol-gel plate optode at different pH -values. The value I/I_{pH3} is the intensity at a particular wavelength relative to the intensity at the pH 3 buffer. The spectra on the right hand side were corrected by relating I/I_{pH3} to the average of the I/I_{pH3} for the range of wavelengths between 750 and 850 nm (Equation (4.4)). The measurements are in the order of increasing pH -values except for the dark blue line which was the last measurement and which was taken at a pH -value of 3. There was no data for wavelengths between 654-659 nm because of the strong line of the Deuterium light source.

As can be seen, there is a clear dependency of the spectra on the pH -value. At pH -values above 9 an elution of the dye was clearly visible to the naked eye. The last measurement at a pH -value of 3 shows high intensities at wavelengths between 400 and 550 nm, a range where the dye absorbs light at low pH -values. As the intensities are based on the first measurement at a pH -value of 3, there should be a straight line at $I/I_{pH3} = 1.00$. This deviation is an indication that an elution has taken place during the measurements.

Figure (4.12) shows the result of a fit to Equations (4.11) and (4.12) with the data from a Sol-gel plate optode. The crosses correspond to Equation (4.11) with measured intensity values, while the line corresponds to Equation (4.12) with a fitted value for the pK_a^* . All measured values are near the calibration curve, but an accurate determination is only possible for values near the pK_a^* -value (7.28) because the red curve is steeper in this range.

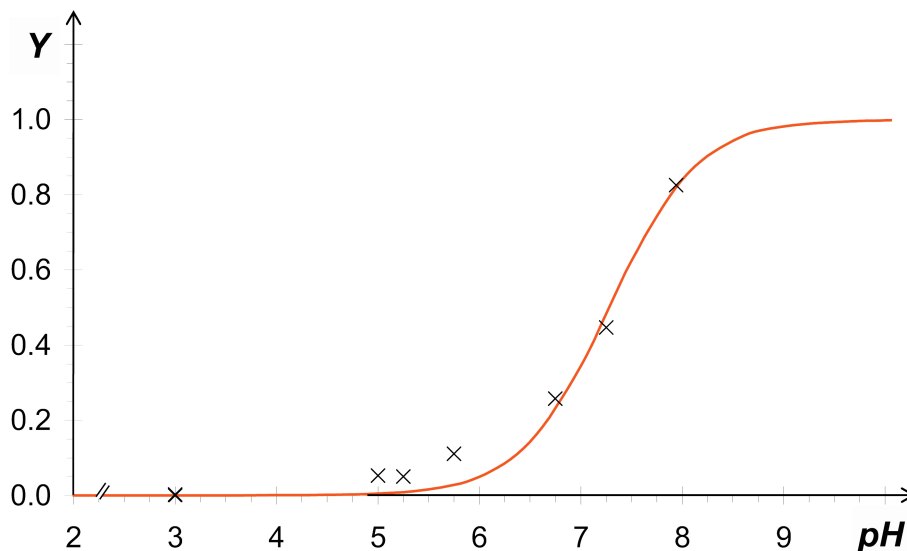


Figure 4.12: The intensity relation for the fit of measured values on Equations (4.11) and (4.12). The values on the Y-axis are Y_r (Equation (4.12)) for the red line, and the crosses represent the Y_l -values obtained from the spectral data according to Equation (4.11) at the corresponding pH -values. The measurements were carried out using a Sol-gel plate optode with different buffers at ambient pressure. The pK_a^* -value in Equation (4.12) was found by trial. The best fit was achieved with $pK_a^* = 7.28$ in Equation (4.12).

Results with Optodes on a Sapphire Window of a High Pressure Cell

These tests were similar to those carried out with glass plates in cuvettes, described in the last chapter. But in these experiments a sapphire window from a high pressure cell was used instead of the cuvette. All glass plate optodes described in Chapter 3.3.2 as well as one dual lifetime referenced (DLR) optode commercial available from PreSens were tested.

The setup is pictured in Figure (4.13).

The first tests were carried out at ambient pressure by dipping the optode, which was fixed on the sapphire window, into a buffer solution inside a darkened housing. No pH -dependent signal was found for all optodes made in our own laboratories, although a colour change was visible to the eye. This could be attributed to reflections on the air/sapphire, sapphire/adhesive, adhesive/glass and glass/immobilisation matrix interfaces.

Another disadvantage of the ion exchanger and the polyamide optodes is the fast bleeding-out of the dye.

Although the setup for the optodes from PreSens are similar to the optodes made in our laboratories, a significant change in the signal was detected. The most probable reason for this difference is the use of a fluorescence indicator dye (7; 8-Hydroxy-1, 3, 6-Pyrenetrisulfonic acid) instead of BTB. Another potential

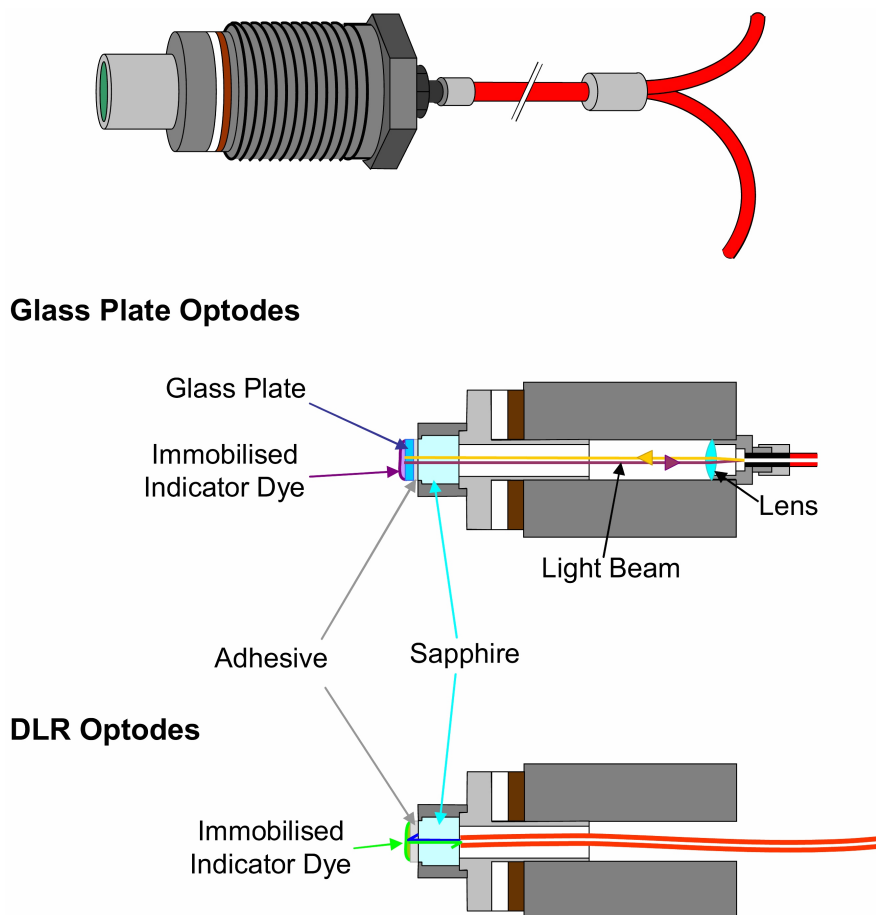


Figure 4.13: Setup for the pH -measurements using optodes fixed on a high pressure window. The picture at the top shows the high pressure window unit with an optode from the outside. The two pictures below show cross-sectional drawings. The picture in the middle is the setup for the glass plate optodes made in our own laboratories. The bottom picture shows the setup with the commercially available DLR optode from PreSens.

reason for this could be the fact that the optode from PreSens has one interface less than the optodes made in our laboratories (the indicator was immobilised in a hydrogel which was fixed with a silicone as adhesive; all other optodes had a glass plate between the immobilisation matrix and the adhesive (see Figure (4.13))).

The setup for the measurements taken with the dual lifetime referenced optode from PreSens differs somewhat from the other measurements as it is based on the dual luminophor reference method. This method needs a special light source and a special photodetector; a complete instrument including these components was used. This instrument needs no branched fibre, as the light beams are separated

inside the instrument. As the fibre that belongs to this instrument had a different connector than those used in the previous measurements, it was not possible to connect it to the lens. Thus, the fibre was fixed by an adhesive strip directly into the drill hole leading to the sapphire (see Figure (4.13) bottom). The DLR optode operates with a pH -independent long decay time reference dye and a short decay time indicator dye which changes the intensity of its fluorescence based on the pH -value; both luminophores have similar excitation and absorption spectra. Besides the intensity, the average decay time was also measured to determine the ratio of the intensities of the fluorescent dyes. Thus, the signal was internally referenced and therefore insensitive to any fluctuations of the light source or to changes in the optical path (see also Chapter 2.3.3).

The light source was a blue LED with sinusoidally modulated intensity (modulation frequency: 49 kHz; GaN, $\lambda_{max} = 470$ nm, the same type of LED as the blue one in Figure (2.5), Chapter 2.3.3). The light was detected with a single photodiode located behind a filter which is translucent for the emitted yellow-green light. Using an RS 232 interface it was possible to control the measuring device with a computer. The output signal contained information about both intensity and phase shift of the emitted light.

Figure (4.14) shows the detected signals of both the phase shift and intensity measured at ambient pressure with different buffer solutions. Both signals vary significantly with the pH -value and a fit similar to that for the Sol-gel plate optodes (but with the tangent of the phase angle Φ , for the derivation see [208]) leads to an accurate fit as can be seen in Figure (4.15).

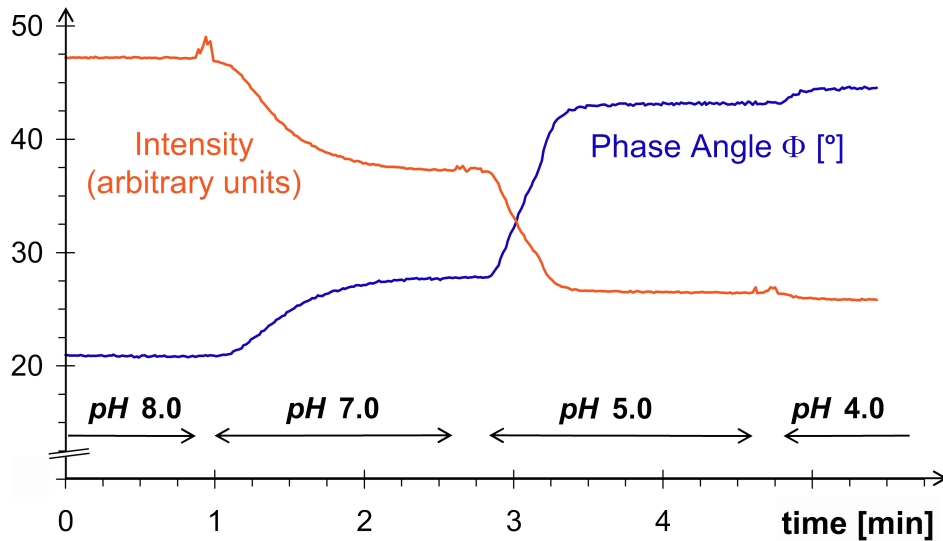


Figure 4.14: Intensity of the emitted light (red) and the phase angle Φ (blue) between the exciting light and the emitted signal. These values were achieved with DLR optodes with different buffers at ambient pressure.

The fact that the phase shift is less susceptible than the intensity to interferences, such as those caused by movements of the window and the optical fibre during the changing of buffer solutions, can be seen by comparing both curves; this is especially distinct between the buffers at pH -values of 8.0 and 7.0.

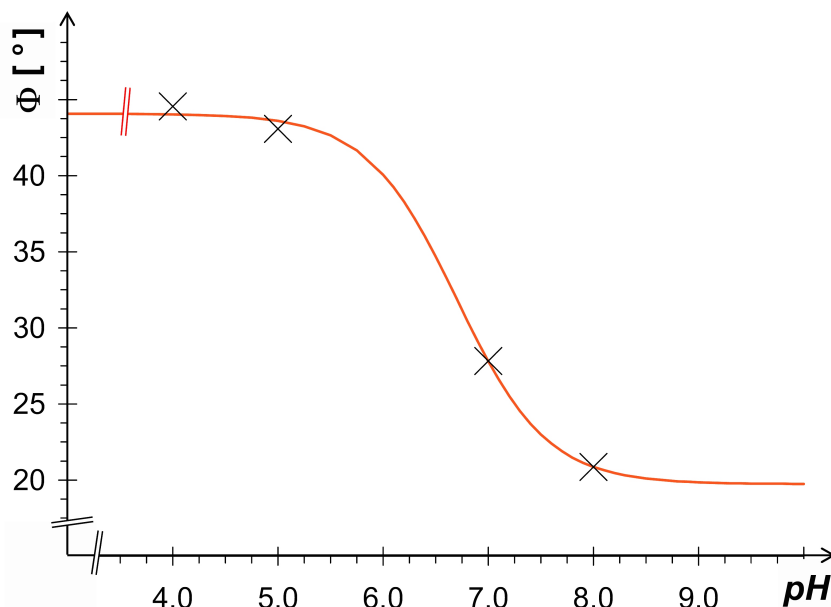


Figure 4.15: The phase angle Φ as function of the pH -value; achieved with DLR optodes with different buffers at ambient pressure. The crosses are the average of the measured buffers pictured in Figure (4.14). The red line fits to a spline of $\ln(\tan(\Phi))$ on $\frac{a_1}{10^{(pK_a^* - pH)} + 1} + a_2$ to these values (A derivation of this correlation is given in [208]). The best agreement was found with $a_1 = 0.80323$, $a_2 = -7.8340$ and $pK_a^* = 6.871$.

As the results of the measurements through a high pressure window were only reliable for the DLR optodes from PreSens, these optodes were chosen for the high pressure tests. For these tests, an optode with a thicker luminescent layer than that used at ambient pressure was implemented. The result was a stronger signal, but with the disadvantage of a slower response.

Figure (4.16) shows data from both phase shift and intensity, measured at different pressures and with different buffer solutions.

Both the phase shift and the intensity showed a significant dependency on the pH -value and pressure. But both signals do not revert to their original value after pressurisation, especially with alkaline pH -values, and this makes calibration impossible. A possible reason for this phenomenon are potential changes in the lumiphores, such as bleeding-out or decomposition. Another reason could be changes in the immobilisation matrix leading to charge differences between the phase interfaces (similar to Reaction (14) in Chapter 2.2) which would influence the equilibrium of the indicator dye.

In Figure (4.16) the different response of the two curves with regard to pressure change is remarkable. This can be most clearly observed during the pressure reduction with the citrate buffer. Unlike the phase shift, light intensity is not only a function of the pH -value and pressure, it depends also on the gradient of pressure. Such differences are caused by changes in the optical path (fluctuation of the light source is another variant, but was ruled out as it has no dependence on pressure). As the differences only appear when the pressure changes, there seems to be a movement of the optode on the window during this process.

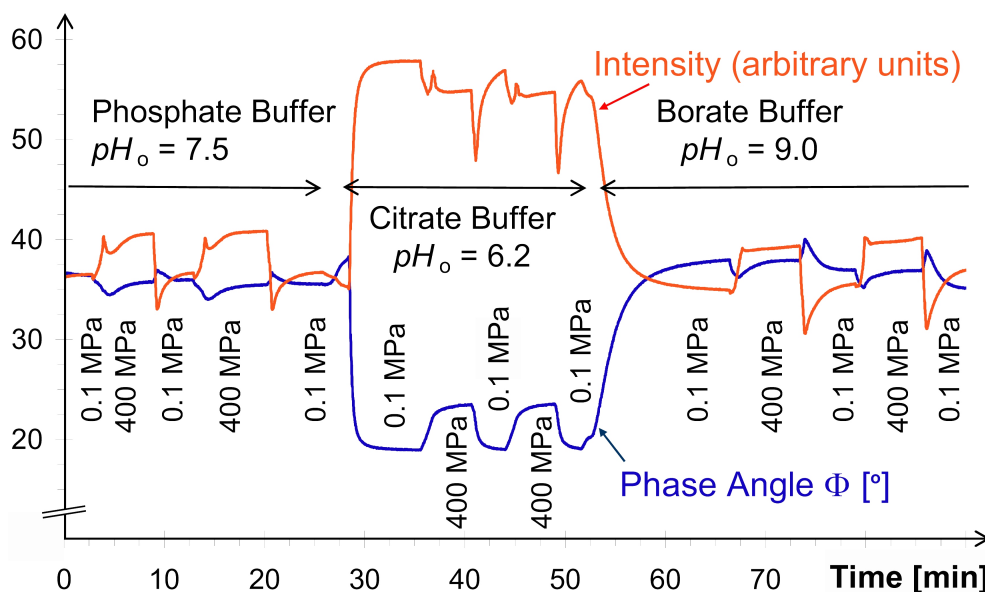


Figure 4.16: Intensity of the emitted light (red) and the phase angle Φ (blue) between the exciting light and the emitted signal. These values were achieved using DLR optodes with different buffers and at different pressures.

Results with Optodes as Detecting Layer Directly on the Glass Fibre

In order to test the optodes with the pH -sensitive layer directly on the end of the fibre, the fibre was coupled with a direct contact to the branched fibres (see Figure (4.17)).

The branch in the fibre was created by arranging the two fibres side by side in an SMA-SMA coupler. The direct contact between the measuring fibre and the branched fibre in an SMA-SMA coupler caused a loss in light, but nevertheless the light was sufficient for the measurements. Results were only adequate if both ends of the fibres stayed close together to avoid reflections. Figure (4.18) shows the spectra achieved with a Sol-gel fibre. The spectra were taken in transmission mode with a reference ("white") spectra at a pH -value of 3. The final value was an average of 20 records, each with an integration time of 500 ms.

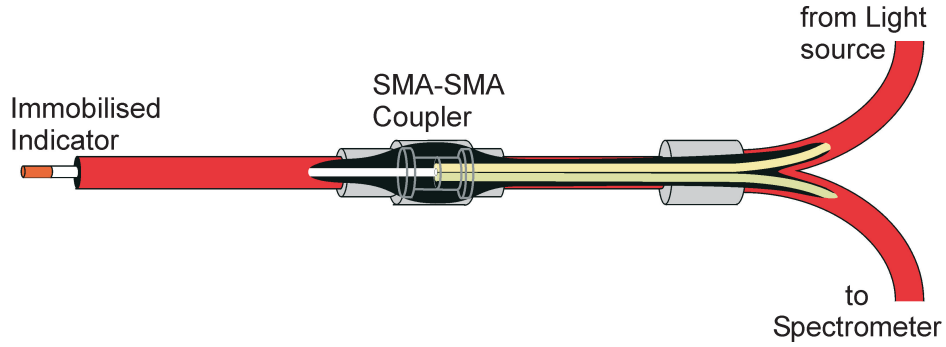


Figure 4.17: Setup for the measurements with the optode directly on the fibre.

Compared to the spectra of the Sol-gel plate optode in Figure (4.11), the peak at high pH -values between 300 and 550 nm is more noticeable in the spectra of the Sol-gel fibre (see also the blue and the brown line in Figure (4.10)). The reason for this is that over time the indicator dye bleeds out. The range of 366-391 nm is a range where both forms of the indicator dye show similar absorption behaviour. Thus a decrease in absorption in this range is an indication of a decreasing concentration of both forms of the indicator dye. Figure (4.19) shows the result of the fit of the measured values using Equation (4.8).

A ratio of the fitted value I_{375}^o with the intensity I_{375} for this measurement shows that there is only about one third of the indicator dye left when compared with the first measurement at a pH -value of 3:

$$\begin{aligned}
 \frac{\lg \frac{I_{375;1}}{I_{375}^o}}{\lg \frac{I_{375;2}}{I_{375}^o}} &= \frac{-\alpha_{375} d c_{\Sigma_1}}{-\alpha_{375} d c_{\Sigma_2}} \\
 \frac{c_{\Sigma_1}}{c_{\Sigma_2}} &= \frac{\lg \frac{I_{375;2}}{I_{375}^o}}{\lg \frac{I_{375;1}}{I_{375}^o}} \\
 &= 0.31.
 \end{aligned} \tag{4.14}$$

Here, $I_{375;1}$ is the average intensity between 366 and 391 nm of the first measurement, $I_{375;2}$ that of the actual measurement and c_{Σ_1} and c_{Σ_2} are the sums of the concentrations of both forms of the indicator dye of the first and the actual measurement.

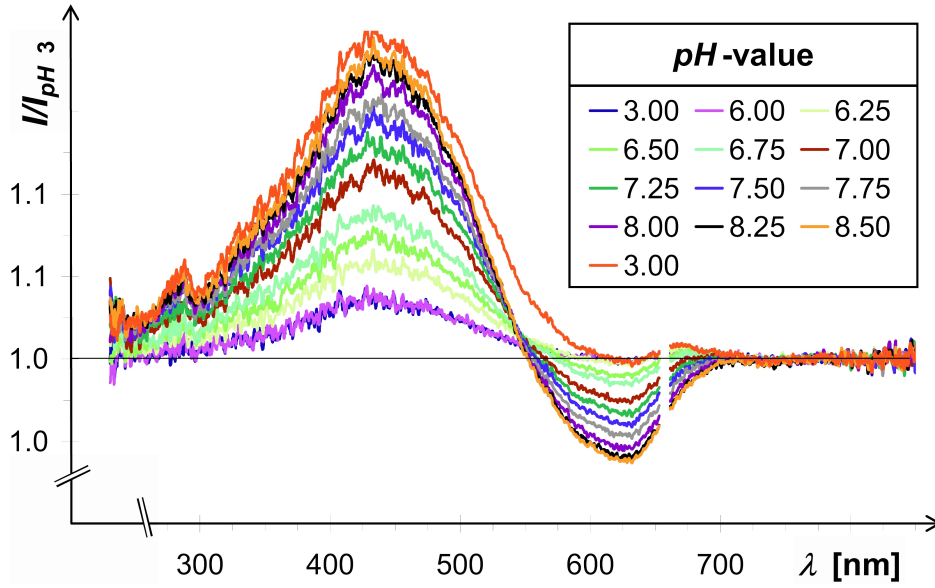


Figure 4.18: Spectra obtained with a Sol-gel fibre optode at different pH -values. The value I/I_{pH3} is the intensity relative to the intensity at the same wavelength in a pH 3 buffer, corrected by relating the averages of the values between 750 and 850 nm (Equation (4.4)). The measurements are in the order of increasing pH -values, except for the last measurement at a pH -value of 3 (red). There is no data for the wavelengths 653-662 nm because of the intense lines from the Deuterium light source.

While the bleeding out of the indicator dye occurred as the pH -value of the calibration buffers was increasing (except the last value), the level of accuracy observed can be misleading. To verify this, a second fibre optode was made in the same manner as the one described above. In contrast to the measurements with the fibre optode just discussed, the ordering of the pH -values of the buffers was random, to avoid the overlay of the following two effects: changing spectra due to changing pH -values, and bleeding out of the indicator dye. The spectra are similar to those of the first fibre optode. A fit to Equation (4.6) is shown in Figure (4.20).

As can be seen in the comparison of Figures (4.19) and (4.20), the fit on the measurements with a random order of pH -values shows less agreement of Equations (4.12) with (4.11). Therefore the results of the fibre optode measured in a regular order of pH -values should be handled with care. The results obtained with the Sol-gel ball optodes were similar to those with Sol-gel fibres, but a less intensive signal was recorded and this led to a greater signal-to-noise ratio.

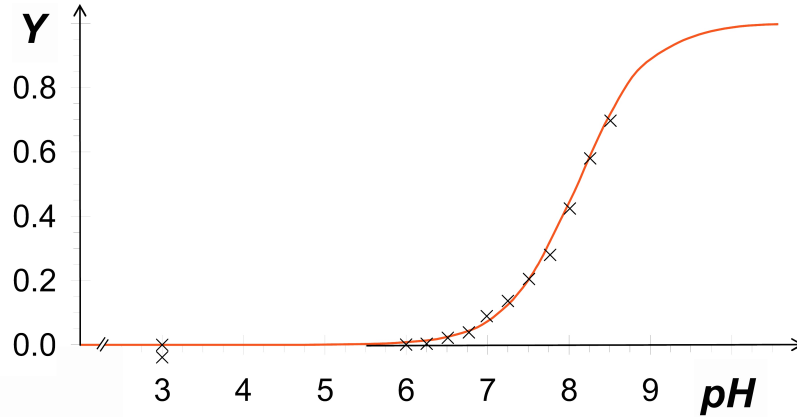


Figure 4.19: The fit of the intensity relationship of measured values using Equation (4.11) and those based on Equation (4.12). Measurements were carried out using Sol-gel fibre optodes with different buffers at ambient pressure. The values were recorded as the pH -value increased, except for the last value at a pH value of 3. The Y -axis for the red line is Y_r of Equation (4.12). The Y -axis for the crosses is Y_l which was obtained from the spectral data according to Equation (4.11) at the corresponding pH -values. The pK_a^* -value in Equation (4.12) was found by trial. The best fit was found with $pK_a^* = 8.10$.

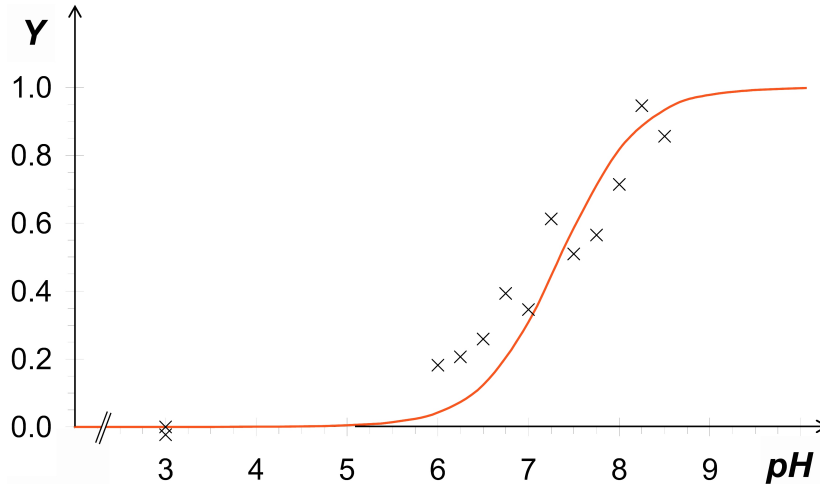


Figure 4.20: The fit of the intensity relationship of measured values using Equation (4.11) and those based on Equation (4.12). Measurements were carried out using the Sol-gel fibre optodes with different buffers at ambient pressure. The Y -axis for the red line is Y_r of Equation (4.12). The Y -axis for the crosses is Y_l which was obtained from the spectral data according to Equation (4.11) at the corresponding pH -values. The pK_a^* -value in Equation (4.12) was found by trial. The best fit was found with $pK_a^* = 7.21$. In contrast to Figure (4.19), the buffers were sampled in a random order.

4.3 Results of the Investigations into pH -Inhomogeneities in High Pressure Vessels

As mentioned earlier, pH -value strongly influences biochemical reactions. Thus, a knowledge of the pH -value throughout the sample would be helpful. A generation of pH -gradients will take place if inhomogeneous samples are pressurised. The results presented here show that the time necessary to homogenise the pH -value can be long compared to the time usually applied for high pressure treatment of food.

The measurements were implemented as described in Chapter 3.4. Figure (4.21) shows a typical run of the intensities of transmitted light at selected wavelengths of an experiment with an absorption indicator dye.

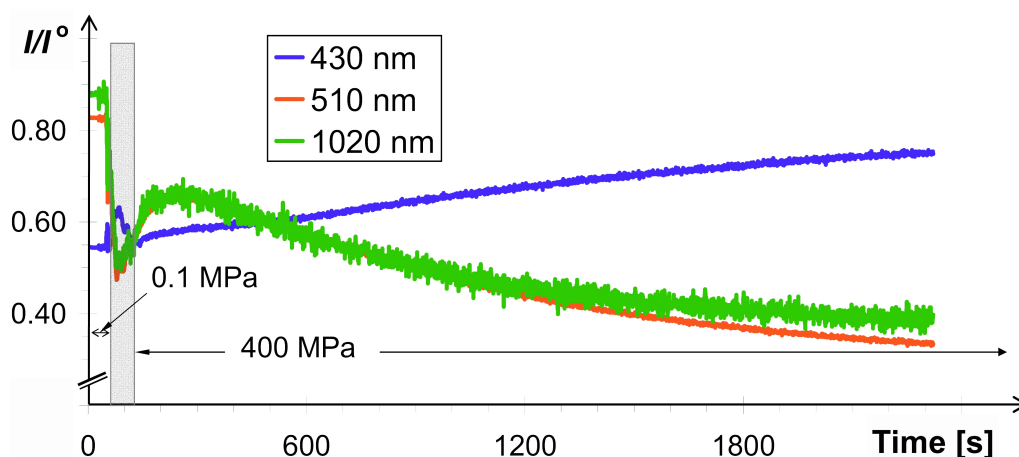


Figure 4.21: Progression of pH -homogenisation in a high pressure vessel at 400 MPa. A 1.1 M HCl solution is forced into an optical cell filled with a 0.1 M Imidazole buffer (Imidazole/ HCl pH 7.0). Both solutions contain the indicator dye Phenol Red (0.4 ml of indicator dye solution (0.1 g Phenol Red in 1 l 20% Ethanol) in 100 ml Buffer/ HCl). During the mixing of the two solutions the colour of the indicator dye changes (at the beginning most of the optical path contains the Imidazole buffer). This colour change is pictured for the intensities at wavelengths where the greatest changes appear (430, 510 and 1020 nm, see Figure (4.22)). The value I/I° is the intensity I of the light passing the sample relative to the intensity I° with water in the measuring cell at ambient pressure.

The spectra for this indicator dye at 400 MPa with different pH -values is pictured in Figure (4.22).

It was found that the homogenisation time in the optical cell (2 ml) is between 10 minutes and 5 hours for experiments where 1 M HCl or KOH is pressurised in a 0.1 M buffer solution. The measurements only yield interpretable results if a solution of a strong acid or base with high molality (about 1 mol/kg) is pressurised

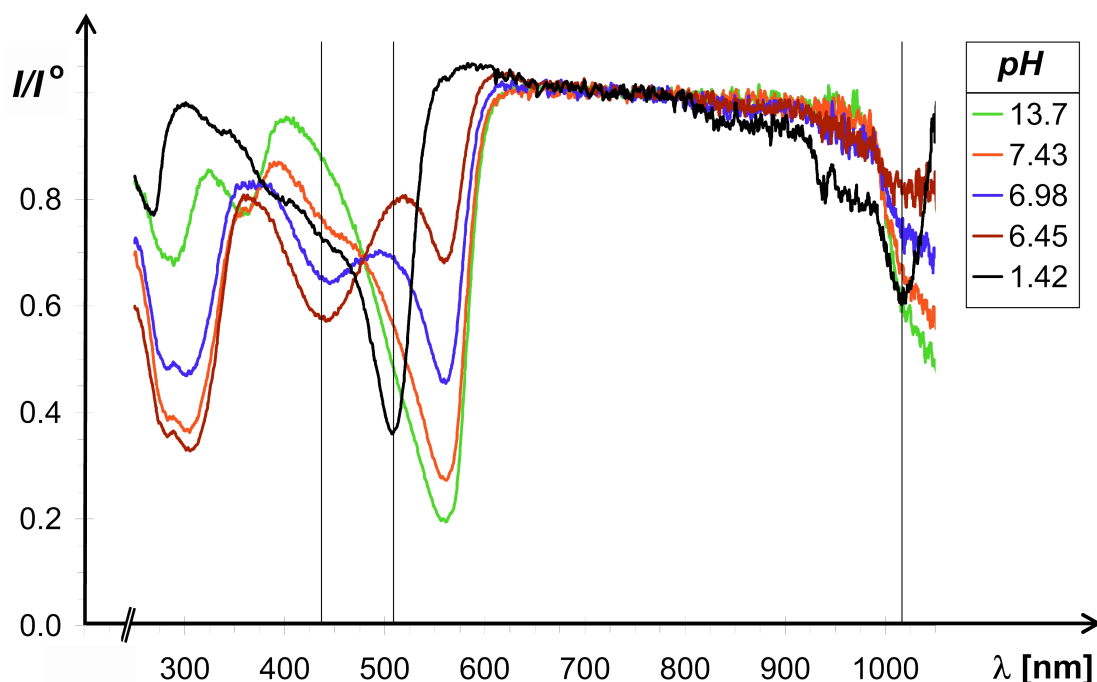


Figure 4.22: Spectra of the indicator dye Phenol Red at 400 MPa for different pH -values (0.1 ml of a indicator solution (10 mg Phenol Red in 100 ml 20% Ethanol) in 25 ml Buffer). Apart from the spectra at pH -values of 13.7 and 1.42 the measured spectra are from a mixture of the different forms of Phenol Red similar to that of Phenolphthaleine in Reaction (21). The wavelengths in which the absorptions are plotted against the time in Figure (4.21) are marked by a black line.

in a buffer solution with lower molality (about 0.1 mol/kg). The reason for this is possibly a mixing due to a forced convection by the added solution. The homogenisation caused by such a mixing is so fast that it is difficult to follow. If the added solution has a high molality the convection is small due to the higher density.

An example of measurements with fluorescent indicator dyes is given in Figure (4.23). The optical cell was filled with Phosphoric acid containing the indicator dye (1 ml Phosphoric acid 80% + 1 ml Florescein Solution (1 g/100 ml Ethanol) + Water up to 100 ml). In this solution a 1 M KOH solution was pressurised containing the same amount of the indicator dye. It was possible to observe with the help of the camera a boundary between the alkaline part of the solution with a yellow-green fluorescence and the acitic part which showed no fluorescence. To illustrate this, the top of Figure (4.23) shows three pictures taken during the experiment. It took about 4 hours for this boundary to travel the distance of the window (diameter: 6 mm). This is also the time in which a sharp increase in emitted light was observed at the spectrometer (see Figure (4.23 bottom)).

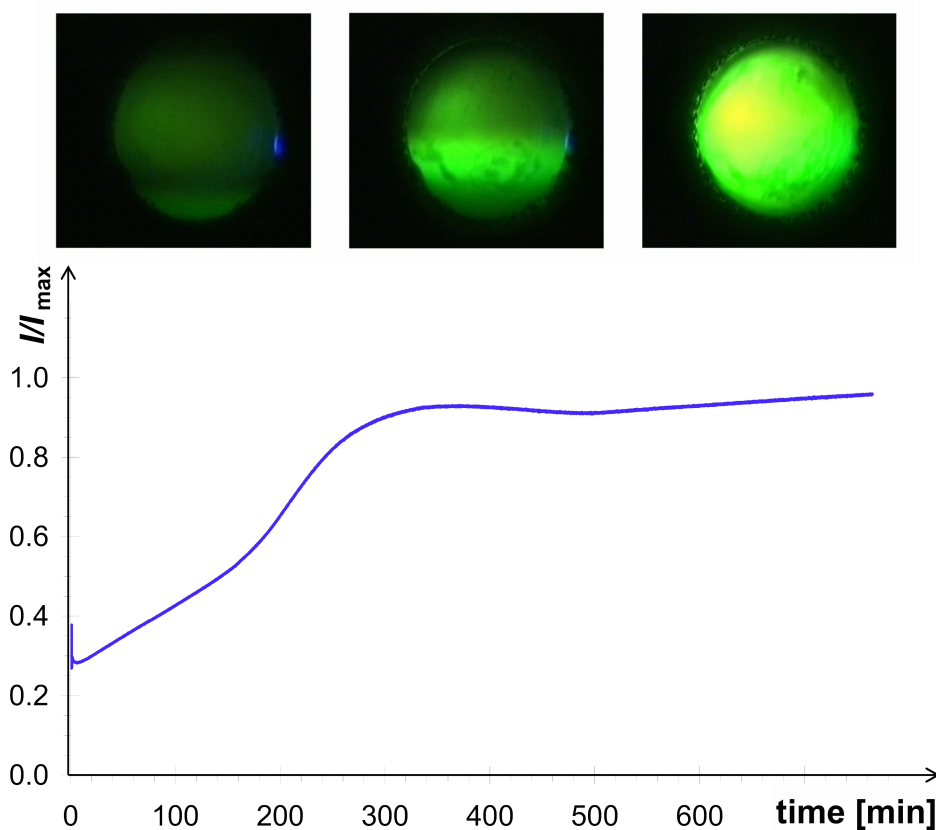


Figure 4.23: Progression of pH -homogenisation in a high pressure vessel at 400 MPa. A 1 M KOH solution is forced into an optical cell filled with diluted Phosphoric acid. Both solutions contain the indicator dye Fluorescein. During the mixing of both solutions the fluorescence of the indicator dye increases (at the beginning most of the optical path contains the Phosphoric acid; in acidic solutions there is no fluorescence of Fluorescein). The top part shows three pictures taken with the video camera, the picture on the left was recorded just after the pressure increase caused by pressurising the alkaline solution in the cell; the middle picture was taken after 2:31 hours and the right picture shows the end of the experiment after 6:27 hours when all of the observed part of the sample was alkaline. The intensity of the fluorescence observed by the spectrometer is plotted on the bottom for the wavelengths where the greatest intensity of emissions appear (500-520 nm, arithmetic average). I_{max} is the highest observed intensity at this range of wavelengths (500-520 nm, arithmetic average).

4.4 Conclusions and Outlook

During high pressure processing of food, the pH -value affects many phenomena and processes, e.g. protein properties such as denaturing, gelification, enzymatic activities, the growth and mortality of microorganisms, the germination or inactivation of bacterial spores, and chemical reactions such as Maillard Browning. At high pressure, the pH -value varies significantly with the absolute pressure level due to changing dissociation constants of attendant acids and bases. The equilibria of reactions forming or dissipating ions or those which change the charge of existing ions, such as the dissociation of acids or dissolving of salts, depend on pressure as equilibrium constants and activity coefficients are both functions of pressure. In particular, acid-base reactions, which are responsible for the pH -value of the medium and for reactions of food ingredients such as proteins, play an important role in high pressure microbiology and food science. To understand more about such reactions it is important to recognise the pressure behaviour of such reactions. In this thesis the background and the most important methods from previous studies to determine this pressure behaviour were introduced and discussed, specifically for reactions affecting the pH -value. The reason for the changes of equilibrium constants with pressure and the basis for the calculation is the volume change accompanying a reaction. This volume change is caused mainly by the electrostatic interaction between an ion and surrounding water. A comprehensive theory has not yet been proposed, but some models described in the literature show an adequate agreement with existing measurements and can be used to interpret experimental results.

A starting-point for a theory describing the interaction between ion and water could be a comparison of the pressure behaviour of equilibrium constants with the many other properties influenced by these interactions. These properties are activity coefficients, reaction rates, equilibrium constants, conductivities, viscosities, densities, refraction indices, electrode processes, dielectric permittivities and so on as functions of pressure, temperature and ionic strength in different solvents. Many experiments have been performed to explain these properties, but models derived from this experimental data often account for only one or a few of these properties. For example, the model of different structures occurring in liquid water, which has been proven to explain such properties as how pressure and temperature affects density and viscosity of water, has not been applied in characterising the behaviour of activity coefficients, reaction rates, equilibria constants and refraction indices. An account on the findings of all experiments and developed models could be useful in finding a theory to describe the complicated interactions between ions and solvents which are a key to understanding the behaviour of ionic solutions under high pressure.

The pressure dependency of the pH -value of food cannot be predicted as its composition is often unknown, and even with a known composition many equilibrium constants are still unknown. The study of the high pressure handling of

food requires simple and fast measuring methods for the determination of fundamental thermodynamic values such as the pH -value. Thus a pH -measuring device was developed for application at pressures of up to 450 MPa. Different methods of pH -measurement are discussed and tested for a possible adaption to high pressure. Various methods should in theory be applicable to high pressure, they are based on either electrochemical or optically detectable reactions. Electrochemical methods suffer from difficulties with the reference element. Either such reference elements show interactions with the sample solution or a liquid junction, integrated in the device to avoid such interactions, causes inaccuracies. Among the optical methods, measurement of the pH -value using the colour change of indicator dyes has been proved to have the greatest potential.

An optical in-situ pH -measurement system with absorbance measurements of indicator dyes for fluid food at pressures of up to 450 MPa was developed for use in the pH -range of 2.0 to 8.0. Through a high pressure cell with sapphire windows a light beam passes the sample and the intensity modifications were observed with a spectrometer. For analysis of the spectral data and the calculation of the pH -value, chemometric methods were used. The calibration was performed with buffer systems, whose pressure dependency is known from theoretical calculations. The achieved accuracy was 0.24 pH -units.

Compared to the large influence of small changes in the pH -value on biological media and food ingredients the precision reached is not great, but exact pH -measurements are rarely possible even at ambient pressure. For an example, [246] describes a comparison of different laboratories which measured pH -values with a glass electrode according to a very elaborate method. They allowed the electrode 30 minutes to settle for both calibration and measurement and used no liquid junction. As the potential of the reference Ag|AgCl-electrode depends on the Cl^- -concentration if no liquid junction is used, the Cl^- -concentration was determined by a further analysis step (gravimetries or titration). Using these methods they reached an accuracy of 0.02 pH -units. As common laboratory measurements cannot normally afford such a time-consuming method, routine measurements with glass electrodes show accuracies of about 0.05 to 0.1 pH -values.

Until now, the effects of temperature and interactions between food ingredients such as alcohol or proteins with some of the indicator dyes have not been considered. Such interactions are described in literature (e.g. [202, 203, 247]) and consequently, it must be examined in which way the accuracy of the system is influenced by these interactions. While the pH -value and sensitivity on the pH -value is also influenced by temperature, and high-pressure food treatment is often accompanied by additional heat or at least self-heating due to compression, it is necessary to extend the calibration to include temperature.

For opaque and strongly coloured samples which cannot be measured using the described system, an adaptation of the used configuration was tested with indicator dyes fixed at the end of a fibre optic cable, or on a film on a sapphire

window integrated into the high pressure vessel. Instead of the transmitted light, the reflected or emitted light was measured. Further benefits include an easier setup and a better protection of the indicator substances against reactions with proteins or alcohol.

Most of the methods tested to immobilise indicator dyes were not able to fix the dyes for an adequate time. Among them only Sol-gel showed enough stability to take some measurements. The best fixation of the dyes was achieved by using a commercially available optode made from a hydrophobe polymer as immobilisation matrix. This optode used a fluorescence indicator dye and was the only optode whose signal-to-noise ratio was high enough to reach a satisfactory accuracy when included in the high pressure setup. For the other optodes, the ratio between the light passing the indicator layer and that being reflected elsewhere onto the optical path was too low. But for the fluorescence optodes with a good signal this signal showed a drift during high pressure measurements, possibly due to ionic reactions on the surface, leading to potential differences which influence the equilibrium of the indicator dye. During this work it was not possible to eliminate such reactions or to find a way to correct their influence, but this could be a starting point for further investigations.

The investigations about the time needed for homogenisation, if pH -gradients appear, are not comprehensive, but nevertheless show that in some cases the time required for such an adjustment is great compared to the time commonly used in pressure treatments of food. Even in the small measuring cell used, with diameter 1 cm, homogenisation times of up to 5 hours could be observed. Therefore, the assumption often used that pH -value is always evenly distributed across a sample is not valid.

Chapter 5

Appendix

5.1 Auxiliary Calculations

5.1.1 Derivation of Equations Used in the Text

Calculations of the Sensitivity σ

Following, the detailed calculation steps which lead from Equation (2.2) and (2.3) to equation (2.4) in Chapter 2.1 are itemised.

$$\begin{aligned}
 \frac{K_a^*}{a_{(H^+)}} &= \frac{c_\Sigma}{c_{(HA)}} - 1 \\
 c_{(HA)} &= c_\Sigma \frac{a_{(H^+)}}{K_a^* + a_{(H^+)}} \\
 \frac{1}{c_\Sigma} \left(\frac{dc_{(HA)}}{dpH} \right) &= \frac{1}{c_\Sigma} \left(\frac{dc_{(HA)}}{da_{(H^+)}} \frac{da_{(H^+)}}{dpH} \right); \quad a_{(H^+)} = 10^{-pH} \\
 &= -\frac{\ln(10) K_a^* a_{(H^+)}}{(K_a^* + a_{(H^+)})^2} \\
 &= -\frac{\ln(10)}{\frac{K_a^*}{a_{(H^+)}} + 2 + \frac{a_{(H^+)}}{K_a^*}} \\
 &= -\frac{\ln(10)}{10^{(pH - pK_a^*)} + 2 + 10^{(pK_a^* - pH)}} \tag{5.1}
 \end{aligned}$$

1

¹With the assumption that the accuracy of a_{HA} is independent from the value of a_{HA} .

Calculations of the Sensitivity $\partial I/\partial pH$ for pH -Measurements with Indicator Dyes (Chapter 2.1)

The pH -value measurement with indicator dyes is based on absorption measurement, described by the law of Lambert and Beer (4.5). If other errors such as protein errors, incorrect concentration of the indicator dyes and changes of the cell geometry are excluded, the inaccuracy of the measurement is a result of only the error in the determination of I and I° . A reasonable definition for the sensitivity σ_I (the subscript I denotes measurements with indicator dyes) is therefore (as in Chapter 2.1 with that HA as the coloured form of the indicator dye):

$$\sigma_I \equiv \left| \frac{\partial I}{\partial pH} \right| + \left| \frac{\partial I^\circ}{\partial pH} \right| = \left(\left| \frac{\partial I}{\partial c_{HA}} \right| + \left| \frac{\partial I^\circ}{\partial c_{HA}} \right| \right) \cdot \left| \frac{\partial c_{HA}}{\partial pH} \right| \quad (5.2)$$

using the same assumption $\partial c_{HA} \approx \partial a_{HA}$ as in Chapter 2.1 it is possible to include Equation (2.4):

$$\sigma_I \equiv \frac{\partial I}{\partial pH} + \frac{\partial I^\circ}{\partial pH} = \left(\frac{\partial I}{\partial c_{HA}} + \frac{\partial I^\circ}{\partial c_{HA}} \right) \cdot \frac{\ln(10)}{10^{(pK_a^* - pH)} + 2 + 10^{(pH - pK_a^*)}}. \quad (5.3)$$

The derivations $\frac{\partial I}{\partial c_{HA}}$ and $\frac{\partial I^\circ}{\partial c_{HA}}$ can be derived from the law of Lambert and Beer (Equation 4.5):

$$\frac{I}{I^\circ} = e^{-\alpha d c_{HA}} \quad (5.4)$$

$$\frac{\partial I}{\partial c_{HA}} = -I^\circ \alpha d \cdot e^{-\alpha d c_{HA}} \quad (5.5)$$

$$\begin{aligned} \frac{\partial I^\circ}{\partial c_{HA}} &= I \alpha d \cdot e^{\alpha d c_{HA}} \\ &= I^\circ \alpha d \quad (\text{with (5.4)}) \end{aligned} \quad (5.6)$$

A combination of Equations (5.3), (5.5), (5.6) and (2.2) leads to:

$$\sigma_I = \frac{I^\circ \alpha d \ln(10) \cdot \left(e^{-\frac{\alpha d c_{HA}}{10^{(pH - pK_a^*)} + 1}} + 1 \right)}{10^{(pK_a^* - pH)} + 2 + 10^{(pH - pK_a^*)}}. \quad (5.7)$$

Using the derivatives from σ_I it is possible to obtain the optimal values for light intensity, absorption index, length of the optical pathway, concentration of the indicator dye and the pH -value of optimal sensitivity for a given pK_a^* -value. As the derivations lead mostly to complicated equations which can only be solved numerically, they are not given here. But some remarks describing the findings are itemized:

- The sensitivity is proportional to I° , it is limited only by the range of the photodiode. Note that the calculations are based on only one indicator dye. If a mixture of indicator dyes is used, I° is the light intensity if only the considered indicator dye is omitted.

- There is an optimum in sensitivity for the product αdc_Σ . This means that indicator dyes with high absorption indices and measuring cells with a long optical pathway require less concentration of the dye. The optimum for the product αdc_Σ is reached when $\frac{I}{I_0} \approx 0.35$ for the indicator dye being in the coloured form.
- In contrast to Equation (2.4) there is not always optimal sensitivity for $pH = pK_a^*$. It exists an product αdc_Σ which has an optimal sensitivity for a given pH -value. But for a sensible combination of α , d and c_Σ the pH -value of the highest sensitivity is near the pK_a^* -value.

Calculation of the Influence of Antimony Hydroxide on the Electric Potential of an Antimony pH -Electrode (Chapter 2.2)

The electric potential of an Antimony electrode as a function of the activity of Antimony ions in solution is (compare to Equation (2.13)):

$$U_{15a} = U_{15a}^* + \frac{RT}{3F} \ln(a_{(Sb^{3-})}). \quad (5.8)$$

The dissociation products for Antimony Hydroxide and water are:

$$K_{15b} = \frac{a_{(Sb^{3-})} \cdot a_{(OH^-)^3}}{a_{(H_2O)}} \quad (5.9)$$

$$K_W = \frac{a_{(H^+)} \cdot a_{(OH^-)}}{a_{(H_2O)}}. \quad (5.10)$$

Equation (5.8) combined with (5.9) and (5.10) gives:

$$\begin{aligned} U_{15a} &= U_{15a}^* + \frac{RT}{3F} \ln \left(\frac{1}{K_{15b} \cdot a_{(OH^-)^3}} \right) \\ &= U_{15a}^* + \frac{RT}{F} \ln \left(\frac{a_{(H^+)}}{K_{15b}^3 \cdot a_{(H_2O)} K_W} \right) \\ &= U_{15a}^* + \frac{RT}{F} \left[\ln \left(\frac{1}{K_{15b}^3 \cdot a_{(H_2O)} \cdot K_W} \right) + \frac{\lg(a_{(H^+)})}{\lg(e)} \right] \\ \frac{(U_{15a} - U_{15a}^*) F}{RT} &= \ln \left(\frac{1}{K_{15b}^3 \cdot a_{(H_2O)} \cdot K_W} \right) - \frac{pH}{\lg(e)} \\ pH &= -\frac{\lg(e) F}{RT} (U_{15a} - U_{15a}^*) + \lg \left(\frac{1}{K_{15b}^3 \cdot a_{(H_2O)} \cdot K_W} \right). \end{aligned} \quad (5.11)$$

5.1.2 A Program to Select and Pre-treat the Values from Spectral Data Files

The following PASCAL program, `sw4_exc9.exe`, was written to select data from the ASCII files produced by the spectrometer. The spectrometer controlling program generates new data files containing the spectral data. The name of these files consists of up to 5 alphanumerical signs which must be given by the operator and an ascending number. Four files with adjacent numbers correspond to one measurement using the four spectrometers. For further data processing with Microsoft EXCEL it is convenient to present the information in four files, each representing an individual spectrometer. The program selects, therefore, data from the files which are four numbers apart. A file called `inifile.txt` is needed to tell the program the path and name of the source files and the required wavelength. Following is an example of the content of this `inifile.txt`:

```
UV.txt
340 363 375 400 406 425 438 710 715
ttt
4
5
Phos2\
phos2
1
Phos23\
phos23
1
Phos26\
phos26
1
Ende
```

The first line contains the name of the new data file, the next itemizes the wavelengths which are to be selected. The following line gives the extension of the source files and the next line the step between the numbering of two data files followed by the number of the column in this file. Finally, the source files are specified by the path, the beginning of the name and the first number. In the last line must be written "Ende".

In the above-mentioned example the data for 340, 363,...715 nm from the 5th column of the following itemized files are selected and written in a new file called `UV.txt`.

```
\Phos2\phos2001.ttt,
\Phos2\phos2005.ttt,
\Phos2\phos2009.ttt,
```

```

...
Phos23\phos2301.ttt,
Phos23\phos2305.ttt,
Phos23\phos2309.ttt,
...
Phos26\phos2601.ttt,
Phos26\phos2605.ttt,
Phos26\phos2609.ttt,
...

```

The actual program code is given below:

```

program SW4_excel;

uses dos, crt;

type
  vv = ^lamda;
  lamda= record
    fl: vv;
    ll: double  ;
  end;

var
  fi, fs, fn, fp:  text;
  datneu, ps:  string;
  vl, v2:  vv;
  sp, j, p:  integer;
  d:  double;

procedure LESE(dat1: string; sp: integer);

var ch:  char;
  t:  string;
  vw:  vv;
  i,m:  integer;
  a:  array[1..5] of double;

```

```

Begin
  writeln(fp,' gefunden');
  assign(fs,dat1);
  reset(fs);
  write(fn,dat1,chr(9));
  readln(fs,t);
  write(fn,t,chr(9));
  readln(fs,t);
  write(fn,t,chr(9));
  readln(fs,t);
  write(fn,t,';');
  readln(fs,t);
  readln(fs,t);
  new(vw);
  vw:=vl;
  j:=0;
  d:=0.0;
  while not (eof(fs) or (vw^.ll=0)) do
    begin
      for i:=1 to sp do
        begin
          t:='';
          repeat
            read(fs,ch);
            case ch of
              ' ':;
              ';':;
              chr(13):;
            else t:=t+ch;
          end;
          until((ch=';') or (ch=#13));
          val(t,a[i],m);
        end;
      if ((a[1]>(vw^.ll-1))and(a[1]<(vw^.ll+1))) then
        begin
          d:=d+a[sp];
          j:=j+1;
        end;
      if (a[1]>(vw^.ll+1)) then
        begin
          d:=d/j;
          vw:=vw^.fl;
          write(fn,d:6:4,';');
        end;
    end;
  end;

```



```

                                d:=0;
                                j:=0;
                                end;
                                while ch<>#10 do
                                    read(fs,ch);
                                end;
                                writeln(fn);
                                close(fs);
                                End;

function FileExists(FileName: string): Boolean;
{ Returns True if file exists; otherwise,
  it returns False. Closes the file if
  it exists. }
var
    f: file;
begin
    {$I-}
    Assign(f, FileName);
    Reset(f);
    Close(f);
    {$I+}
    FileExists := (IOResult = 0) and
        (FileName <> '');
end; { FileExists }

procedure Name(var fi: text; p: integer);
Var i, j, k, s: integer;
    datei, datl, pfad,
    trt,z, dat: string;

Begin
    clrscr;
    readln(fi,trt);
    if trt='' then
        readln(fi,trt);
    readln(fi,sp);
    readln(fi,s);
    readln(fi,pfad);

```

```

repeat
  readln(fi,dat);
  readln(fi,i);
  i:=i+p;
  str(i,z);
  if length(dat)>6 then
    repeat
      datei:=dat[1];
      case i of
        0..9:      k:=6;
        10..99:    K:=5;
        100..999: K:=4;
        else      K:=3
      end;
      for j:=2 to k do datei:=datei+dat[j];
      datei:=datei+'~';
      datl:=pfad+datei+z+'.'+trt;
      i:=i+s;
      str(i,z);
      write(fp,'Suche ~datl: ',datl,' i: ', i, ' k: ',k);
      if fileexists(datl) then lese(datl, sp)
      else
        begin
          writeln(fp,' ~',datl,' nicht gefunden');
        end;
      writeln(datl);
    until (not(FileExists(datl)))
  end;
else
  repeat
    datei:=dat;
    case i of
      0..9:      k:=7;
      10..99:    k:=6;
      100..999: k:=5;
      else      k:=2
    end;
    while (length(datei)<k) do datei:=datei+'0';
    str(i,z);
    datl:=pfad+datei+z+'.'+trt;
    write(fp,'Suche datl: ',datl,' i: ', i, ' k: ',k);
  end;
end;

```

```

        if fileexists(datl) then lese(datl, sp)
        else
            begin
                writeln(fp,' ',datl,' nicht gefunden');
                writeln(datl);
            end;
        i:=i+s;
    until (not(FileExists(datl)));
    readln(fi,pfad);
    until ((pfad='Ende') or (eof(fi)));
    close(fp);
End;

```

```

function init(var fi: text):string;

var    text: string;

begin
    if not eof(fi) then readln(fi,text)
    else text:='end';
    init:=text;
end;

```

```

procedure leseinit(var fi: text; vi: vv);

var    re:    double;

begin
    if not eof(fi) then
        repeat
            read(fi,re);
            vi^.ll:=re;
            new(vi^.fl);
            vi:=vi^.fl;
            vi^.ll:=0;
        until(eoln(fi))
    else writeln('Fehler 2 Leseinit');
end;

```

```

Begin
  clrscr;
  if fileexists('inifile.txt')then
  begin
    for p:=0 to 3 do
    begin
      assign(fp,'Protokoll.txt');
      rewrite(fp);
      assign(fi,'inifile.txt');
      reset(fi);
      str(p,ps);
      datneu:=ps+init(fi);
      assign(fn,datneu);
      rewrite(fn);
      new(v1);
      v1^.ll:=0;
      leseinit(fi,v1);
      write(fn,'Datei',chr(9),'Text',chr(9),'Integrationszeit',chr(9),
        'Average\Lambda->');
      v2:=v1;
      while v2^.ll<>0 do
      begin
        write(fn,',',v2^.ll:4:0);
        v2:=v2^.f1;
      end;
      writeln(fn);
      name(fi,p);
      writeln(fn,'Spalte: ',sp);
      close(fn);
      close(fi);
    end;
  end
  else writeln('Nix inifile.txt');
  writeln('Taste druecken');
  repeat until keypressed;
End.

```

Bibliography

- [1] A.M. Matser, B. Krebbers, R.W. van den Berg, P.V. Bartels (2004) *Trends Food Sci. & Tech.*, **15**, 79.
- [2] J.P.P.M. Smelt (1998) *Trends Food Sci. & Tech.*, **9**, 152.
- [3] D.G. Hoover, K. Meterick, A.M. Papineau, D.F. Farkas, D. Knorr (1989) *Food Tech.*, **43**, 99.
- [4] B. Tauscher *Advances in High Pressure Bioscience and Biotechnology*, Ed. by H. Ludwig; Springer, Berlin 1999, 363.
- [5] C.G. Heden (1964) *Bacteriol. Rev.*, **28**, 14.
- [6] V. Herdegen, PhD.-Thesis, Technical University Munich, 1998; Verlag Ulrich Grauer Stuttgart
- [7] D.A. Ledward, D.E. Johnson, R.G. Earnshaw, A.P.M. Hasting (Eds.) *High Pressure Processing of Foods*; Nottingham University Press, 1995.
- [8] W.P. Larson, T.B. Hartzell, H.S. Diehl (1918) *J. Infectious Diseases*, **22**, 271.
- [9] C. Dogan O. Erkmen (2004) *J. Food Eng.*, **62**, 47.
- [10] W.B.C. de Heij, L.J.M.M. van Schepdael, R. Moezelaar, H. Hoogland, A.M. Matser, R.W. van den Berg (2003) *Food Tech.*, **57**, 37.
- [11] S. Balasubramanian, V.M. Balasubramaniam (2003) *Food Res. Int.*, **36**, 661.
- [12] N. Merkulow, PhD.-Thesis, University Heidelberg, 2001.
- [13] A. Molina-Gutierrez, V. Stippl, A. Delgado, M.G. Gänzle, R.F. Vogel (2002) *Appl. Envir. Microbiol.*, **68**, 4399.
- [14] H.M. Ulmer, PhD.-Thesis, Technical University Munich, 2001
(<http://tumb1.biblio.tu-muenchen.de/publ/diss/ww/2002/ulmer.pdf>)

- [15] M. Hayert, J.M. Perrier-Cornet, P. Gervais (1997) *High Pressure Research in the Biosciences and Biotechnology*, Ed. by Heremans, Leuven University Press, 205.
- [16] P. Chilton, N.S. Isaacs, B. Mackey, R. Stenning (1997) *High Pressure Research in the Biosciences and Biotechnology*, Ed. by Heremans, Leuven University Press, 225.
- [17] B. Tauscher (1998) *Flüssiges Obst*, **2/98**, 72.
- [18] H. Frauenfelder, N.A. Alberding, A. Ansari, D. Braunstein, B.R. Cowen, M.K. Hong, I.E.T. Iben, J.B. Johnson, S. Luck, M.C. Marden, J.R. Maurant, P. Ormos, L. Reinisch, R. Scholl, A. Schulte, E. Shyamsunder, L.B. Sorensen, P.J. Steinbach, A. Xie, R.D. Young, K.T. Yue (1990) *J. Phys. Chem.*, **94**, 1024.
- [19] E. Morild (1981) *Adv. Protein Chem.*, **34**, 93.
- [20] I. Seyderhelm, S. Boguslawski, G. Michaelis, D. Knorr (1996) *J. Food Sci.*, **61**, 308.
- [21] L. Smeller, K. Heremans (1997) *High Pressure Research in the Biosciences and Biotechnology*, Ed. by Heremans, Leuven University Press, p. 55.
- [22] G. Weber, H.G. Drickamer (1983) *Q. Rev. Biophys.*, **16**, 89.
- [23] D. Farr (1990) *Trends Food Sci. & Tech.*, **1**, 16.
- [24] J.M. Ames (1998) *Food Chem.*, **62**, 431.
- [25] T. Tamaoka, N. Itoh, R. Hayashi (1991) *Agric. Biol. Chem.*, **55**, 2071.
- [26] V.M. Hill, D.A. Ledward, J.M. Ames (1996) *J. Agric Food Chem.*, **44**, 594.
- [27] J. van Camp, W. Messens, J. Clement, A. Huyghebaert (1997) *J. Agric. Food Chem.*, **45**, 1600.
- [28] J. van Camp, W. Messens J. Clement, A. Huyghebaert (1997) *Food Chem.*, **60**, 417.
- [29] A. Totosaus, J.G. Montejano, J.A. Salazar, I. Guerrero (2002) *Int. J. Food Sci. & Tech.*, **37**, 589.
- [30] J.M. Thevelein, J.A. Van Assche, K. Heremans, S.Y. Gerlsma (1981) *Carbohydrate Research*, **93**, 304.
- [31] N. Kato, A. Teramoto, M. Fuchigami (1997) *J. Food Sci.*, **62**, 359 and 398.

- [32] D. Prieur, G. Erauso, J. Llanos, J.W. Deming, J. Baros (1992) *High Pressure and Biotechnology*, Ed. by C. Balny, R. Hayashi, K. Heremans, P. Masson; Colloque Inserm **224**, 9.
- [33] K.-H. Sohn, H.-J. Lee (1998) *Intern. J. Food Sci. Tech.*, **33**, 359.
- [34] H. Schöberl, PhD.-Thesis, Technical University Munich, 1999; Herbert Utz Verlag München.
- [35] W. De Heij, L. van Schepdeal, R. van den Berg, P. Bartels (2002) *High pressure research*, **22**, 653.
- [36] L. Otero, A.D. Molina, P.D. Sanz (2002) *High pressure research*, **22**, 627.
- [37] S. Denys, L.R. Ludikhuyze, A.M. Van Loey, M.E. Hendrickx (2000) *Biotechnol. Prog.*, **16**, 92.
- [38] C. Hartmann, A. Delgado (2003) *Biotech. Bioeng.*, **82**, 725.
- [39] C. Hartmann, A. Delgado (2003) *J. Food Eng.*, **59**, 33.
- [40] C. Hartmann, A. Delgado (2002) *Biotech. Bioeng.*, **79**, 94.
- [41] F. Werner, A. Delgado, M. Pehl (1999) *Advances in High Pressure Bioscience and Biotechnology*, Ed. by H. Ludwig, Heidelberg, 519.
- [42] A. Delgado, M. Pehl (2000) *Exp. in Fluids*, **29**, 302.
- [43] F. Werner, A. Delgado, M. Pehl (2002) *Trends in High Pressure Bioscience and Biotechnology*, Ed. by R. Hayashi; Elsevier Science B.V., Amsterdam, 429.
- [44] J.C. Cheftel, J. Lvy, E. Dumay (2000) *Food Rev. Int.*, **16**, 453.
- [45] A. LeBail, D. Chevalier, D.M. Mussa, M. Ghoul (2002) *Int. J. Refrigeration*, **25**, 504.
- [46] W. Kowalczyk, C. Hartmann, A. Delgado (2003) *Int. J. Heat Mass Trans.*, **47**, 1079.
- [47] S. Denys, A. Van Loey, S. De Cordt, M. Hendrickx, P. Tobback (1997) *High Pressure Research in the Biosciences and Biotechnology*, Ed. by Heremans, Leuven University Press, 351.
- [48] G. Tammann (1895) *Zeit. Phys. Chem.*, **17**, 725.
- [49] M. Planck (1887) *Ann. Phys. Chem.*, **32**, 426.
- [50] G. Tammann (1910) *Z. Electrochem.*, **15**, 592.

- [51] B.H. Hite (1899) *Bull. W. Va. Univ. Agric. Exp. Sta., Morgatown.*, **58**, 15.
- [52] G.W. Chlopin, G. Tammann (1903) *Z. Hyg. Infektionskrankh.*, **45**, 171.
- [53] B.H. Hite, N.J. Giddings, C.E. Weakly (1914) *W. Va. Univ. Agric. Exp. Stn. Bull.*, **146**, 1.
- [54] P.W. Bridgemann (1914) *J. Biol. Chem.*, **19**, 511.
- [55] W. Kauzmann (1959) *Adv. Prot. Chem.*, **14**, 1.
- [56] C. Tanford (1968) *Adv. Prot. Chem.*, **23**, 212.
- [57] E. Morild (1981) *Adv. Prot. Chem.*, **34**, 93.
- [58] P.W. Bridgemann (1912) *Proc. Am. Acad. Arts Sci.*, **47**, 439.
- [59] R.M. Pytkowicz, D.R. Kester, B.C. Burgener (1966) *Limnol. Oceanog.*, **11**, 417.
- [60] G.N. Somero (1992) *Ann. Rev. Physiol.*, **54**, 557.
- [61] J.G. Clouston, P.A. Wills (1969) *J. Bacteriology*, **97**, 684.
- [62] A.J.H. Sale, G.W. Gould, W.A.J. Hamilton (1970) *Gen. Micobiol.*, **60**, 323.
- [63] J.G. Clouston, P.A. Wills (1970) *J. Bacteriology*, **103**, 140.
- [64] P. Palou, E. Palou (1998) *Nonthermal Preservation of Foods*, Ed. by G.V. Barbosa-Cnovas, R. Usha, New York: Dekker, 276.
- [65] K. Suzuki (1960) *Rev. Phys. Chem. Jpn.*, **29**, 91.
- [66] B. Ly-Nguyen, A.M. Van Loey, D. Fachin, I. Verlent, T. Duvetter, S.T. Vu, C. Smout, M.E. Hendrickx (2002) *Biotech. Prog.*, **18**, 1447.
- [67] F.-G. Klärner, F. Wurche (2000) *J. Prakt. Chem.*, **342**, 609.
- [68] S.D. Hamann (1980) *Rev. Phys. Chem. Jpn.*, **50**, 147.
- [69] T. Asano, W.J. le Noble (1978) *Chem. Rev.*, **78**, 407.
- [70] F.T. Millerno (1971) *Chem. Rev.*, **71**, 147.
- [71] R. Van Eldik, T. Asano, W. J. Le Noble (1989) *Chem. Rev.*, **89**, 549.
- [72] M.G. Evans, M. Polanyi (1935) *Trans. Fara. Soc.*, **31**, 875.
- [73] J. Buchanan, S.D. Hamann (1953) *Trans. Fara. Soc. I*, **49**, 1425.

- [74] B.S. ÉI'Yanov, M.G. Gonikberg (1967) *Bull. Acad. Sci. USSR/Div. Chem. Sci.* 1007.
- [75] B.S. ÉI'Yanov, E.M. Vasylvitskaya (1980) *Rev. Phys. Chem. Jpn.*, **50**, 169.
- [76] N.I. Prokhorova, B.S. ÉI'Yanov, M.G. Goniberg (1967) *Bull. Acad. Sci. USSR*, **3**, 256.
- [77] B.S. ÉI'Yanov (1975) *Austr. J. Chem.*, **28**, 933.
- [78] B.S. ÉI'Yanov, E.M. Gonikberg (1979) *Fara. Trans. I*, **75**, 172.
- [79] D.A. Lown, H.R. Thirsk, Lord Wynne-Jones (1968) *Trans. Fara. Soc. I*, **64**, 2073.
- [80] M. Tsuda, I. Shirotani, S. Minomura, Y. Terayama, (1976) *Buellion Chem. Soc. Jpn.*, **49**, 2952.
- [81] R.C. Neumann, W. Kauzmann, A. Zipp (1973) *J. Phys. Chem.*, **77**, 2687.
- [82] J.L. Kavanau *Water and solute-water Interactions* (1964) Holden-Day, San Francisco.
- [83] H. Tanaka (2000) *J. Chem. Phys.*, **112**, 799.
- [84] G.W. Robinson, C.H. Cho (1999) *Biophys. J.*, **77**, 3311.
- [85] M.-P. Bassez, J. Lee, G.W. Robinson (1987) *J. Phys. Chem.*, **91**, 5818.
- [86] M. Vedamuthu, S. Singh, G.W. Robinson (1994) *J. Phys. Chem.*, **98**, 2222.
- [87] C.H. Cho, S. Singh, G.W. Robinson (1997) *J. Chem. Phys.*, **107**, 7979.
- [88] E. Whalley (1963) *J. Chem. Phys.*, **38**, 1400.
- [89] Y. Liu, T. Ichiye (1999) *Biophys. Chem.*, **78**, 97.
- [90] A.A. Kornyshev, G. Sutmann (1997) *Chem. Phys. Lett.*, **79**, 519.
- [91] B.B. Owen, S.R. Brinkley (1941) *Chem. Rev.*, **29**, 461.
- [92] R.E. Gibson (1934) *J. Amer. Chem. Soc.*, **56**, 4.
- [93] R.E. Gibson (1935) *J. Amer. Chem. Soc.*, **57**, 284.
- [94] G. Tammann (1893) *Zeit. Phys. Chem.*, **11**, 676.
- [95] N.A. North (1973) *J. Phys. Chem.*, **77**, 931.
- [96] B.S. ÉI'yanov, S.D. Hamann (1975) *Austral. J. Chem.*, **28**, 945.

- [97] S.D. Hamann, W. Strauss (1955) *Fara. Trans. I*, **51**, 1684.
- [98] O. Redlich, J. Bigeleisen (1942) *Chem. Rev.*, **30**, 171.
- [99] I.R. Kritschewsky (1938) *Acta Physicochim. U.R.S.S.*, **8**, 181.
- [100] T.J. Webb (1926) *J. Am. Chem. Soc.*, **48**, 2589.
- [101] P. Mukerjee (1961) *J. Phys. Chem., Ithaca*, **65**, 740.
- [102] M. Born (1920) *Zeit. Physik*, **1**, 45.
- [103] M. Nakahara (1975) *Rev. Phys. Chem. Jpn.*, **44**, 57.
- [104] E. Hückel (1925) *Physik. Zeit.*, **26**, 93.
- [105] H. Harned, N.D. Embree (1935) *J. Am. Chem. Soc.*, **57**, 1669.
- [106] H. Harned, G.L. Kazanjin (1936) *J. Am. Chem. Soc.*, **58**, 1912.
- [107] D.M. Murray-Rust, H. Hartley (1929) *Proc. Roy. Soc.*, **A126**, 84.
- [108] G. Scatchard (1925) *J. Am. Chem. Soc.*, **47**, 2098.
- [109] H.S. Harned, R.A. Robinson (1928) *J. Am. Chem. Soc.*, **50**, 3157.
- [110] H. Harned, N.D. Embree (1934) *J. Am. Chem. Soc.*, **56**, 1050.
- [111] H. Harned, B.B. Owen (1940) *Chem. Rev.*, **26**, 31.
- [112] V.K. LaMer, F. Brescia (1940) *J. Am. Chem. Soc.*, **62**, 617.
- [113] B.B. Owen (1933) *J. Am. Chem. Soc.*, **55**, 1922.
- [114] F.J. Millero (1970) *J. Phys. Chem.*, **74**, 356.
- [115] H.S. Harned, B.B. Owen (1930) *J. Amer. Chem. Soc.*, **52**, 5079.
- [116] A.G. Macdonald (1992) *High Pressure and Biotechnology*, Ed. by C. Balny, R. Hayashi, K. Heremans, P. Masson; Colloque Inserm **224**, 67.
- [117] P.T.T. Wong (1986) *Physica B*, **140**, 847.
- [118] A. Pqueux (1972) *Symp. Soc. Exp. Biol.*, **26**, 483.
- [119] T. Liu, E. Diemann, H. Li, A.W.M. Dress, A. Müller (2003) *Nature*, **426**, 59.
- [120] R.G. Earnshaw (1995) *High Pressure Processing of Foods.*, Ed. by D.A. Ledward, D.E. Johnson, R.G. Earnshaw, A.P.M. Hasting; Nottingham University Press, 37.

- [121] M.F. Patterson, M. Quinn, R. Simpson, A. Gilmor (1995) *High Pressure Processing of Foods*, Ed. by D.A. Ledward, D.E. Johnson, R.G. Earnshaw, A.P.M. Hasting; Nottingham University Press, 47.
- [122] P. Butz, H. Ludwig (1986) *Physica B*, **140**, 875.
- [123] M. Voldrich, J. Dobis, L. Tich, M. Cerovsky, J. Kratka (2004) *J. Food Eng.*, **61**, 545.
- [124] J. Raso, M.M. Gongora-Nieto, G.V. Barbos-Canovas, B.G. Swanson (1998) *Int. J. Food Microbiol.*, **44**, 125.
- [125] C. Hölters, B. Sojka, H. Ludwig (1997) *High Pressure Research in the Biosciences and Biotechnology*, Ed. by Heremans, Leuven University Press, 225.
- [126] E.Y. Wuytack, S. Boven, C.W. Michiels (1998) *Appl. Environ. Microbio.*, **64**, 3220.
- [127] P. Großand H. Ludwig (1992) *High Pressure and Biotechnology*, Ed. by C. Balny, R. Hayashi, K. Heremans, P. Masson; Colloque Inserm **224**, 57.
- [128] K. Carl, H. Ludwig (1991) *High Pressure Research*, **7**, 767.
- [129] T. Treude, F. Janßen, W. Queisser, U. Witte (2002) *Deep-Sea Research I*, **49**, 1281.
- [130] B.R. de Forges, J.A. Koslow, G.C.B. Poore (2000) *Nature*, **405**, 944.
- [131] Y. Todo, A.J. Gooday, J. Hashimoto, A.J. Gooday (2005) *Science*, **307**, 689.
- [132] P.J.R. Uwins, R.I. Webb, A.P. Taylor (1998) *American Mineralogist.*, **83**, 1541.
- [133] J. Cowen (2003) *Science*, **299**, 120.
- [134] A.A. Yayanos, A.S. Dietz, R. Van Boxel (1979) *Science*, **205**, 808.
- [135] A.A. Yayanos, A.S. Dietz, R. Van Boxel (1981) *Proc. Nat. Acad. Sci. USA*, **78**, 5212.
- [136] A. Williams, J.A. Koslow, P.R. Last (2001) *Mar. Ecol. Prog. Ser.*, **212**, 247.
- [137] F. Abe, K. Horikoshi (1997) *High Pressure Research in the Biosciences and Biotechnology*, Ed. by Heremans, Leuven University Press, 209.

- [138] C.W. Michiels, K. Peeters, C. Soontjens, E. Wuytack, K. Hauben (1997) *High Pressure Research in the Biosciences and Biotechnology*, Ed. by Heremans, Leuven University Press, 217.
- [139] K. Heremans, F. Wuytack (1980) *Fed. Europ. Biochem. Soc. Lett.*, **117**, 161.
- [140] J. Barciszewski, J. Jurczak, S. Porowski, T. Specht, V.A. Erdmann (1999) *Eur. J. Biochem.*, **260**, 293.
- [141] N.S. Isaacs, P. Chilton (1995) *High Pressure Processing of Foods*, Ed. by D.A. Ledward, D.E. Johnson, R.G. Earnshaw, A.P.M. Hasting; Nottingham University Press, 58.
- [142] R. Hayashi, Y. Kawamura, S. Kunugi (1987) *J. Food. Sci.*, **52**, 1107.
- [143] S.P.L. Sörensen (1909) *Biochem. Zschr.*, **21**, 131 and 159.
- [144] I. Mills *IUPAC, Quantities, Units and Symbols in Physical Chemistry*, Blackwell, Oxford 1993, pp.60.
- [145] R.P. Buck, S. Rondinini, A.K. Covington, F.G.K. Baucke, C.M.A. Brett, M.F. Camões, M.J.T. Milto, T. Mussini, R. Naumann, K.W. Pratt, P. Spitzer, G.S. Wilson (2002) *Pure Appl. Chem.*, **74**, 2169.
- [146] A. Delgado, M. Pehl (1998) *High Pressure Bioscience and Biotechnology*, Ed. by H. Ludwig, Heidelberg, 519.
- [147] Y.J. Cho, PhD-Thesis, Gerhard-Mercator-University Duisburg, 1994.
- [148] J. Seemann, F.-R. Rapp, A. Zell, G. Gauglitz (1997) *Fresenius J. Anal. Chem.*, **359**, 100.
- [149] H.M. Heise, A. Bittner (1997) *Fresenius J. Anal. Chem.*, **359**, 93.
- [150] M.Y. Salem, E.S. El-Zanfaly, M.F. El-Tarras, M.G. El-Bardicy (2003) *Anal. Bioanal. Chem.*, **375**, 211.
- [151] W.J. LeNoble (1967) *Progr. Phys. Org. Chem.*, **5**, 207.
- [152] D.E. Yates, S. Levine, T.W. Healy (1974) *Fara. Trans. I*, **70**, 1807.
- [153] F.G.K. Baucke (1994) *Anal. Chem.*, **66**, 4519.
- [154] H. Kaden, K. Jüttner, H. Jahn, M. Berthold, K.-M. Mangold, S. Schäfer (2000) *Chem. Ing. Tech.*, **72**, 1534.
- [155] H. Kaden, H. Jahn, M. Berthold, K. Jüttner, K.-M. Mangold, S. Schäfer (2001) *Chem. Eng. Technol.*, **24**, 1120.

- [156] M. Jovanovic, A. Dekanski, G. Vlajnic, M.S. Jovanovic (1997) *Electroanalysis*, **9**, 564.
- [157] D.L. Harne, L.J. Bousse, J.D. Meindl (1987) *IEEE Trans. Electron Devices*, **ED-34**, 1700.
- [158] W. Kordatzki: *Taschenbuch der praktischen pH-Messung* (1938) Müller & Steinicke, München.
- [159] S.N. Lvov, X.Y. Zhou, D.D. Macdonald (1999) *J. Elec. Anal. Chem.*, **463**, 146.
- [160] K. Sue, M. Uchida, T. Usami, T. Adschiri, K. Arai (2004) *J. Supercrit. Fluids*, **28**, 287.
- [161] K. Sue, K. Murata, Y. Matsuura, M. Tsukagoshi, T. Adschiri, K. Arai (2001) *Rev. Sci. Instr.*, **72**, 4442.
- [162] K. Eklund, S.N. Lvov, D.D. Macdonald (1997) *J. Electroanal. Chem.*, **437**, 99.
- [163] J.V. Dobson (1972) *J. Electroanal. Chem.*, **35**, 129.
- [164] D.D. Macdonald, P.R. Wentrec, A.C. Scott (1980) *J. Electrochem. Soc.*, **127**, 1745.
- [165] W.L. Bourcier, G.C. Ulmer, H.L. Barnes (1987) *Hydrothermal Experimental Techniques* Ed. by G.C. Ulmer, H.L. Barnes, Wiley-Interscience, New York, 157.
- [166] S.D. Hamann (1963) *J. Phys. Chem.*, **67**, 2233.
- [167] A. Distéche, S. Distéche (1965) *J. Electrochem. Soc.*, **112**, 350.
- [168] A. Distéche (1959) *Rev. Sci. Instruments*, **30**, 474.
- [169] A. Distéche (1962) *J. Electrochem. Soc.*, **109**, 1084.
- [170] A. Distéche, M. Dubuisson (1960) *Dubuisson Bull. Inst. Océanographique Monaco*, **1174**, 1.
- [171] A.M. Whitfield (1969) *J. Electrochem Soc.*, **116**, 1042.
- [172] S. Ben-Yaakov, I.R. Kaplan (1968) *Rev. Sci. Instruments*, **39**, 1133.
- [173] C. Culberson, D.R. Kester, R.M. Pytkowicz (1967) *Science*, **157**, 59.
- [174] D.J.G. Ives, G.J. Janz (1961) *Reference Electrodes*, Academic Press, New York.

- [175] E. Nilsson, PhD-Thesis, University Stockholm, 1983.
- [176] S. Yao, M. Wang, M. Madouz (2001) *J. Electrochem. Soc.*, **148**, 29.
- [177] H. Galster, *pH measurements-Fundamentals, Methods, Applications, Instruments* (1991) VCH Publishers, New York .
- [178] R.E.F. Einerhand, W.H.M. Visscher, E. Barendrecht (1989) *Electrochim. Acta*, **34**, 345.
- [179] C.C. Liu, B.C. Bocchicchio, P.A. Overmyer, M.R. Neuman (1980) *Science*, **207**, 188.
- [180] W.T. Grubb, L.H. King (1980) *Anal. Chem.*, **52**, 270.
- [181] A. Fog and R.P. Buck (1984) *Sens. Actuators*, **5**, 137.
- [182] G. Milazzo *Elektrochemie, Theoretische Grundlagen und Anwendungen* (1952) Springer Wien.
- [183] J.V. Dobson, P.R. Snodin, H.R. Thirsk (1976) *Electrochim. Acta.*, **21**, 527.
- [184] L.B. Kriksunov, D.D. Macdonald, P.J. Millett (1994) *J. Electrochem. Soc.*, **141**, 3002.
- [185] K. Ding, W.E. Seyfried (1996) *Science*, **272**, 1634.
- [186] K. Ding, W.E. Seyfried (1995) *Geochim. Cosmochim. Acta*, **59**, 4769.
- [187] D.D. Macdonald, S. Hettiarachchi, S.J. Lenhart (1988) *J. Sol. Chem.*, **17**, 719.
- [188] D.D. Macdonald, S. Hettiarachchi, H. Song, K. Makerla, R. Emmerson, M. Heim (1992) *J. Sol. Chem.*, **21**, 849.
- [189] H.A. Lubs, S.F. Acree (1916) *J. Am. Chem. Soc.*, **38**, 2772.
- [190] H.A. Lubs, W.M. Clark (1915) *J. Wash. Acad. Sci.*, **5**, 609.
- [191] H.A. Lubs, W.M. Clark (1916) *J. Wash. Acad. Sci.*, **6**, 481.
- [192] I.M. Kolthoff *Gebrauch der Farbindikatoren* (1926) Justus Springer Berlin.
- [193] B. Cohen (1927) *U.S. Pub. Health Rep.*, **41**, 3051.
- [194] A.B. Clark, H.A. Lubs (1918) *J. Am. Chem. Soc.*, **40**, 1940.

- [195] E. Ross, J. Köthe, R. Naumann, W. Fischer, U. Jäschke, W.-D. Mayer, G. Wieland, E. Merck, E.J. Newman, C.M. Wilson: Indicator Reagents in *Ullmann's Encyclopedia of Industrial Chemistry*, Ed. by B. Elvers, S. Hawkins, M. Ravenscroft, G. Schultz **A 14** VCH Weinheim. 127.
- [196] J.M. Kolthoff *Die Massanalyse* (1928) Justus Springer Berlin .
- [197] M. Chierici, A. Fransson, L.G. Anderson (1999) *Marine Chem.*, **65**, 281.
- [198] S. Palitzsch (1911) *Compt. Rend. Carlsberg*, **10**, 162.
- [199] G.D. Christian (1975) *CRC Crit. Rev. Anal. Chem.*, **5**, 119.
- [200] I.M. Kolthoff (1922) *Rec. Trav. Chim.*, **41**, 54.
- [201] J. Kielland (1937) *J. Am. Chem. Soc.*, **59**, 1675.
- [202] M. Winkler, Habil., University Dresden, 1984.
- [203] A. Thiel, F. Wülfken, A. Daßler (1924) *Z. anorg. allg. Chem.*, **136**, 406.
- [204] E.R. Bishop, E.B. Kitt, J.H. Hildebrand (1922) *J. Am. Chem. Soc.*, **44**, 135.
- [205] W. Gottwald *UV-VIS Spektroskopie für Anwender*, Wiley-VCH Weilheim; ISBN 3-527-28760-4.
- [206] U. Kosch, PhD.-Thesis, University Regensburg, 1998.
- [207] O.S. Wolfbeis *Fiber Optic Chemical Sensors and Biosensors* (1991) CRC Press, Boca Raton, Florida,
- [208] PreSens (Precision Sensing GmbH) *PDD-470 fiber-optic phase detection device* (Instruction Manual).
- [209] J. Lin (2000) *Trends Anal. Chem.*, **19**, 541.
- [210] M. Wollenweber, PhD.-Thesis, Technical University Munich, 1996.
- [211] G. Vishnoi, T.C. Coel, P.K. Pillai (1999) *Proc. SPIE*, **3538**, 319.
- [212] S. Zhang, S. Tanaka, Y.A.B.D. Wickramasinghe, P. Rofle (1995) *Med. Bio. Eng. Comp.*, **33**, 152.
- [213] A. Dybko, R.S. Romaniuk, J. Maciejewski, Z. Brzózka (1992) *Int. J. Optoelec.*, **7**, 443.
- [214] O. Ben-David, E. Shafir, I. Gilath (1997) *Chem. Mater*, **9**, 2255.

- [215] J.Y. Ding, M.R. Shahriari, G.H. Sigel (1991) *Elec. Lett.*, **27**, 1560.
- [216] B.D. Gupta, S. Sharma (1998) *Optics Comm.*, **154**, 282.
- [217] U.H. Manyam, M.R. Shahriari, M.J. Morris (1999) *Proc. SPIE*, **3540**, 10.
- [218] B.D. Gupta, S. Sharma (1997) *Optics Comm.*, **140**, 32.
- [219] S.A. Grant, R.S. Glass (1997) *Sens. Actuat.*, **B 45**, 35.
- [220] D.A. Nivens, Y. Zhang, S.M. Angel (1998) *Anal. Chim. Acta.*, **376**, 235.
- [221] U. Kosch, I. Klimant, O.S. Wolfbeis (1999) *Fres. J. Anal. Chem.*, **364**, 48.
- [222] O.S. Wolfbeis, R. Reisfeld, I. Oehme (1996) *Struc. Bond.*, **85**, 51.
- [223] J. Lin, C.W. Brown (1997) *Trends Anal. Chem.*, **16**, 200.
- [224] M. Hayert, J.-M. Perrier-Cornet, P. Gervais (1999) *J. Phys. Chem. A*, **103**, 1785.
- [225] K.G. Lipphard, A. Jost (1976) *Ber. Bunsenges. Phys. Chem.*, **80**, 125.
- [226] W. Fichter, H. Kaden, R. Müller, P. Czerney (1999) *Feinwerktech. Messtech.*, **107**, 26.
- [227] A. Dybko, W. Weóblewski, E. Roźniecka, K. Poźniakb, J. Maciejewski, R. Romaniuk, Z. Brzózka (1998) *Sens. Actuat.*, **B 51**, 208.
- [228] J.A. Ferguson, B.G. Healey, K.S. Bronk, S.M. Barnard, D.R. Walt (1997) *Anal. Chim. Acta*, **304**, 123.
- [229] M.W. Grant (1973) *Fara. Trans. I*, **69**, 560.
- [230] A.E. Hopkinsa, K.S. Sella, A.L. Solia, R.H. Byrneba (2000) *Marine Chem.*, **71**, 103.
- [231] S.D. Hamann, M. Linton (1974) *Fara. Trans. I*, **70**, 2239.
- [232] A. Molina-Gutierrez, B. Rademacher, M.G. Gänzle R.F. Vogel (2002) *Trends in High Pressure Bioscience and Biotechnology*, Ed. by R. Hayashi; Elsevier Science B.V., Amsterdam, 295.
- [233] A. Molina-Höppner, W. Doster, R.F. Vogel, M.G. Gänzle (2004) *Appl. Environ. Microbiol.* **70**, 2013.
- [234] I. Van Opstal, S.C. Vanmuysen, C.W. Michiels (2003) *Int. J. Food Microbiol.*, **88**, 1.

- [235] P. Debye, E. Hückel (1923) *Phys. Zeit.*, **24**, 185.
- [236] L. Sigg, W. Stumm *Aquaristische Chemie* (1944) Teubner, Stuttgart, 523.
- [237] S.D. Hamann (1984) *Fara. Trans. I*, **80**, 2541.
- [238] E. Pfeil (1974) Patent from Behringerwerke: DE 2436257.
- [239] K. Neisius, W. Bäumer (1968) Patent from Merck: DE 1698247.
- [240] S. Motellier, M.H. Noire, H. Pitsch, B. Dureault (1995) *Sens. Actuat.*, **B29**, 354.
- [241] R. Zusman, C. Rottman, M. Ottolenghi, D. Avnir (1990) *J. Non-Crystalline Solids*, **122**, 107.
- [242] M.A. Villegas, L. Pascual (1999) *Thin Solid Films*, **351**, 103.
- [243] A. Dybko, J. Maciejewski, R.S. Romaniuk, W. Wroblewski (1993) *Proc. SPIE (Biochem. Medical Sens.)*, **2085**, 131.
- [244] M. Otto *Analytische Chemie* (1995) VCH Weinheim Chap. 6.2.2 (pp. 222-225).
- [245] B.G.M. Vandeginste, D.L. Massart, L.M.C. Buydens, S. De Jong, P.J. Lewi, J. Smeyers-Verbeke *Data Handling in Science and Technology 20B: Handbook of Chemometrics and Qualimetrics B* (1998) Elsevier Science Amsterdam, Chap. 36 (pp. 358-366).
- [246] Deutscher Kalibrierdienst (2002) *Abschlussbericht DKD-Ringvergleich pH-Wert 2002* (<http://www.dkd.info/dkd-ring/ph-wert2002.pdf>).
- [247] M. Herbst, P. Pionthek (1970) *Pflügers Arch.*, **313**, 186.

Curriculum Vitae

Personal Data:

Family name: Stippl
Christian names: Volker Michael
Address: Itzling 6, 85354 Freising, Germany
Date of Birth: November 10, 1966
Place of birth: Achern, Germany
Family status: Unmarried
Nationality: German

Education:

1986 Baccalaureate: Technisches Gymnasium Bühl
1986-1988 Civil service
1988-1995 University of Karlsruhe
Study of chemistry with the certificate: Graduate chemist
1996-2001 Technical University of Munich (TUM)/Weihenstephan
Study of brewing sciences with the certificate:
Graduate engineer
Since 2001 PhD-student
Lehrstuhl für Fluidmechanik und Prozessautomation, TUM
Supported by a Scholarship from
"Fleischmannfonds zur Förderung des Brauernachwuchses"
(July 2000 - July 2002)